EXPLORING PASSIVE HEARTBEAT DETECTION USING A HYDRAULIC BED SENSOR SYSTEM

A Thesis
presented to
the Faculty of the Graduate School
University of Missouri-Columbia

In Partial Fulfillment
Of the Requirements for the Degree
Master in Science

---

by

Licet Rosales

Dr. Marjorie Skubic, Thesis Supervisor

Dec 2011

The undersigned, appointed by the dean of the Graduate School, have examined the thesis entitled

EXPLORING PASSIVE HEARTBEAT DETECTION USING A HYDRAULIC BED SENSOR SYSTEM

Presented by Licet Rosales,

A candidate for the degree of
Master of Science in Electrical Engineering,
And hereby certify that, in their opinion, it is worthy of acceptance.

Professor Marjorie Skubic, PhD.,

Professor Marilyn Rantz, PhD.,

Professor Dominic Ho, PhD.,

.... To my parents for their continuous support

ACKNOWLEDGMENTS

Foremost, I would like to thank my advisor, Prof. Marjorie Skubic, who shared with me a lot of her expertise and research insight. I also like to express my gratitude to the members of the center of eldercare and rehabilitation technology faculty, students and staff, whose thoughtful advice often served to give me a sense of direction during my MS studies.

Contents

List of Figures

List of Tables

ABSTRACT

Sleep monitoring of heartbeat, respiration and restlessness can help to detect sleep disturbances which may be indicative of poor health and functional deficits, especially in older adults. This work investigates a new hydraulic bed transducer configuration, in order to improve its ability to capture heartbeat signals from different body types and proposes a new approach for detecting heartbeats from a ballistocardiogram (BCG) signal using the k-means clustering algorithm. The system's ability to capture heartbeat signals was improved by increasing the sensitivity of the transducer, varying its length, volume of water, and positioning. The transducer placement experiments were conducted on two participants based on two criteria: 1) Visual observation of the transducer signal to verify the occurrence of heartbeats in the BCG signal, and 2) A reliability index based on the percentage of heartbeats effectively detected by the system. Additional testing on a diverse group of six participants (ranging in age and body type) was performed to validate the transducer arrangement proposed. Results showed that the system was able to capture the occurrence of heartbeats for seven out of eight participants.

The BCG signals captured by the new transducer arrangement were tested to explore a new approach for detecting individual heartbeats using the k-means clustering algorithm and features extracted from the BCG signal. The performance criteria used in the evaluation was the percentage of correct detection of heartbeats derived from the confusion matrix. The percentage of correct detection for five ballistocardiogram signals acquired from different body types, tested in the laboratory setting with a coil spring mattress were in the range of 91.X% to 99.7%. When tested in residential living with an air mattress, the results were 83.3% which indicate the need for further investigation in feature selection and machine learning.

Finally, the Windowed Peak to Peak Deviation (WPPD) algorithm and the new approach for detecting heartbeats using the k-means algorithm were compared to the Ground Truth signal by computing the beat-to-beat distance and the heart rate.

Chapter 1

Introduction

1.1 Problem statement

There is a growing awareness of the need for new ways to improve the well-being of older adults at home.Technology use and advances in wireless and wired communications may serve as a strategy to extend independence and provide the means for home monitoring. Taking advantage of this, TigerPlace, a retirement community especially designed to help residents age in place, provides in-home monitoring through sensor networks installed in the apartments of volunteer residents. An important component of this integrated sensor network is the bed sensor system, which was installed in 40 apartments [4]. The bed sensor transducer is a pneumatic strip placed on top of the bed mattress, underneath the bed linens, that captures heartbeat, respiration and restlessness and reports them in a qualitative way [5]. Heart and respiration rates are reported as low, normal and high while bed restlessness is reported as one of four levels, depending on the duration of body motion. The need for quantitative measures of heart and respiration along with noninvasive monitoring motivated the development of a new transducer [6] (which is filled with water and placed under the mattress) and a new algorithm for extracting the heartbeats from the Ballistocardiogram (BCG) signal.
So far the Hydraulic Bed Sensor (HBS) system has reported promising results in detecting heartbeat and respiration, using the Windowed-Peak-to-Peak deviation (WPPD) algorithm for extracting heartbeats. Recent results reported in [1] suggest the devel-

opment of a tuning stage for two parameters, the window size (ws) used when the WPPD signal is being computed and the cutoff frequency (fc2) used for the lowpass filter WPPD signal.

1.2 Approach and contribution

This work reviews the results presented in [1] and addresses the specific problem of 1) finding a transducer arrangement capable of capturing heartbeat signals from different body types and 2) developing a new approach for detecting individual heartbeats in the BCG signal using clustering techniques.

In order to determine a transducer arrangement robust enough to capture the occurrence of heartbeat in the ballistocardiogram (BCG) signal from different body types, different volumes of water, lengths and transducer positioning were tested, in the attempt to increase its sensitivity. A new algorithm called VFM peak detection was developed for scoring the percentage of valid, false and missed peaks detected on the WPPD signal compared to a Ground Truth (GT) signal. The selection of the transducer arrangement was conducted in a laboratory setting on two participants and then validated on 1) five other participants and 2) a Tiger Place resident.

Once the selection process of the transducer arrangement was completed, a new approach for heartbeat detection on the BCG signal using the k-means algorithm (HbD-KM) was presented. The preliminary results for heart rate estimation and number of heartbeats detected were compared to the WPPD results in order to observe their effectiveness with respect to the GT signal.

Chapter 2

Related Work and Background

2.1 Related work

2.1.1 Eldercare and in-home monitoring

Technology is being applied across many environments to help older adults. Sensors, video, and telecommunications are being engineered into their homes to help caregivers monitor their well-being and support their everyday activities. In this sense, considerable research efforts have been focused towards in-home monitoring, where 24/7 monitoring of health and activities is intended to reduce emergency events and make efficient management of existing conditions [7]. Technology use will also facilitate the detection of early signs of illness, rapid intervention to health changes and/or decline, supporting the desire to maintain independence in their own homes, which is routinely identified as a passionate priority for people as they age [8].

2.1.2 Noninvasive long-term monitoring of heartbeat, respiration and body motion

2.1.2.1 Ballistocardiography

Ballistocardiography is a technique that measures the mechanical activity of the heart and produces a graphical representation (Ballistocardiogram) of repetitive motions of

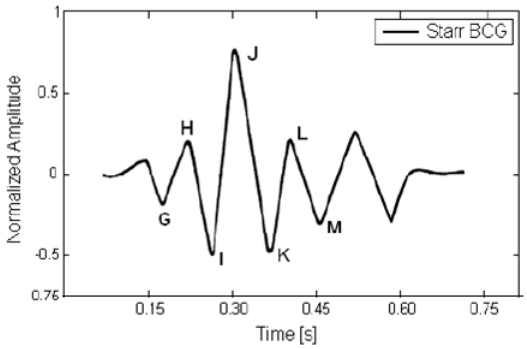

Figure 2.1: BCG Waves

the human body arising from the sudden ejection of blood into the great vessels with each heart beat [9]. These mechanical motions due to cardiac and hemodynamic events can be recorded from multiple locations and with multiple types of sensors leading to a confusing number of techniques and signals, sometimes related, sometimes not [10]. For this reason, the Scarborough-Talbot Report approved by the Committee on Ballistocardiographic Terminology decided to keep the terminology of the ballistocardiogram waves proposed by Starr (Figure 2.1), which is described below.

Ballistocardiogram Waves The ballistocardiogram waves may be separated in three major groups, the pre-systolic (frequently disregarded), the systolic and the diastolic [3].

Pre-Systolic Group

- F wave: (rarely seen) headward wave preceding G, related to pre-systolic events, not an after-vibration.
- G wave: small footward wave which at times precedes the H wave.

Systolic Waves

- H wave: headward deflection that begins close to the peak of the R wave (from the electrocardiogram) – maximum peak synchronously or near the start of ejection.

- I wave: footward deflection that follows the H wave, occurs early in systole.
- J wave: largest headward wave that immediately follows the I wave, occurs late in systole.
- K wave: footward wave following J, occurs before the end of systole.

The I and J waves are also referred to as ejection waves.

Diastolic Waves

- L and N waves: two smaller headward deflections which usually follow K.
- M wave: footward deflection between L and N.
- Smaller subsequent waves may be visible, and are named in sequence.

2.1.2.2 Monitoring heartbeat, respiration and restlessness

Several researchers are developing approaches to monitor vital signals using BCG, due to recent technological improvements, namely in the field of piezoelectric sensors [3]. This technique is promising when considering noninvasive long-term monitoring and especially sleep monitoring, that it is why, new systems and digital signal processing techniques intend to measure heartbeat, respiration, body motion and positioning as accurate as possible, in order to detect changes and capture patterns. Some of these systems are briefly described below.

1) Watanabe et al. [11] developed a noninvasive pneumatics-based system capable of measuring heartbeat through a thin, air-sealed cushion placed under the bed mattress, and compute heart rate by applying simple Fast Fourrier Transform (FFT), achieving a 94.7% of correct detection and 100% when segments with high content of noise , due to body motion, are not being considered in the computation. Additional measures for respiration, snoring, and body movements were computed..

2) Zhu et al. [12] designed a system placed under the pillow, which can noninvasively extract effectively heartbeat and respiration in real time. It is composed of two incompressible vinyl tubes, filled with water in a preloaded internal pressure of 3

kPa and sandwiched between two acrylic boards, separated 13 cm to each other. It uses a Wavelet Transformation (WT) for the estimation of heart rate and respiration rhythm. The sensitivity and positive predictivity reached compared to an piezoelectric device were 99.17% and 98.53%, respectively. Similarly, for respiration rhythm, compared with detections from nasal thermistor signals, results were 95.63% and 95.42%, respectively.

3) Mack et al. [5] proposed a system that uses noninvasive analysis of physiological signals (NAPS), developed to measure heart rate, breathing rate, and musculoskeletal movement. The system measurements of heart rate and breathing rate accurately detected heartbeat, averaged over the prescribed 30-s epochs, to within less than 2.72 beats per minute of ECG, and accurately detected breathing rate, averaged over the same epochs, to within 2.10 breaths per minute of RIP bands used in polysomnography. This system has already proven useful as a qualitative sleep assessment tool in an assisted living environment, and shows promise as a general sleep analysis tool for elderly living environments [4].

4) Bruser et al. [2] implemented a system consisted of a single sensing unit which was attached to one of the slats in a slatted bed frame. The sensing unit was composed of four strain gauges which formed a full Wheatstone bridge, glued to the center of the slat to measure its deformation. It presents and approach that autonomously learns and detects BCG peak patterns corresponding to individual heartbeats, using a modified version of the k-means algorithm. It computes the heart rate based on the beat-to-beat distance. Its effectiveness detecting heartbeats reached correct detection of 96.87%, false negatives:0.28% and false positives:0.13%. It also reports a beat-to-beat interval error of 14.16 ms and the mean heart rate error of 0.39 bpm averaged over 10 s long epochs.

5) Beattie et al. [13]presented a method of predicting the position of an individual lying on the bed using load cells placed under each of the bed supports to detect and monitor patients with sleep apnea. They found that sleeping position may alter the characteristic respiration signal detected by the load cells. Four positions were detected (back, right, left, stomach) by computing the means of the angle of displacement for

each breath in the center of pressure (of the weight on the bed) signal.

The computation of the beat-to-beat interval, based on the detection of the heartbeats in the BCG signal is also proposed by [5]. The technique consists of isolating individual BCG waves by examining changes in the relative positions of any local minima in the waveform. This is implemented using different imposed upper limit levels for the heart rate, starting with a beat-to-beat period of one-third of a second (corresponding to 180 beats per minute) and continuing by consistently incrementing the period by one-twentieth of a second to a final upper limit corresponding to approximately 80 beats per minute. The heart rate is reported only if the values reported are consistent across the majority of the nine readings. Unlike Mack et al. [5], that compute the beat-beat distance to estimate the heart rate, but does not report the intervals for further analysis, Bruse et al. [2] present an approach that estimates the location of the heartbeat and uses this information to compute the beat-to-beat interval , which opens the possibility for a Heart Rate Variability (HRV) analysis.

If the criteria of comfort and practical installation is evaluated, the systems presented in [5] and [12] may generate discomfort for the user and introduce additional artifacts if the transducers are not kept in the same position, which for [11] and [2] is not an issue.

Although the measure of heartbeat and respiration is an important functionality for a bed sensor, the BCG signal waveform can help to identify cardiac conditions. Xinsheng et al. [14] proposed an automatic BCG-signal classification algorithm based on artificial neural networks (ANNs). It uses the BCG signal to determine whether a person suffers from a cardiac condition. It uses a fast wavelet transform program to decompose the BCG signal into a prototype wavelet with its scaled and shifted versions. Then the small approximated signal which still has the significant information is presented to the neural network classifier. The algorithm classified normal condition, hypertension and heat attack risk; the classification results of wavelet coefficients reached 95.39 % of correct classification.

Additional considerations about the position of the person on the bed can help to estimate a complete sleeping pattern [7]. Gaddam et al. [15] developed a bed sensor

based on force sensors placed under the four legs of a bed. The system does not provide heart or respiration rates but it can estimate the person's position on the bed. This is achieved by estimating the position of the actual loading points enabling the system to detect the person's position. Initial test results reported an error within 2 and 10 % and it is envisaged that it will be extended to detect abnormalities in sleeping pattern.

Nukaya et al. [16]proposed a bed sensor system, consisted of piezoceramics bonded to stainless steel plates placed beneath each of the four legs of the bed. The system detects heartbeat, respiration, body movement, position change and scratching motion of a person lying on the bed. Heartbeat can be extracted from any of the piezoceramics, by band-pass filtering the signal using a bandwidth ranging from 3 to 7 Hz, full-wave rectified and low-pass filtered at a moving average of 150 points. Graphs shows the correlation between the signal extracted and the pulse oximetering used as reference. The detection of the person's position was demonstrated by showing the contribution of each piezoceramic device when different movements and postures were tested.

2.2 Background

2.2.1 Network sensors at TigerPlace (Columbia, MO)

TigerPlace, an active retirement community developed by Americare in affiliation with the MU Sinclair School of Nursing [17] and the Center for Elder care and Rehabilitation Technology at the University of Missouri have been working on maintaining and improving the quality of life of their residents. Sensor networks have been installed in the apartments of volunteer residents in order to support in-home monitoring for the purpose of capturing activity patterns using passive sensing. Changes in these patterns may indicate declining health [18]. These changes are compared to changes in the health conditions as part of ongoing research to develop early illness recognition methods. To date, over forty sensor networks have been installed in homes of elderly residents [4].

The integrated sensor network include a bed sensor developed by colleagues at the University of Virginia [5]. It is a pneumatic strip placed on top of the bed mattress,

underneath the bed linens, that captures qualitative heartbeat and respiration as well as restlessness in the bed. Bed restlessness is reported as one of four levels, depending on the time for continuous movement, while heart and respiration rate are reported as low, normal and high. The need for quantitative measure of heart rate and respiration motivated the development of a new transducer along with a new algorithm for detecting heartbeats and computing heart rate [6]. The next section describes briefly the hydraulic bed sensor (HBS) system and the algorithm developed for detecting heartbeats.

2.2.2 Hydraulic bed sensor (HBS)

The transducer construction and improvements are described in [6] and [1] respectively. The criteria used was: comfort for the user, practical installation and watertight durability. The HBS system is shown in Figure 2.2

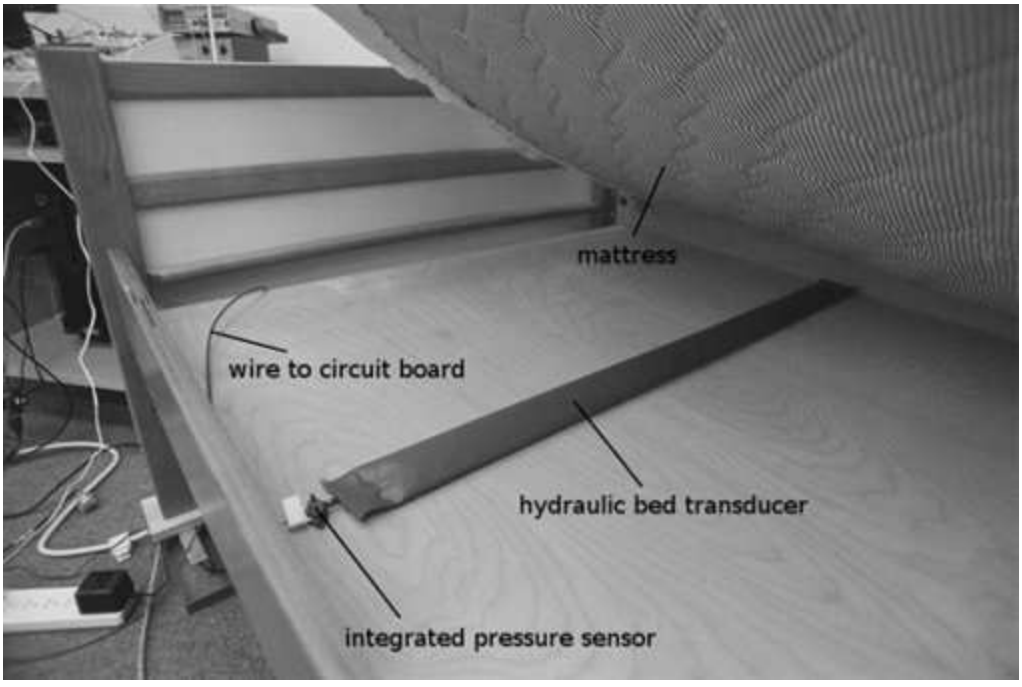

Figure 2.2: Hydraulic Bed Sensor (HBS) System

The transducer output is connected to a pressure sensor [19], which in turn goes to an Amplification/Filtering card (AFC) shown below in figure 2.3. The AFC amplifies

the transducer output (voltage ranging between 0 and 5 volts) by a factor of 10 using an inverting operational amplifier circuit (741 op-amp [20]). Then an 8th-order integrated Bessel Lowpass Filter (Maxim MAX7401 [21]) with a corner frequency of 38 Hz suppresses the high frequency noise in the amplifier's output. This LPF output is fed to a 12-bit Analog-to Digital converter (ADC) at sampling rate of 100 Hz [1].

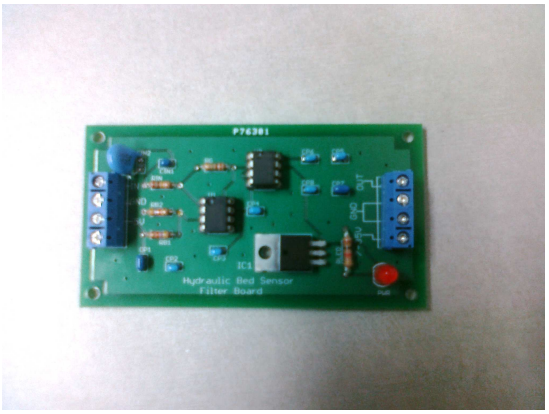

Figure 2.3: Amplification/Filtering Card

Signal processing - Heartbeat detection using Windowed Peak to Peak deviation (WPPD)

Heise et al. [1] show that heartbeats can be extracted from the BCG signal by computing the windowed Peak-to-Peak Deviation (WPPD). The WPPD signal is computed by finding the difference between the most negative and the most positive within a sliding window as in equation (2.1).

$$WPPD(t) = MAX_i^{i+ws}[signal(i)] - MIN_i^{i+ws}[signal(i)] \ ... \ (2.1)$$

Figure 2.4 shows the effectiveness of the WPPD algorithm in extracting the heartbeats.

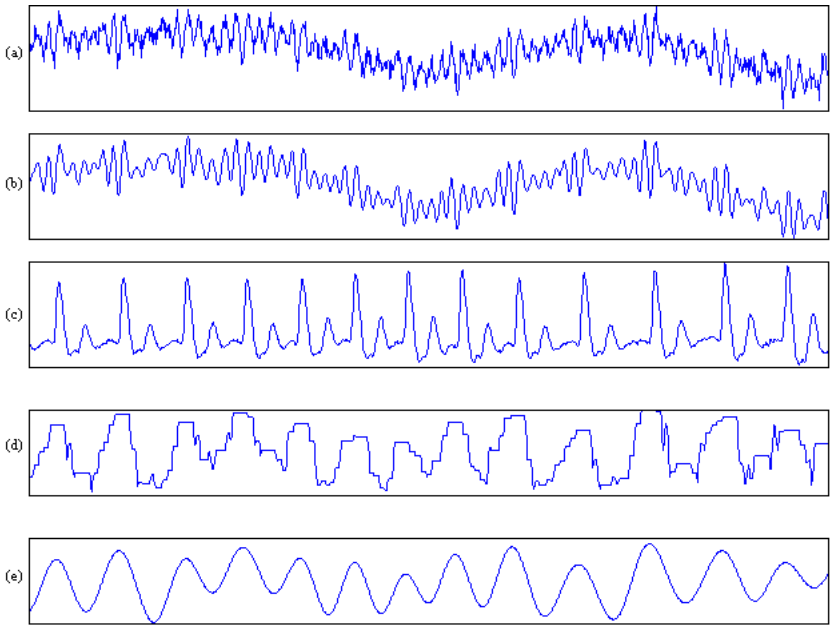

Figure 2.4: Ten-second data segment being processed using WPPD algorithm Figure extracted from [6]). (a) shows ten seconds of the signal coming from the ADC, (b) shows the signal after 10 Hz lowpass filtering, (c) shows the corresponding Ground Truth signal coming from the piezoresistive pulse sensor, (d) shows the WPPD signal for a window size (ws) of 250 ms (or 25 samples) and (e) shows the WPPD signal after 2 Hz lowpass filtering.

Heart rate computation

The algorithm for computing heart rate counts the number of the peaks (heartbeats) over 15-second (non-overlapping) segments and multiplies the count by 4 in order to get a measure expressed in beats per minute (bpm).

2.2.3 Limitations of the HBS system

The evaluation trial presented in [1] studied the performance of the HBS system compared to a GT signal [22], when two parameters of the WPPD algorithm were varied. These parameters were the window size (ws) used when the WPPD signal is being computed and the cutoff frequency (fc2) used for lowpass filter the WPPD signal. The ws&fc2 combination proposed in [6] was ws=25 and fc2=2 Hz . The new values tested

in [1] were ws=[15, 25, 40, 60] and fc2=[1, 1.5, 2]. The data was collected over 10 minutes, in which each subject was asked to lie on his/her back for two minutes, turn to the right side for two minutes, return to the back for two minutes, turn to the left side for two minutes, and finally return to the back for a final two minutes (approximately ten minutes in total). The HBS signal is illustrated in Figure 2.5.

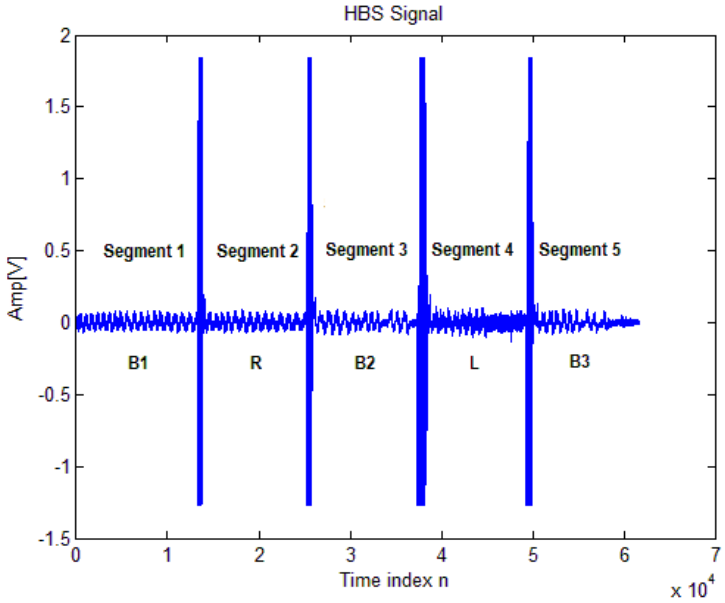

Figure 2.5: Ten minute segment-Evaluation trial [1]
Transients indicate bed motion, while the relatively flat sections show the subject following the pattern of the experiment (back (B1), right side (R), back (B2), left side (L), back (B3).

Results from this study conducted on five subjects as shown in Table 2.1, indicate that the heartbeat detection, if the right combination of parameters is chosen, can be accurate to within 8 beats per minute up to 97.5% of the time.

	Gender	Age	Weight [kg]	Height [cm]	Prior cardiac history
Subject #1	male	24	113	183	No
Subject #2	male	30	79	187	No
Subject #3	female	31	53	163	Yes
Subject #4	female	56	68	163	No
Subject #5	male	67	76	177	Yes

Table 2.1: Participants for [1]

Then the problem would be to find the combination of ws&fc2 that can lead to the correct estimation of number of heartbeats detected using the WPPD algorithm. If so, which would be the criteria for choosing the values for ws and fc2?

Before answering this question, data collected for this evaluation trial were processed again. This time, instead of segmenting the HBS signal into 15-second segments for reporting the number of heartbeats detected, the count was performed over the whole signal. Table 2.2, which corresponds to the data collected from Subject 5, shows the count of heartbeats for four different window sizes (ws) and three cutoff frequencies (fc2) used to smooth the WPPD signal.

B1	# hb GT=126		
# hb HBS			
ws \fc2	1 Hz	1.5 Hz	2 Hz
15	106	125	141
25	105	124	135
40	101	120	129
60	98	117	134

(a) Segment 1-B1

R	# hb GT=79		
# hb HBS			
ws \fc2	1 Hz	1.5 Hz	2 Hz
15	62	78	132
25	61	81	120
40	59	81	120
60	51	74	94

(b) Segment 2-R

B2	# hb GT=96		
# hb HBS			
ws\ fc2	1 Hz	1.5 Hz	2 Hz
15	70	97	133
25	67	97	133
40	66	91	115
60	59	82	110

(c) Segment 3-B2

L	# hb GT=68		
# hb HBS			
ws \fc2	1 Hz	1.5 Hz	2 Hz
15	50	68	80
25	49	69	73
40	48	66	69
60	46	59	72

(d) Segment 4-L

B3	# hb GT=85		
# hb HBS			
ws \fc2	1 Hz	1.5 Hz	2 Hz
15	70	84	89
25	69	84	87
40	65	83	83
60	55	78	96

(e) Segment 5-B3

Table 2.2: Number of Heartbeats computed for twelve combinations of window sizes (ws) and cutoff frequencies (fc2), for segments B1, R, B2, L, B3, from the signal shown in Figure 2.5.
(a) 2-minute segment where subject 5 was asked to lie on his back. (b) 2-minute segment when subject 5 was asked to lie on his right side (c) 2-minute segment when subject 5 was asked to lie on his back (d) 2-minute segment when subject 5 was asked to lie on his left side (e) 2-minute segment when subject 5 was asked to lie on his back
.

The results shown in Table 2.2 correspond to the segments B1, L, B2, R and B3 shown in Figure 2.5. The ws&fc2 combination closer or equal to the heartbeat count scored by the GT signal for the first two minutes, segment B1, is not the same for the one that gives a better estimate for the next 2-minute segments, and so on. To get a better

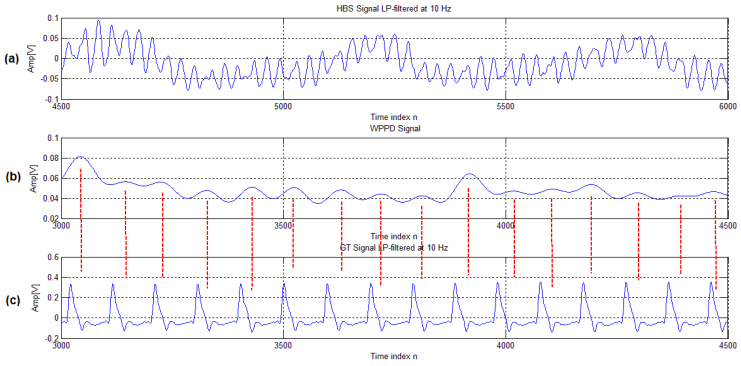

Figure 2.6: Fifteen-second data segment being processed to extract heartbeats using the WPPD algorithm
(a) shows the signal after 10 Hz lowpass filtering, (b) shows the WPPD signal computed using a ws = 15 and fc2 = 1 Hz; and (c) shows the corresponding signal from the piezoresistive pulse sensor, used as ground truth for showing heartbeats.

understanding of what is the effect of using these different combinations in the WPPD algorithm, plots for these combinations were generated and are shown in Appendix 6.2. From Figures in Appendix A.1 the WPPD signal is generated for ws=[15,25,40,60] and fc2=[1,1.5,2]. The WPPD algorithm seems to extract the heartbeats in a consistent way for all the ws&fc2 combinations. Two of these combinations are presented below in Figures 2.7 and 2.6, where (b) and (c), for both cases, show that a shift with respect to the GT signal, is introduced in the location of most of the peaks. They also show that for Figure 2.7 an additional peak that does not line up with the GT signal is present.

In addition to the WPPD peaks that do not line up to the GT signal, Figures in Appendix A.1, show that some peaks get missed for some combinations.

Observation 1: Since the heartbeat counter considers all the peaks generated by the WPPD algorithm as heartbeats, then it is necessary to implement an automated algorithm able to identify whether the peak is a heartbeat or a false peak. The appearance of false peaks can be related to noise or body motion.

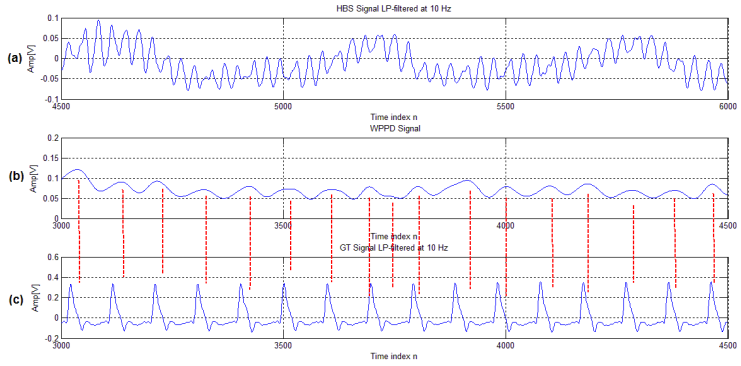

Figure 2.7: Fifteen-second data segment being processed to extract heartbeats using the WPPD algorithm
(a) shows the signal after 10 Hz lowpass filtering, (b) shows the WPPD signal computed using a ws = 40 and fc2 = 2 Hz; and (c) shows the corresponding signal from the piezoresistive pulse sensor, used as ground truth for showing heartbeats.

Looking at the data shown in Appendix A.2 and A.3, after lowpass filtering at 10 Hz the HBS signals at 10 Hz, only three 15-second segments for subject 2 and five 15-second-segment for subject 4, showed the occurrence of heartbeats, characterized by a pattern that lines up with the GT signal. For all figures (a) shows the HBS signal after lowpass filtering at 10 Hz and (b) shows the GT signal. The number of heartbeats from HBS and GT signals were counted by visual observation and are displayed in the upper right of (a) and (b). HBS signals captured from subject 1, 3 and 5, did not show the presence of heartbeats for any of the 15-second segments of the trial.
This shows that for some of the participants (subject 2 and subject 4) the transducer was able to capture heartbeat for only short periods of time. This may be due to the variation on age, weight, height and prior cardiac conditions reported. For instance, body type characterized by the subject's weight and height will vary the pressure applied to the transducer in different proportions. The Subject's height will determine the distance between the heart and the transducer.

Observation 2: The observation of the data captured by the transducer after lowpass filtering at 10 Hz showed that the system is not capturing heartbeat signals for all the subjects, and may therefore require modifications on the transducer construction and positioning.

Chapter 3

Methodology

As was shown in Section 2.2.3, a transducer arrangement capable of capturing the occurrence of a heartbeat from different body types is needed. To address this, different lengths, volumes of water, positions and number of transducers were tested, in order to improve the sensitivity of the transducer.

The analysis used to assess the different transducer placement was based on two criteria:

1. Comparison of the Windowed Peak to Peak Deviation (WPPD) signal computed from the transducers and the WPPD signal computed from the Ground Truth (GT), in terms of percentage of valid peaks and false peaks.

2. Visual observation of the transducer signal after lowpass filtering at 10 Hz, to verify the occurrence of heartbeats in the BCG signal.

Once the selection process was concluded, Sections 3.3 and 3.4 present a system overview along with an approach for computing heart rate using the k-means algorithm to find the location of the heartbeat on HBS signal.

3.1 Selection process of the transducer placement on the bed

This section describes the methodology followed for finding a robust arrangement capable of capturing heartbeat and respiration from different body types. To achieve this goal, different lengths, volumes of water, positions and number of transducers

were tested to improve the sensitivity of the transducer, as was suggested by [6]. The following series of experiments were intended to determine a transducer arrangement capable of capturing heartbeats and to identify the region of the bed where this arrangement remains sensitive enough to detect them.

3.1.1 Laboratory setting

The testing was performed using a twin-sized coil spring mattress with a height of 7 inches. The following procedure was carried out to determine and validate the arrangement.

1. Transducer arrangement selection-Testing group 1: Two subjects were tested for five different configurations. They were asked to lie down on their backs while the data was acquired. Two consecutive readings of 2.5 minutes were taken for every configuration to check its repeatability.The signal captured from the transducers was correlated to the MLT1010 Pulse Transducer [22]described in Section 3.1.2, which was used as a ground truth for the heartbeat. Observation of the HBS signal after lowpass filtering at 10 Hz and algorithms for scoring the performance of each transducer arrangement were run in order to determine the system's ability for capturing heartbeats. The main objective of these experiments were to determine a transducer arrangement suitable for both of them.

2. Transducer arrangement validation-Testing group 2: Five subjects were tested for the transducer arrangement selected. They also were asked lie down on their backs for 2.5 minutes for two consecutive readings.The signal captured from the transducers was correlated to the pulse signal captured by the pulse piezoelectric device worn for the participant (MLT1010 Pulse Transducer [22]). Observation of the HBS signal, LPF at 10 Hz and algorithms for scoring the performance were run in order to determine the system ability for capturing heartbeats.

3.Validating the transducer arrangement-Testing group 3: Three participants from the testing group of [1]were tested for the transducer arrangement selected. They

were asked to repeat the protocol used in [1], where the data were collected over 10 minutes, in which each subject was asked to lie on the back for two minutes, turn to the right side for two minutes, return to the back for two minutes, turn to the left side for two minutes, and finally return to the back for a final two minutes.The signal captured from the transducers was correlated to the MLT1010 Pulse Transducer. Observation of the HBS signal, LPF at 10 Hz and algorithms for scoring the performance were run in order to determine the system's ability for capturing heartbeats.

3.1.1.1 Testing groups

The information about the participants is listed in Tables 3.1 , 3.2 and 3.3 for testing group 1, testing group 2 and testing group 3.

Testing group 1

	Gender	Age	Weight [kg]	Height [cm]	Prior Cardiac History
Subject # 1(*)	Female	32	53.0	163	Yes
Subject # 2	Male	32	86.4	173	No

Table 3.1: Testing Group 1
(*)Subject#1 is Subject#3 in the testing group of [1]

Testing group 2

	Gender	Age	Weight [kg]	Height [cm]	Prior Cardiac History
Subject # 1	Male	24	86.0	180	No
Subject # 2	Male	26	63.6	170	No
Subject # 3	Female	30	58.0	160	No
Subject # 4	Male	32	86.4	173	No
Subject # 5	Female	32	53.0	163	Yes

Table 3.2: Testing Group 2

Testing group 3

	Gender	Age	Weight [kg]	Height [cm]	Prior cardiac history
Subject #1	male	24	113	183	No
Subject #3	female	31	53	163	Yes
Subject #4	female	56	68	163	No

Table 3.3: Testing Group 3-Participants for [1]

3.1.1.2 Experiment protocol

Subjects from testing group 1 and 2 described in Tables 3.1 and 3.2, respectively, lay for periods of two minutes on their backs. Piezoelectric pulse sensor worn on the finger (Heartbeat Ground Truth), which is kept in place using using a velcro strip around the finger.

Subjects from testing group 3 described in Table 3.3, lay for periods of two minutes on their backs, right side, back, left side, and back again. Piezoelectric pulse sensor worn on the finger.

3.1.1.3 Transducer placement

Transducer - Length and Volume of water

The combinations of length and volume of water tested are shown in Table 3.4. All the transducers were built using the procedure and materials described in [1].

Combination Length&Volume	Length [in]	Vol [oz]	Percentage of fullness [%]
1	36.0	20	60
2	36.0	30	70
3	21.8	16	70

Table 3.4: Length and Volume Combinations
Percentage of fullness is estimated by measuring the length of the transducer filled with water divided by the full length of the transducer.

Transducer arrangements proposed

The transducer arrangements to be tested are described in Table 3.5 and shown in Figures 3.1, 3.2, 3.3 and 3.4.

HBS-Arrangement	No. of Transducer	Position	Figure	Distance to Headboard [in]				Distance to right side * [in]			
				T1	T2	T3	T4	T1	T2	T3	T4
1	4	H	3.1	7	12	18	24	0.2	0.2	0.2	0.2
2	2	T	3.2	15	16.5			8	19		
3	1	V	3.3	1,12 (**)				19			
4	4	V	3.4	2	2	2	2	8	15	22	29

Table 3.5: Transducer arrangements

H: Transducer(s) placed horizontally
V:Transducer(s) placed vertically
T: Combination of two transducers, one placed horizontally (T1) and the other placed vertically (T2)
(*) Distance to the right side of the bed
(**)The transducer was placed at 1 in first and then at 12 in, respectively to the bed headboard.

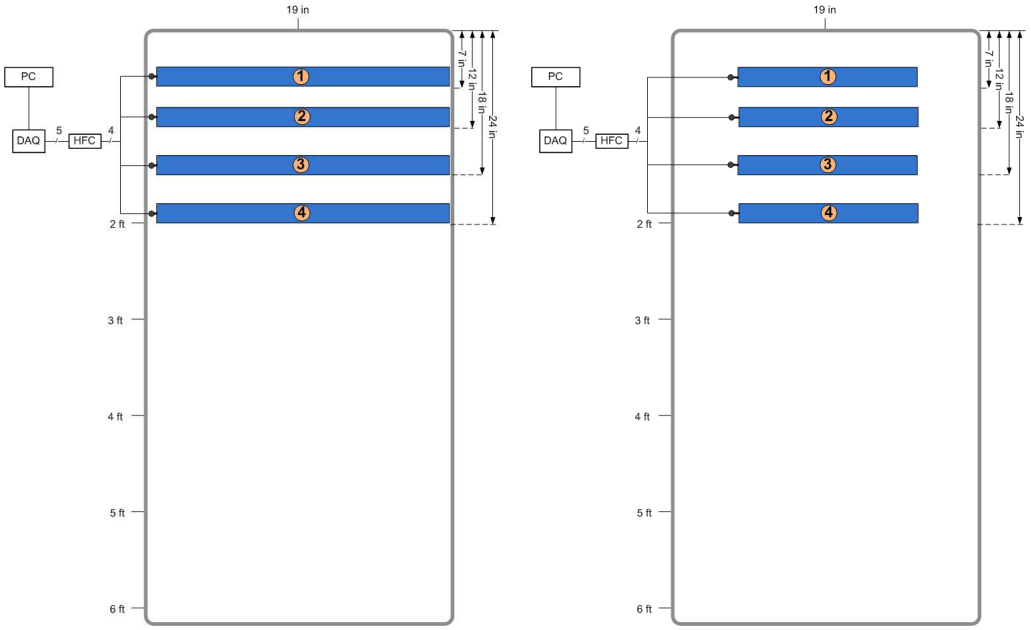

(a) Variation 1 (b) Variation 2

Figure 3.1: Transducer arrangement 1

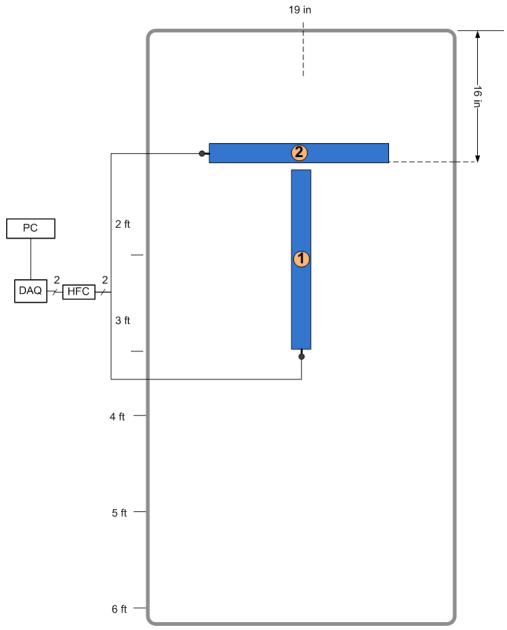

Figure 3.2: Transducer arrangement 2

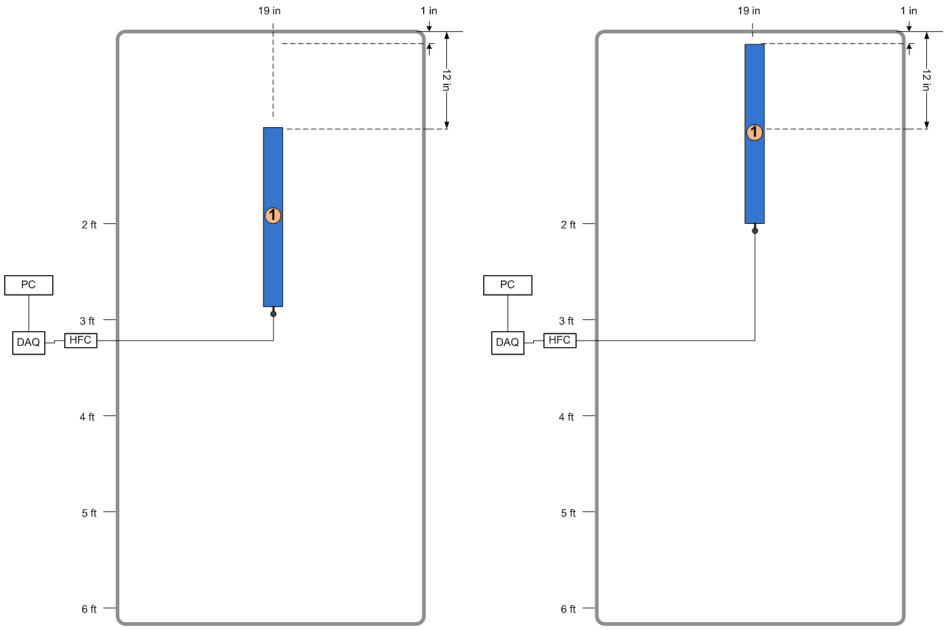

(a) Variation 1 (b) Variation 2

Figure 3.3: Transducer arrangement 3

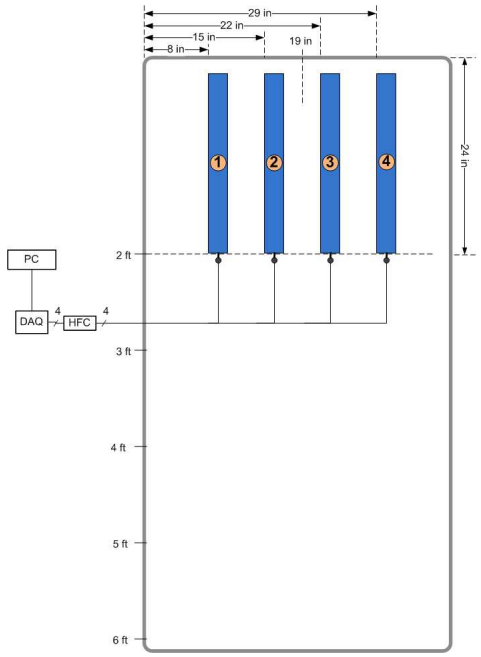

Figure 3.4: transducer arrangement 4

Experiments

Transducers (T1, T2, T3 and T4) were built the same way as described in [1]. Different lengths and volumes of water were combined; the combinations are shown in Table 3.4, along with different transducer arrangements. The arrangement positions are detailed on Table 3.5 and shown in Figures 3.1, 3.2, 3.3 and 3.4.

The experiments are listed in Table 3.6,

Exp	Combination Len&Vol	HBS Arrangement	No. of transducers	Testing. group
1	1	1	4	1
2	2	1	4	1
3	3	1	4	1
4	3	2	2	1
5	3	3	1	1
6	3	3	1	1
7	3	4	4	1
8	3	4	4	2
9	3	4	4	3

Table 3.6: List of Experiments

3.1.2 Ground Truth Signal

GT signal for validating the output of the hydraulic bed sensor is collected via a piezoelectric pulse sensor (MLT1010) [22] attached to the subject's finger. The MLT1010 Pulse Transducer uses a piezoelectric element to convert force applied to the active surface of the transducer into an electrical signal. In order for it to produce a signal, a change in force must be applied to the active surface of the transducer. Expansion and contraction of the finger circumference, due to changes in blood pressure, can be detected by the transducer. A typical output is 50-200 mV but can reach as high as 500 mV .

3.1.3 Scoring the performance

The criteria used for scoring the ability of the system for capturing heartbeat was based on:

1. Computation of the reliability index: Comparison of the WPPD signal computed from the transducers (HBS signal) and the WPPD signal computed from the GT signal, in terms of percentage of valid peaks and false peaks.

2. Visual observation of the transducer signal (HBS signal) after lowpass filtering at 10 Hz to verify the occurrence of heartbeats.

Section 3.1.3.1 describes the algorithm developed for obtaining the percentage of valid peaks (Peaks extracted from the HBS signal, computed using the WPPD algorithm that line up with the peaks extracted using the WPPD algorithm from the GT signal and false peaks.

3.1.3.1 Valid-False-Missed (VFM) peak detector

The erroneous estimation of number of heartbeats extracted applying the WPPD algorithm, presented in Section 2.2.3, show the need for developing an algorithm that compares one by one the peaks detected by the WPPD algorithm and the GT signal, in order to make a fair comparison between the HBS signal and GT signal. To automate the comparison between the HBS signal and the GT signal the algorithm applies the WPPD algorithm to the GT signal, using a ws=40 and fc2=1.5Hz.

VFM peak detector algorithm overview

As shown in Figure 3.5, the WPPD HBS signal presents some shifting with respect to the WPPD GT Signal. Although peaks 1 to 9 do not show a precise alignment to the WPPD GT, they seem to correlate; in this case, the VFM-peak detector will consider these peaks as "Valid Peaks". Continuing the analysis, peaks 10 and 11 do not show a clear correspondence to the WPPD GT signal; in this case the algorithm will consider the one that is closer to the WPPD GT signal as a "Valid peak " and the other as a "False peak".

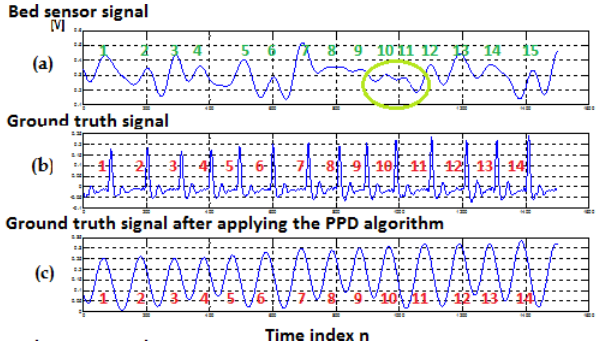

Figure 3.5: WPPD transducer signal computed using ws=25 and fc2=1.5. (a) is the transducer signal, (b) is the GT signal and (c) is the WPPD GT signal.

The algorithm works with the HBS and GT indexes computed from the WPPD HBS and WPPD GT signal, using the matlab function $findpeaks$. Each index corresponds to the location of an HBS peak, which is considered as a heartbeat. The peaks are represented by their locations or indexes. If the HBS peak lines up with the GT peak, it will be considered as a "valid" peak. But, due to the shifting observed on the WPPD HBS signal, an interval around the GT index was computed, allowing the HBS index some margin of shifting. In this sense, if the HBS index falls into the interval computed around its respective GT index, the HBS peak is considered as a "valid peak". If an HBS index falls outside the GT intervals, then it is considered as a "false" peak and if none of the HBS indexes fall into this interval then a "missed" peak will be reported.

For the algorithm to perform properly, an additional alignment stage is required, to ensure that the first HBS indexes tested are not a false peaks, in which case a wrong assignment will be carried along the whole HBS signal giving erroneous values. Therefore, the VP detector algorithm was designed with two main stages 1) the WPPD HBS and WPPD GT alignment and 2) the assignment of "Valid", "False" and "Missed " peaks.

WPPD HBS and WPPD GT alignment

The alignment between the WPPD HBS and WPPD GT signals uses one GT index at a time to determine whether the WPPD HBS and WPPD GT signals are aligned. The signals will be aligned when three WPPD HBS peaks fall into the intervals computed around three WPPD GT peaks. Some assumptions had to be made in order to perform the alignment and peaks assignment. These parameters are: 1) *min_5pts_dist*: Minimum distance between GT index and HBS index, 2) *Per_p2p_dist*: Percentage to be considered for computing the intervals around the GT index. For instance, if J_G^3 is the GT index and *Per_p2p_dist*=30 % , then the interval will be computed based on the distances to the GT indexes, $d1'$ and $d2'$; in this case, the interval will be delimited by [30 % * $d1'$, 30 % * $d2'$]. Figure 3.6 shows the alignment process in a graphical way.

(1) It starts computing the distance between the GT index J_G^2 and five consecutive HBS indexes $J_H^1, J_H^2, J_H^3, J_H^4, J_H^5$. If the minimum distance is less than *min_5pts_dist* then the HBS indexes are temporary aligned to J_G^2.

(2) Next the intervals around J_G^3, J_G^4 are computed and J_H^3, J_H^4 are tested to verify whether or not they fall into these intervals . If they fall into the intervals the temporary alignment becomes permanent.

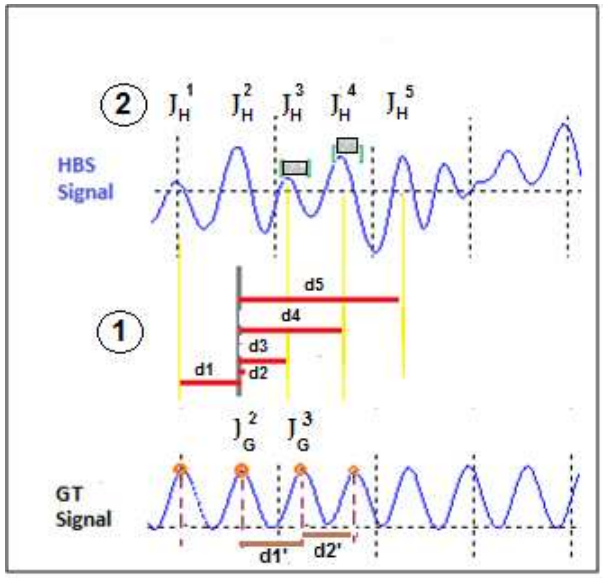

Figure 3.6: WPPD HBS and WPPD GT Alignment
J_G^2 : is the GT index corresponding to the second peak of the WPPD GT signal,
$J_H^1, J_H^2, J_H^3, J_H^4, J_H^5$: are HBS indexes,
$d1$: is the distance between J_G^2 and J_H^1, $d2$: is the distance between J_G^2 and J_H^2, $d3$: is the distance between J_G^2 and J_H^3 and so on,
$d1'$: is the distance between J_G^3 and J_G^2, $d2$': is the distance between J_G^3 and J_G^4.

The flow chart for the WPPD HBS and WPPD GT signal alignment is depicted in Figure 3.7.Variables such as *Align* are used to indicate whether the alignment was reached or not. If i *Align* = 0, then WPPD HBS and WPPD GT signals are not aligned and the next GT index has to be tested; if *Align* =1, then WPPD HBS and WPPD GT signals are aligned and the VFM Assignment starts and the alignment ends; contrary if *Align* = 3, then all of the GT indexes were evaluated and the WPPD HBS and WPPD GT signals could not be aligned.

The variable *iter* represents the number of elements (indexes) to be evaluated. Whereas *min_L* is the smallest number of elements between HBS and GT indexes.

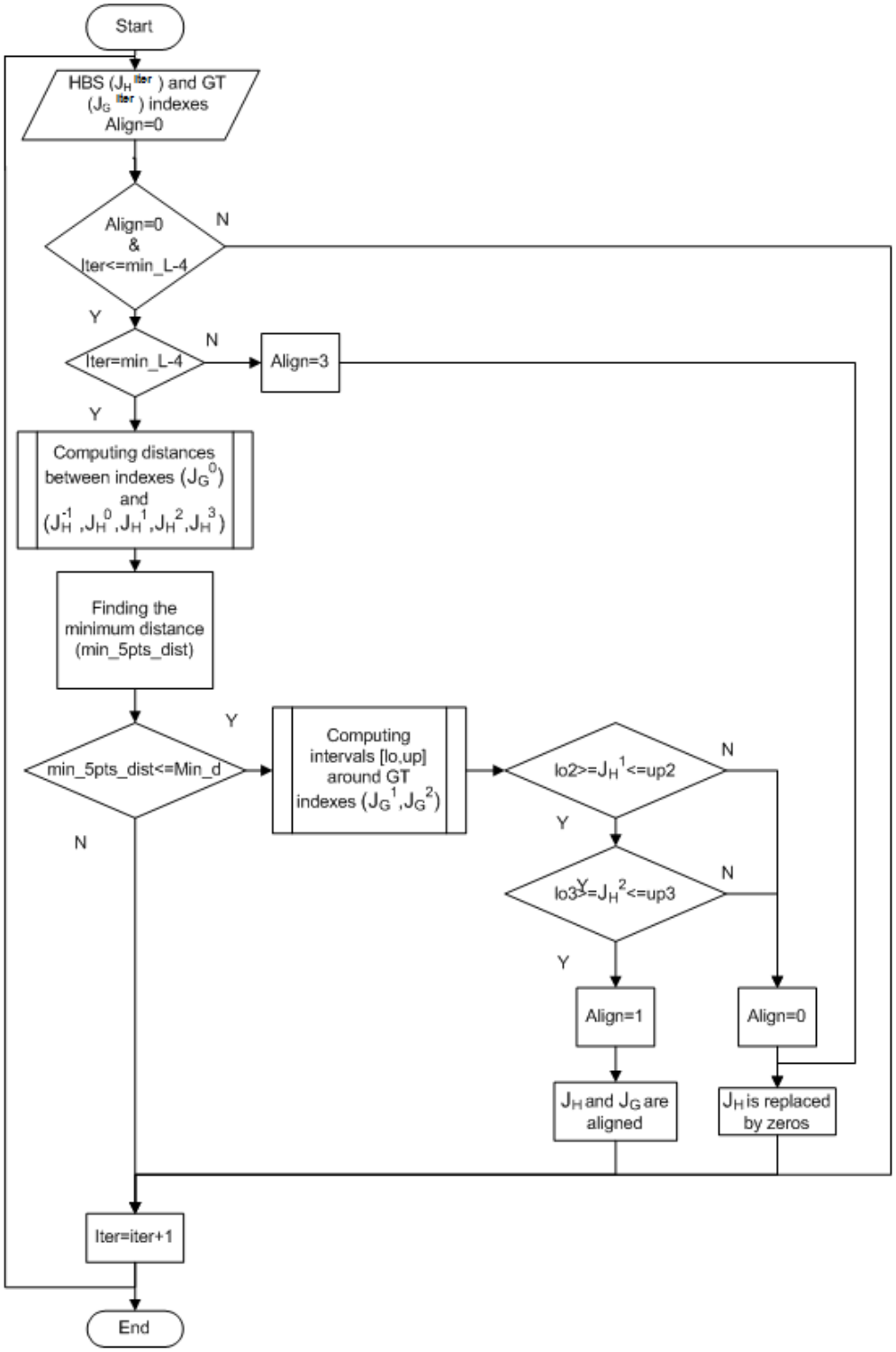

Figure 3.7: WPPD HBS and WPPD GT signal alignment flow chart

VFM (Valid-False-Missed) peak assignment

Once the alignment stage is done, the VFM assignment stage starts computing intervals around the GT indexes J_G. As explained above, the same procedure is used to compute the intervals around the GT indexes. Figure 3.8 shows the intervals generated for J_G^2 in order to determine whether the HBS peak J_H^2 is considered valid or false. In this case, the interval *[j+1]* will be computed using *d1*, *d2* and a percentage (*Per_p2p_dist*), where *lo2= Per_p2p_dist*d1* and *up2=Per_p2p_dist*d2*.

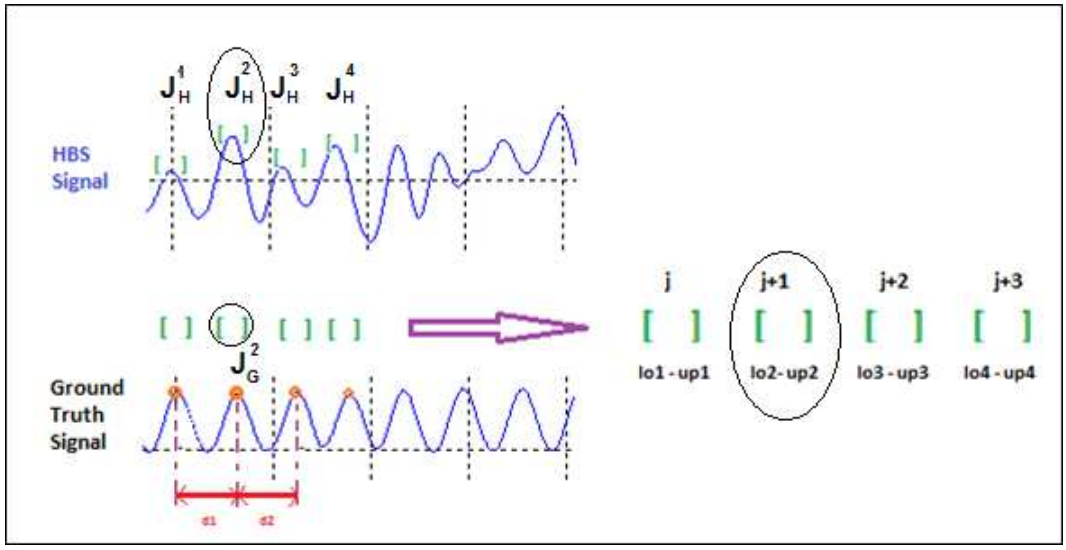

Figure 3.8: Intervals 1
J_G^2 : is the GT index corresponding to the second peak of the WPPD GT signal,
$J_H^1, J_H^2, J_H^3, J_H^4$: are HBS indexes,
$d1$: is the distance between J_G^2 and J_G^1, $d2$: is the distance between J_G^2 and J_G^3,
$[lo2, up2]$: interval computed around J_G^2 based on the $d1$ and $d2$,
$[lo1, up1]$, $[lo3, up3]$ and $[lo4, up4]$ are the intervals computed around J_G^1 , J_G^3 and J_G^4 respectively.

Once the intervals are computed, the algorithm will categorize the peaks into:

- Valid peaks: The HBS index falls into the interval computed around the GT index

- False peaks: The HBS index falls out of the interval computed around the GT index, if more than one HBS index falls into the interval, the closer index to the GT index will be considered as a valid peak and the rest as false peaks.

- Missed peaks:No HBS index falls into the interval computed around the GT index

Figure 3.9 shows an example in which the system reports a missed peak (M) for the first interval. It also identifies two false peaks (F) that fall between the first and second and the third and fourth intervals, respectively, and reports the ones that fall into the second, third, fourth and so on as valid peaks.

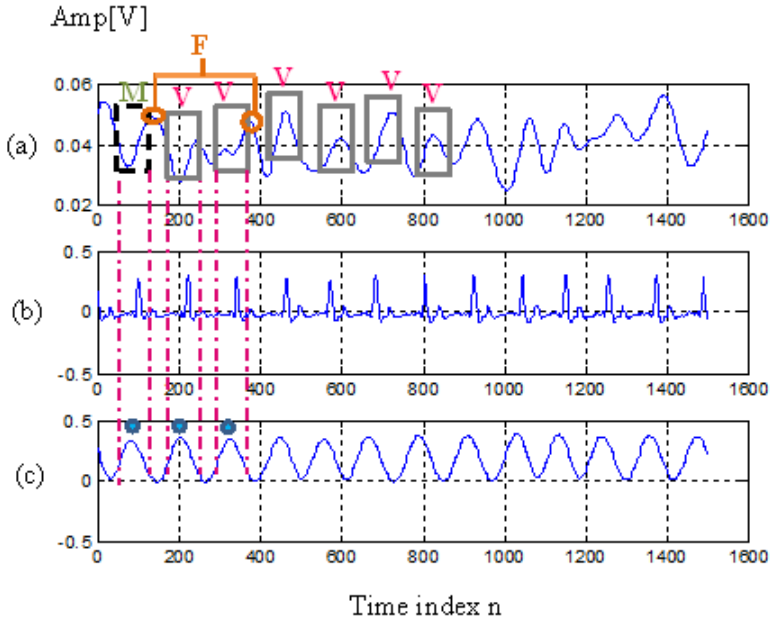

Figure 3.9: VFM Assignment
(a) is the HBS WPPD signal, (b) is the GT signal and (c) is the WPPD GT signal

The VFM assignment is described in the flow chart depicted in Figure 3.10,where *L_HBS* and *L_GT* are the lengths of the the vectors that contain the HBS and GT indexes and *"min_i2i"* is the difference between the indexes J_G^2 and J_H^2. If this distance is greater than *min_i2i*, the system outputs *0* for all the percentages of valid, false and missed peaks. If it is less than *min_i2i*, then the intervals are computed around the

GT J_G^2 indexes. Depending on whether the HBS indexJ_H^2 falls into the interval *[lo2, up2]*, three cases are considered. CASE 1 assumes J_H^2 is a valid peak and verifies this, computing the intervals for the next HBS indexes J_H^3, J_H^4. CASE 2 assumes J_H^2 is a false peak, because it falls outside the interval *[lo2, up2]*, and it is less than *lo2*; the analysis is then run on $J_H^3, J_H^4, J_H^5, J_H^6$. And CASE 3 verifies whether the index J_H^2 falls into the intervals *[lo3, up3]* or [*lo4,up4];* if it is greater than *up2* then a missed peak is reported.

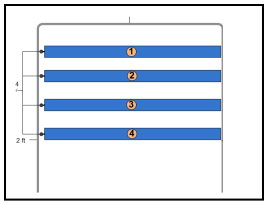

Figure 3.10: VFM Assignment flow chart

VFM peak detector demonstration

The VFM peak detector output creates a vector that contains the peaks categorized as valid and false (VF-vector), and another for the ones categorized as missed peaks (M-vector). Each HBS index is assigned to two possible values:

'2' if the HBS index is considered as a valid peak

'1' if the HBS index is considered as a false peak

The GT index is assigned to two values:

'-1' if there is no HBS index that falls into the intervals computed for the GT index

'0' if an HBS index falls into the interval.

Figure 3.11 shows the output of the VFM-peak detector.

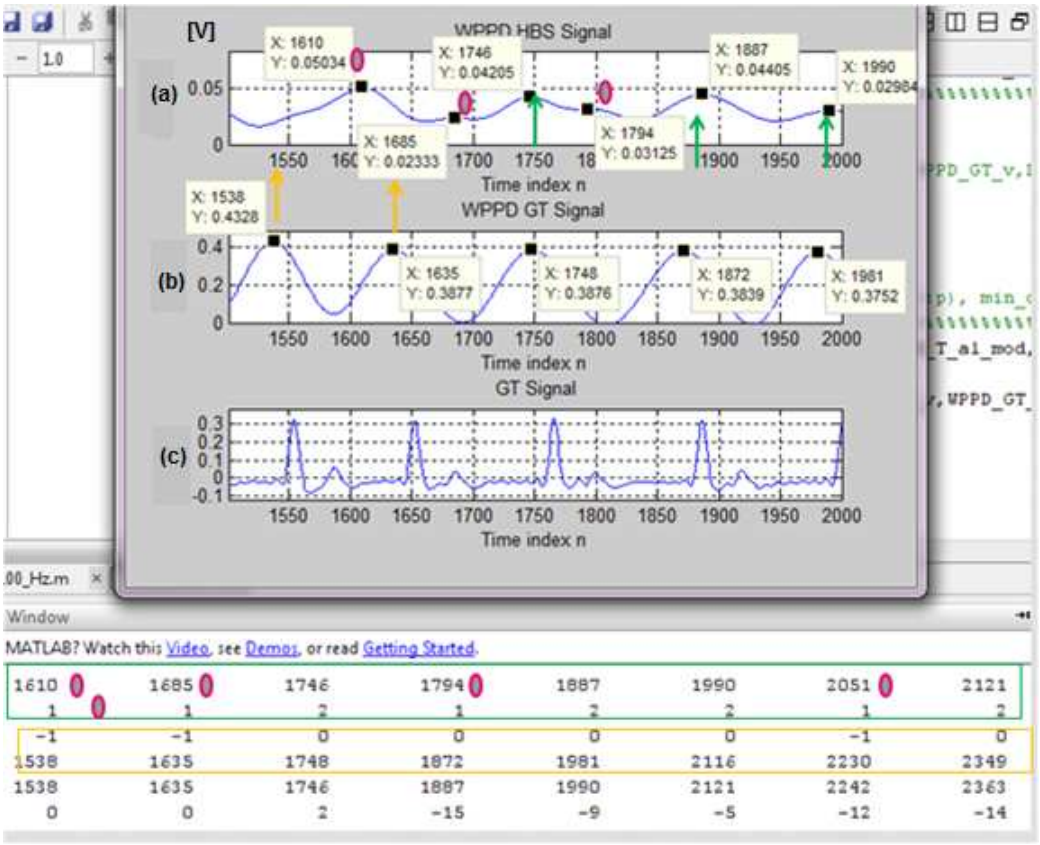

Figure 3.11: VFM-peak detector output
(a) and (b) are the WPPD signals for the HBS and GT signals and (c) shows the GT signal.
VFM-peak detector output: row 1 shows the HBS indexes, row 2 is the VF-vector, row 3 is the M-vector, row 4 shows the GT indexes, row 5 shows the HBS indexes and the auxiliary indexes computed when a missed peak is reported, finally row 6 shows the difference between the row 4 and 5, which is expected to be less than the value assigned to *min_i2i*.

For this five-second data, the HBS index 1610, 1685 and 1794 are assigned as false peaks (VF-vector=1); they have a red circle on top of them to show the shift with respect to the GT indexes. Indexes 1746, 1887, 1990 and 2121 are assigned as valid peaks (VF-vector=2); which is verified looking at (a) and (b) The M-vector assigns -1 to the GT indexes 1538 and 1635 indicating that the HBS signal does not have any index that falls into the intervals created for these three GT indexes.
Once the VFM peak detector is run, the VF-vector and M-vector are used to compute the percentages for Valid, False and Missed Peaks, which will be used to score the ability of the transducer for capturing heartbeats.

Limitations of the VFM peak detector

The VFM peak detector is not able to differentiate whether the HBS peak is produced by a movement or noise. If this peak falls into one of the intervals generated using the GT indexes, then it is considered as a valid peak. If the HBS signal presents a shift greater than the one considered for the interval computation, then the VFM peak detector will assign an output of 0 for the valid, false and missed peaks percentages, because the alignment stage will not be able to align the WPPD HBS and WPPD GT signals.

3.1.3.2 Data processing

All the data acquired from the transducer arrangements proposed in Section 3.1.1.3 were processed following the flow chart shown in Figure 3.12.

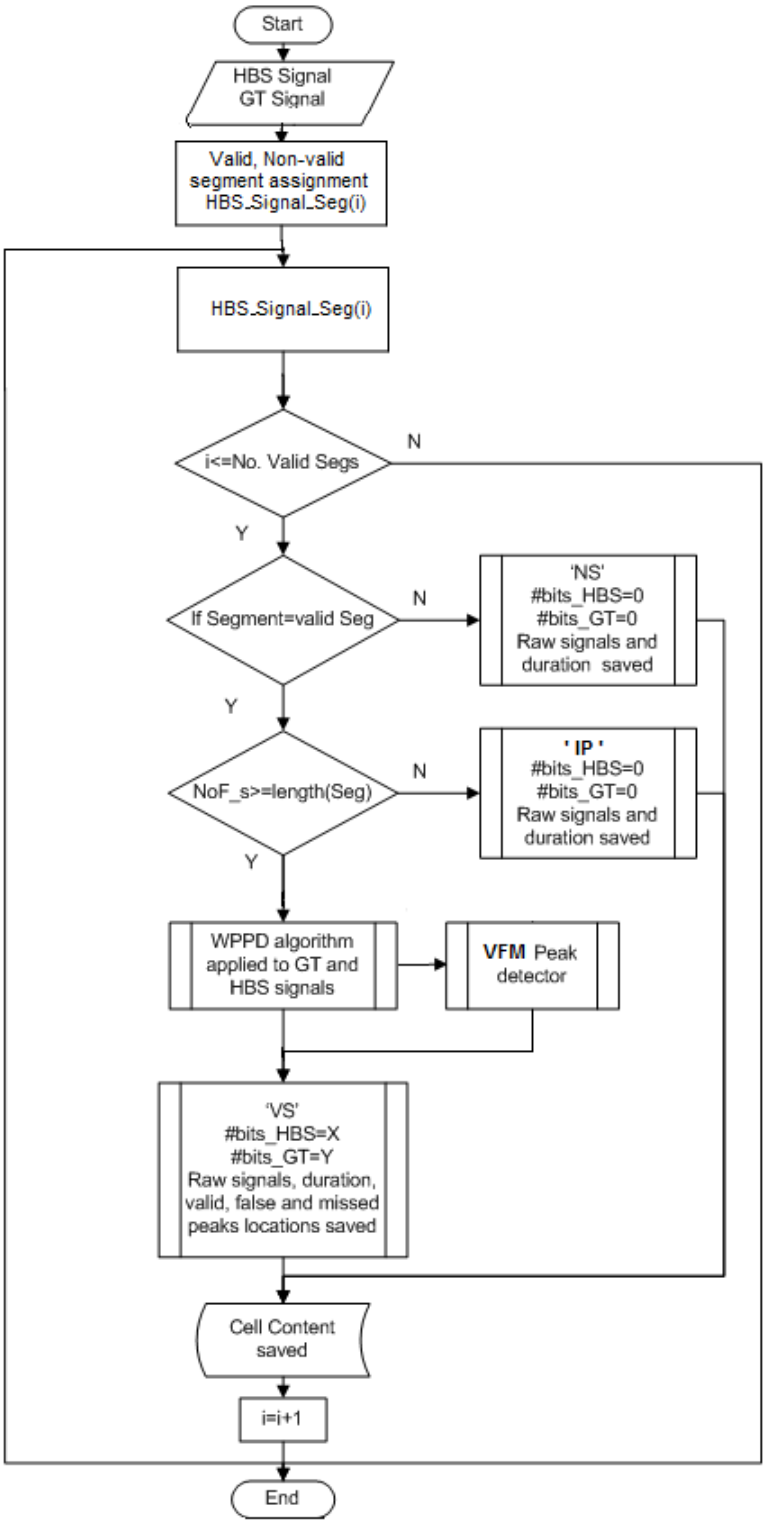

Figure 3.12: Data Processing

The extraction of valid segments is needed in order to remove bed motion [1], represented as transients in Figure 3.13.

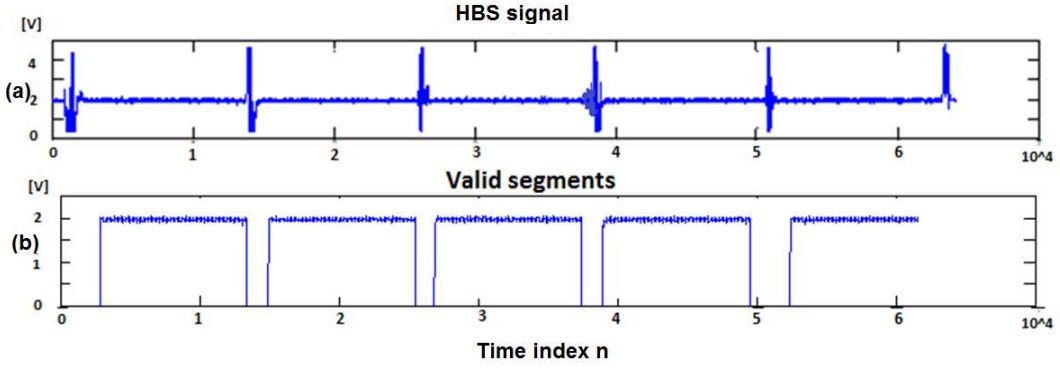

Figure 3.13: Extraction of valid segments
(a) The non-restlessness segments, shown as flat sections are extracted and shown in (b) using two thresholds (±1 standard deviation computed over the whole data).

If the segment is considered as non-valid, then the label *NS* (Noisy Signal) is assigned and the number of heartbeats computed for the HBS and GT are set to zero.
If the segment is considered as valid and its length is less than *NoF* (minimum number of samples needed to perform the WPPD algorithm and filtering), then the signal is labeled as *IP* (Insufficient Points).
If the segment is considered as valid and its length is greater than '*NoF*' then the signal is labeled as *VS* (Valid Signal). The WPPD algorithm is then applied to the HBS and GT signal for a combination of four window sizes (ws=[15 25 40 60]) and three cutoff frequencies for lowpass filtering the WPPD HBS signal, fc2 =[1 1.5 2]. These results are evaluated by the VFM peak detector, in order to determine the percentages of valid, false and missed peaks for each combination of ws and fc2.
As shown in Figure 3.12, the duration of the segment and the original HBS and GT signals are saved for all the possible cases.

VFM peak detector applied to the WPPD GT signal

It was observed that when the WPPD algorithm is applied to a signal that exhibits a peak that stands out, the WPPD peaks formed when different combinations of window

sizes and cutoff frequencies (fc2) are combined, remain almost constant. This was verified when the GT signal was evaluated with respect to itself, using the data processing described in Section 3.1.3.2.

Figure

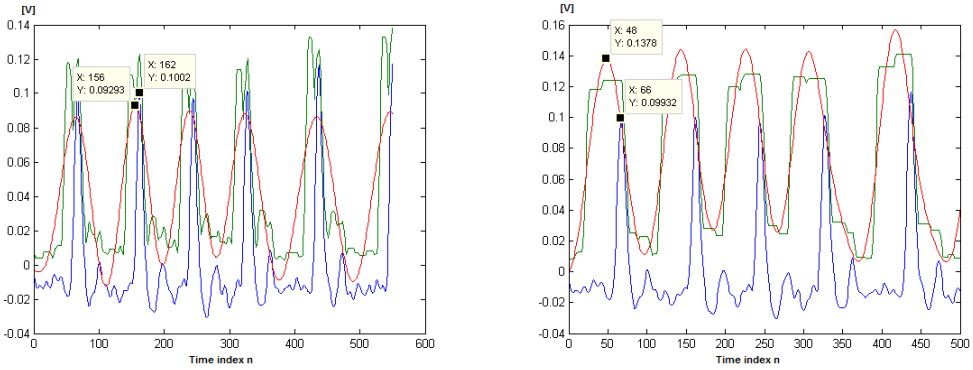

(a) ws=15, fc2=1.5 (b) ws=40, fc2 =2

Figure 3.14: WPPD GT signal
GT signal was evaluated respect to itself using the WPPD algorithm for two combinations of window size (ws) and cutoff frequency (fc2). Signals shown: GT signal, GT signal after using a certain ws and after lowpass filtering at a certain fc2.

Both combinations show consistently the same peaks.Table 3.7 verifies this by showing high percentages of valid peaks (V%) and low percentages of false peaks (F%) for eight combinations of ws&fc2.

		fc2=1 Hz		fc2=1.5 Hz		fc2=2 Hz	
		V [%]	F [%]	V [%]	F [%]	V [%]	F [%]
T1	ws=15	0.00	0.00	99.35	0.00	99.09	0.52
	ws=25	0.00	0.00	99.35	0.00	99.22	0.52
	ws=40	0.00	0.00	99.35	0.00	99.35	0.00
	ws=60	0.00	0.00	98.57	0.26	98.96	0.39

Table 3.7: Ground Truth Signal VFM peak detector results
Percentages of valid peaks (V%) and false peaks (F%) for twelve combinations of ws&fc2, where ws=[15, 25, 40, 60] samples and fc2 =[1, 1.5, 2] Hz.

3.1.3.3 Visual observation of the HBS lowpass filtered

Table 3.7 shows that, if the signal to be processed by the WPPD algorithm exhibits peaks with higher amplitudes than the ones around them, then the WPPD peaks computed for different ws&fc2 combinations show a high percentage of valid peaks and a low percentage of false peaks. Note that the expected waveform of the BCG signal contains the J-wave, the largest headward wave of the BCG signal [3], If the J-wave is captured by the system, then the VFM peak detector will score high values for V% and low values for F%. In order to do a fair observation and verify the presence of BCG-J, which indicates the occurrence of a heartbeat, the signal was lowpass filtered at 10 Hz [1], in order to keep the cardiac and respiration components and remove high frequency signals.

3.2 Results of the transducer placement experiments

This section shows the results of the experiments described in Table 3.6. Sample HBS signals are shown in this section. The complete set is included in Appendix B. The analysis used to assess the different arrangements was based on two criteria:

1. The reliability index computed from the output of the VFM-peak detector, which basically compares the WPPD signal computed from the transducers and the WPPD signal computed from the GT signal, in terms of the percentage of valid peaks and false peaks. The greater percentage of valid peaks and the smaller percentage of false peaks the better. The HBS signal resembles the heartbeat; if the heartbeat is well defined by a prominent peak (the J-wave), then the percentages of valid peaks %V will be greater while the percentages of false peaks %F will be smaller.

The percentage of Missed (M) peaks was not included, but can readily be derived by subtracting the percentage of Valid peaks from 100%.

2. The observation of the transducer signal lowpass filtered at a cutoff frequency of 10 Hz.

Assumptions made for the VFM peak detector were: *Per_p2p_dist*=0.3 (30%), *Min_5pts_dist*=20 samples and *Min_i2i*=40 samples;

3.2.1 Experiment 1

Transducer Arrangement: Figure 3.1a, four horizontal transducers

Combination of Length and &Volume: 1, Table 3.4.

Subject 1

		fc2=1 Hz		fc2=1.5 Hz		fc2=2 Hz	
		V [%]	F [%]	V [%]	F [%]	V [%]	F [%]
T1	ws=15	0.0	0.0	56.9	35.8	69.9	52.8
	ws=25	0.0	0.0	36.6	46.3	48.8	57.7
	ws=40	0.0	0.0	0.0	0.0	28.5	38.2
	ws=60	0.0	0.0	0.0	0.0	24.4	27.6
T2	ws=15	0.0	0.0	4.1	62.6	0.0	0.0
	ws=25	0.0	0.0	0.0	0.0	0.0	0.0
	ws=40	0.0	0.0	0.0	0.0	0.0	0.0
	ws=60	0.0	0.0	8.1	56.9	0.0	0.0
T3	ws=15	24.4	22.0	59.3	37.4	0.0	0.0
	ws=25	0.0	0.0	48.0	47.2	0.0	0.0
	ws=40	0.0	0.0	26.8	67.5	0.0	0.0
	ws=60	0.0	0.0	0.0	0.0	36.6	63.4
T4	ws=15	0.0	0.0	38.2	57.7	49.6	56.9
	ws=25	0.0	0.0	15.4	61.8	30.1	74.0
	ws=40	0.0	0.0	0.0	0.0	0.0	0.0
	ws=60	0.0	0.0	0.0	0.0	0.0	0.0

Table 3.8: Experiment 1-Subject 1-Test 1
V% and F% are the percentages of valid and false peaks respectively for twelve combinations of ws&fc2 computed for transducer T1, T2 , T3 and T4. Window sizes: ws=[15,25,40,60] and cutoff frequencies: fc2=[1, 1.5, 2] Hz.

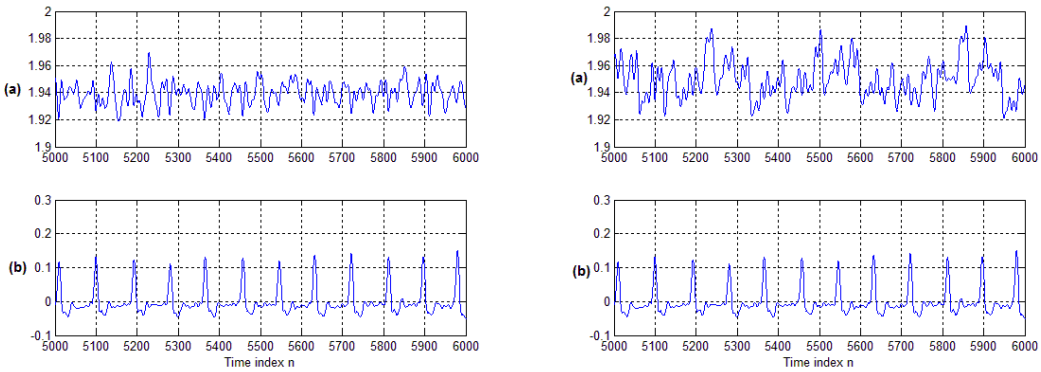

(a) T1

(b) T2

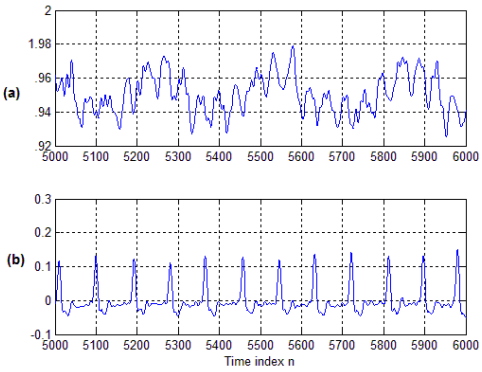

(c) T3

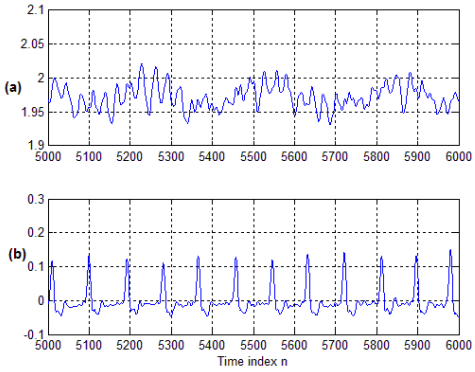

(d) T4

Figure 3.15: Experiment 1-Subject 1-Test 1
(a) shows the HBS signal after lowpass filtering at 10 Hz. (b) GT signal captured by a piezoelectric device worn on the subject's finger. T1, T2, T3 and T4 are the transducers tested.

Subject 2

		fc2=1 Hz		fc2=1.5 Hz		fc2=2 Hz	
		V [%]	F [%]	V [%]	F [%]	V [%]	F [%]
T1	ws=15	0.0	0.0	34.8	43.5	0.0	0.0
	ws=25	23.9	20.7	0.0	0.0	31.5	55.4
	ws=40	19.6	17.4	30.4	34.8	41.3	47.8
	ws=60	0.0	0.0	39.1	19.6	54.3	35.9
T2	ws=15	0.0	0.0	41.8	37.3	0.0	0.0
	ws=25	0.0	0.0	33.6	43.6	0.0	0.0
	ws=40	0.0	0.0	36.4	28.2	55.5	51.8
	ws=60	0.0	0.0	31.8	25.5	54.5	45.5
T3	ws=15	0.0	0.0	63.6	9.1	54.5	22.7
	ws=25	0.0	0.0	31.8	9.1	59.1	18.2
	ws=40	0.0	0.0	36.4	0.0	0.0	0.0
	ws=60	0.0	0.0	36.4	0.0	36.4	0.0
T4	ws=15	22.7	19.5	83.6	9.4	84.4	25.0
	ws=25	21.9	19.5	93.0	3.1	91.4	14.8
	ws=40	21.9	18.0	87.5	4.7	87.5	13.3
	ws=60	17.2	19.5	69.5	13.3	75.8	20.3

Table 3.9: Experiment 1-Subject 2-Test 1
V% and F% are the percentages of valid and false peaks respectively for twelve combinations of ws&fc2 computed for transducer T1, T2 , T3 and T4. Window sizes: ws=[15,25,40,60] and cutoff frequencies: fc2=[1, 1.5, 2] Hz.

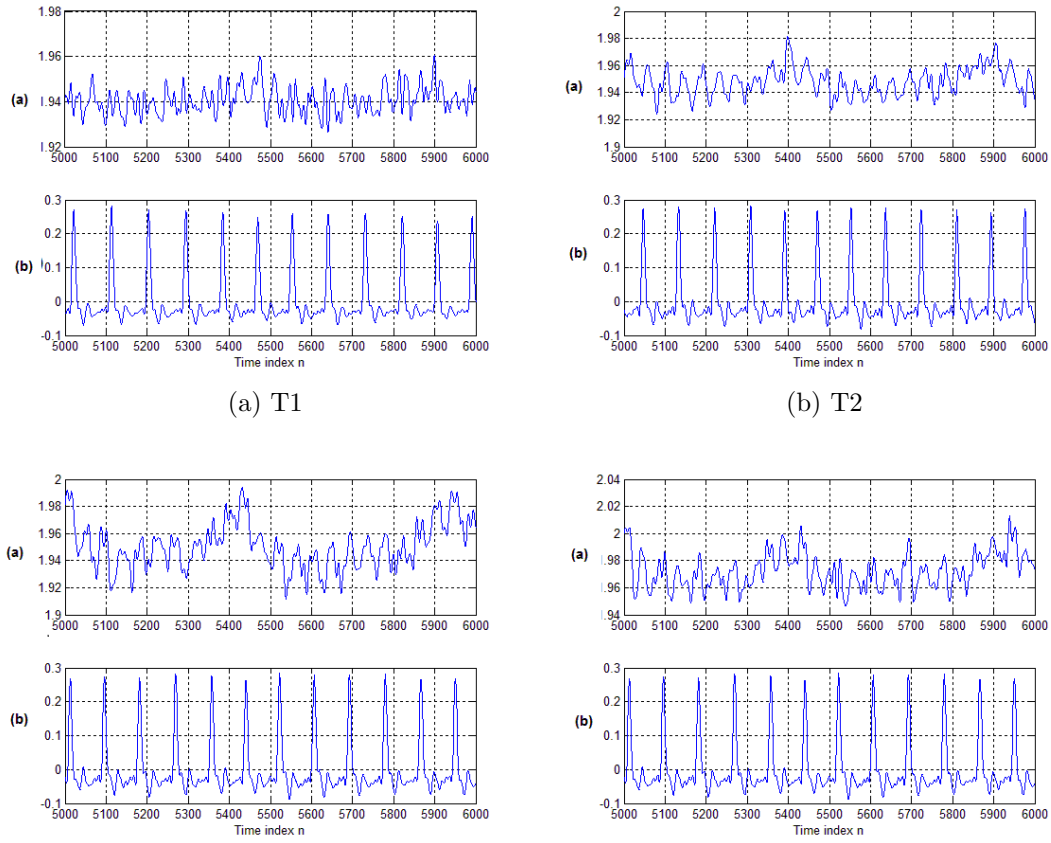

(a) T1 (b) T2

(c) T3 (d) T4

Figure 3.16: Experiment 1-Subject 2-Test 1
(a) shows the HBS signal after lowpass filtering at 10 Hz. (b) GT signal captured by a piezoelectric device worn on the subject's finger. T1, T2, T3 and T4 are the transducers tested.

Discussion

The main objective of this experiment was to identify the bed region in which the heartbeat signal can be better captured for both participants. It was expected that either T1, T2, T3 or T4, would be able to capture the occurrence of heartbeats. But Figures 3.15 and 3.16 show that any transducer captures it. The observation was performed on the whole signal. From the percentages of valid (V%) and false (F%) peaks presented in Tables 3.8 and 3.9, for both cases and all of the transducers, F% was greater than the percentage of valid peaks for most of the combinations. The same

results were observed when the experiment was repeated. This low percentage of valid peaks and the plots shown in Figures 3.15 and 3.16 shows the need of testing other transducer arrangements, as the arrangement tested for either subject 1 or subject 2 did not work.

(*)The value of 0 % means that the VFM peak detector could not complete the alignment process between the HBS and GT signals. This means that the VFM peak detector could not find three consecutive WPPD HBS peaks that lined up to the WPPD GT peaks. In this particular table, the VFM peak detector could not complete the alignment for almost all the the transducer arrangements and combinations of ws and fc2 =1 Hz.

3.2.2 Experiment 2

Transducer Arrangement: Figure 3.1a, four horizontal transducers.
Combination of Length and &Volume: 2, Table 3.4.

Discussion

This experiment repeats the transducer arrangement tested in Experiment 1, but explores the effect of increasing the volume of water from 20 to 30 oz.

Subject 1: The arrangement does not seem able to capture heartbeats; this is demonstrated in Figure B.5 where neither T1, T2, T3 nor T4 shows a distinguishable heartbeat pattern. Table B.3 reflects this situation. The high percentage of valid peaks for each transducer are reported and listed below along with their respective percentage of false peaks and ws&fc2 combinations.

T1:	V% =62.1,	F% = 58.3	for ws=60 & fc2=2
T2:	V% = 0.0,	F% = 0.0	for all the ws & fc2 combinations which mean that the WPPD HBS and WPPD GT signal could not be aligned.
T3:	V% = 85.4,	F% = 34.0	for ws=25 & fc2=2
T4:	V% = 84.5,	F% = 35.0	for ws=25 & fc2=2

This high percentages of false peaks for T1, T3 and T4, make this arrangement unsuitable for this subject.

Subject 2: Percentage of valid peaks & Percentage of false peaks: (V%≥85 & F%≤15) as reported in Table B.4 are listed in order to see the number of ws&fc2 combinations that fall into this interval.

T1: V% = 90.5, F% = 5.6 for ws=15 & fc2=1.5
V% = 88.9, F% = 7.9 for ws=15 & fc2=2
T2: V% = 81.0, F% = 11.9 for ws=25 & fc2=2
T3: V% = 71.4, F% = 42.9 for ws=25 & fc2=2
T4: V% = 87.3, F% = 9.5 for ws=40 & fc2=1.5

Looking at Figure B.6a, only T1 shows a pattern of three consecutive peaks for each heartbeat. This is reflected in the number of ws&fc2 combinations that scored higher values for T1 compared to T2, T3 and T4.
Two combinations of ws&fc2 are in the range of V%≥85 and F%≤ 15, suggesting that the position and volume for T1 can capture effectively the heartbeat signal from subject 2.

3.2.3 Experiment 3

Transducer Arrangement: Figure 3.1b, four shorter horizontal transducers
Combination of Length and &Volume: 3, Table 3.4.

Discussion

In order to find an arrangement that can capture heartbeats from subject 1 as well as subject 2, this experiment uses shorter transducers under the assumption that keeping the proportion of volume of water while reducing the length will yield an amplified output, due to the premise that the force exerted each time the heart is beating will be less attenuated if the distance to the pressure sensor is smaller.

The 36-inches transducer filled with 30 oz. of water seems to be filled to about 70 % of its total length (percentage of fullness is estimated by measuring the length of the transducer filled with water divided by the full length of the transducer), replicating

this, the new 21.8 inches transducer, was filled with 16 oz of water , in order to fill 70 % of its length . The positioning is shown in Figure 3.1b.

Subject 1: Percentage of valid peaks & Percentage of false peaks: (V%≥85 & F%≤15) as reported in Table B.4:

T1: None

T2: V% = 96.0, F% = 0.7 for ws=15 & fc2=1.5
V% = 94.7, F% = 0.0 for ws=25 & fc2=1.5
V% = 94.7, F% = 0.0 for ws=40 & fc2=1.5
V% = 94.0, F% = 2.0 for ws=15 & fc2=2
V% = 94.7, F% = 0.0 for ws=25 & fc2=2
V% = 94.7, F% = 0.0 for ws=40 & fc2=2
V% = 88.7, F% = 7.3 for ws=60 & fc2=2

T3: V% = 82.8, F% = 8.6 for ws=40 & fc2=1.5

T4: V% = 79.5, F% = 5.3 for ws=40 & fc2=1.5

Looking at Figure B.8b and the results from table B.3, T2 is clearly capturing the heartbeat signal, this is shown by looking at the correlations between the HBS signal and the GT signal. Seven ws&fc2 combinations were greater than 85& for the V% and less than 15 % of the F%. Six scored values for V% >than 94% & F%<0.7%.

Subject 2: Percentage of valid peaks&Percentage of false peaks: (V%≥85 & F%≤15) as reported in table B.6:

T1: None

T2: None

T3: None

T4: None

Although the highest percentage of valid and false peaks were V% = 80.8 and F% = 6.7 for T3 computed for ws=40 and fc2 =1.5, Figure B.6c does not show any occurrence of heartbeats.

These results showed that this arrangement can effectively work for subject 1 but cannot be used for subject 2.

3.2.4 Experiment 4

Transducer Arrangement: Figure 3.2, two transducers in a T

Combination of Length and &Volume: 3, Table 3.4

Discussion

Several transducer placements were tried this time. T1 was placed vertically and T2 horizontally, Table 3.2 shows the exact location of each transducer

Subject 1: Percentage of valid peaks & Percentage of false peaks: (V%≥85 & F%≤15) as reported in Table B.4:

T1: None

T2: V% = 93.6 , F% = 2.9 for the ws=15 & fc2=1.5
V% = 83.6, F% = 12.1 for ws=25 & fc2=1.5
V% = 94.3 , F% = 2.1 for ws=40 & fc2=1.5
V% = 92.1, F% = 2.9 for ws=60 & fc2=1.5
V% = 95.0, F% = 1.4 for ws=15 & fc2=2
V% = 92.1, F% = 0.0 for ws=25 & fc2=2
V% = 87.1, F% = 5.0 for ws=40 & fc2=2
V% = 85.0, F% = 7.9 for ws=60 & fc2=2

Looking at Figure B.11 and considering that 8 combinations of ws&fc2 fall into the range (V%≥85 & F%≤15), it is clear that T2 is capturing heartbeat the signal. This was expected given the previous results. T1 instead presents low percentages of valid peaks and the HBS signal showed in Figure B.11a confirms that it is not capturing presence of the heartbeat signal.

Subject 2: Percentage of valid peaks & Percentage of false peaks: (V%≥85 & F%≤15) as reported in Table B.6:

T1: None

T2: V% = 86.1, F% = 14.8 for ws=25 & fc2=1.5
V% = 85.2, F% = 9.6 for ws=40 & fc2=1.5
V% = 85.2, F% = 11.3 for ws=60 & fc2=1.5

Although T2 shows that three ws&fc2 combinations scored values greater than 85% for V% and less than 15% for F%, Table B.12b does not show the presence of the heartbeat signal.

These results show that T1 did not work for any of the participants and T2 was able to capture data from subject 1 but it did not work subject 2.

3.2.5 Experiment 5

Transducer Arrangement: Figure 3.3a, one vertical transducer

Combination of Length and &Volume: 3, Table 3.4.

Discussion

Different placements were tested, Figure3.3b shows the placement for this experiment.

Percentage of valid peaks & Percentage of false peaks: (V%≥85 & F%≤15) as reported:

T1: None

Looking at Tables B.9 and B.10, it is clear that no combinations of ws&fc2 fall into the range (V%≥85 & F%≤15), Figures B.14 and B.15a do not show the presence of any heartbeat signal. It is evident that this position will not give any useful information.

3.2.6 Experiment 6

Transducer Arrangement: Figure 3.3a, one vertical transducer

Combination of Length and &Volume: 3, table 3.4.

Discussion

For this experiment the transducer is placed right in the middle of the bed at 1 inc. respect to the headboard. Figure 3.3b shows the positioning of the transducer.

Subject 1: Percentage of valid peaks & Percentage of false peaks: (V%≥90 & F%≤10) as reported in Table B.11 are listed below :

T1: V% = 90.2, F% = 5.3 for ws=15 & fc2=1.5
V% = 91.0, F% = 24.8 for ws=25 & fc2=1.5
V% = 93.2, F% = 1.5 for ws=40 & fc2=1.5
V% = 93.2, F% = 12.8 for ws=60 & fc2=1.5
V% = 91.7, F% = 2.3 for ws=15 & fc2=2
V% = 91.0, F% = 8.3 for ws=25 & fc2=2

Six ws&fc2 combinations fall into (V%≥90 & F%≤10) and the waveform displayed in Figure B.14, shows the occurrence of heartbeat.

Subject 2: From Table B.12, the Percentage of valid peaks & Percentage of false peaks: (V%≥85 & F%≤15) is:

T1: V% = 91.0, F% = 4.5 for ws=15 & fc2=1.5
V% = 91.7, F% = 13.5 for ws=25 & fc2=1.5
V% =93.2, F% = 3.8 for ws=40 & fc2=1.5
V% =92.5, F% = 6.8 for ws=60 & fc2=1.5
V% =93.2, F% = 3.8 for ws=15 & fc2=2
V% = 94.0, F% = 3.8 for ws=25 & fc2=2
V% = 89.5, F% = 6.8 for ws=40 & fc2=2
V% = 92.5, F% = 7.5 for ws=60 & fc2=2

Eight combinations of ws&fc2, fall into (V%≥90 & F%≤10). Same as subject 1 Table B.12 shows the occurrence of heartbeats. These results show the effectiveness of this arrangement capturing data from different body types.

Reliability index Based on the observations of the the percentage of valid peaks and percentage of false peaks, V% and F%, receptively, V% gets higher values when the HBS signal shows distinguishable heartbeats, while F% gets smaller. If ws&fc2 combinations are being evaluated then the reliability index is defined as the number of ws&fc2 combinations that fall into the range (V%≥90 & F%≤10), which indicates that 90% of the HBS peaks lined up with the GT peaks and 10% HBS peaks were reported as false peaks. Then the reliability index for subject 1 is 6 and 8 for subject 2.

3.2.7 Experiment 7

Transducer Arrangement: Figure 3.4, four vertical transducers

Combination of Length and &Volume: 3, Table 3.4.

Discussion

Figure 3.4 is proposed based on the results obtained in Experiment 6. Additional experiments showed that if the person is not lying on the transducer, its effectiveness of capturing the occurrence of heartbeats reduces drastically. For this reason, four transducers are placed under the mattress, ensuring that at least one of them will be able to capture useful data.

Subject 1: The number of ws&fc2 combinations with a percentage of valid and false peaks that fall into: (V%≥90 & F%≤10) are listed below, this estimation was made using the values of V% and F% reported in Table B.18:

Reliability index:

T1:0

T2:0

T3:3

T4:0

Transducer 3 (T3) is the one that has the greater number of combinations of ws&fc2 that falls into (V%≥90 & F%≤10). This is verified looking at Figure B.26, that shows the presence of the heartbeat in the BCG signal captured by T3.

Subject 2: Table B.19 shows that T3 and T4 have the greater number of ws&fc2 combinations.

Reliability index:

T1:0

T2:0

T3:4

T4:4

Figure B.27d shows the presence of well defined heartbeats for T4 and T2. These results confirm the effectiveness of this arrangement in capturing heartbeats from different body types. This series of experiments identified the bed region where the transducer can effectively capture heartbeat, which is located between 7 in. and 25 in. from the headboard; experiments 2,3,4 and 6 demonstrated this. Additional experiments were performed placing the transducer below 3 ft, with no success capturing the heartbeats.

3.2.8 Experiment 8

Validation of transducer arrangement 3.4

Transducer Arrangement: Figure 3.4, four vertical transducers
Combination of Length and &Volume: 3, Table 3.4.
This experiment was conducted on participants of testing group 2 described in Table 3.2 in order to test the robustness of the transducer arrangement shown in Figure 3.4.

Discussion

Table 3.10 was build based on Tables B.15, B.16, B.17, B.13 and B.14. It shows the number of ws&fc2 combinations that resulted in a high percentage of valid peaks (V%) and a low percentage of false peaks (F%): (V%≥90 & F%≤10).

	Subject 1	Subject 2	Subject 3	Subject 4	Subject 5
T1	0	0	0	0	0
T2	1	2	0	1	0
T3	4	2	8	4	4
T4	4	6	5	0	5

Table 3.10: Number of ws&fc2 combinations with (V%≥90 & F%≤10)

From this table, it can be said that either T3 or T4 can be used to further analysis of the BCG signal for subject 1, for T4 for subject 2 , T3 for subject 3, T3 for subject 4 and T4 for subject 5. This can be verified looking at Figures B.23, B.24, B.25, B.20

and B.21. These results confirm that the placement shown in Figure 3.4 is able to capture effectively the heartbeat from different body types.

3.2.9 Experiment 9

Transducer Arrangement: Figure 3.4, four vertical transducers

Combination of Length and &Volume: 3, Table 3.4.

In this experiment the transducer placement was tested for three participants from the evaluation trial presented in [1]. Subjects 1, 3 and 4 (listed in testing group 3) were asked to repeat the same protocol used in [1].

Discussion

Section 3.11 summarizes the number of ws&fc2 combinations that fall into the range (V%≥90 & F%≤10), for each position tested for subject 1, 3 and 4. The BCG signals are displayed in the Appendix B.9.

The BCG signal extracted from subject 1 did not show the occurrence of heartbeats when he lay on his back, although the WPPD-A scored 6 combinations of ws&fc2. Right and left positions were not tested since no visible heartbeat signal was captured form B1 segment.

Results from subject 3 an 4 showed that the arrangement was able to capture heartbeat signal for all the segments when they lay on their back.

	Subject 1	Subject 3					Subject 4				
	B1	B1	R	B2	L	B3	B1	R	B2	L	B3
T1	0	0	0	0	0	3	3	4	0	0	0
T2	6	4	0	8	0	6	8	7	8	0	8
T3	0	8	0	7	0	7	8	3	8	0	6
T4	0	6	0	2	0	0	8	0	8	0	6

Table 3.11: Number of ws&fc2 combinations with (V%≥90 & F%≤10)
Number of ws&fc2 combinations that present a percentage of valid peaks (V%) and percentage of false peaks (F%): (V%≥90 & F%≤10); computed for T1, T2, T3 and T4 and the segments represented in Figure 2.5 (B1, R, B2, L and B3).

Section 3.11 also shows that the effectiveness of the arrangement decreases when the person lies on her left or right side. That is the case for Subject 3 where no ws&fc2 combinations are in the range (V%≥90%, F%≤10%), but three are scored for (V%≥80%, F%≤15%) when she lay on her right side (R) and four when she lay on her left side (L).

BCG signals for Subject 4, captured when she lay on her right side, shows the occurrence of heartbeat for 3 transducers (T1, T2, and T3). Similarly, when subject 4 lay on her left side zero ws&fc2 combinations are in this range, but four are in (V%≥80%, F%≤15%). BCG signals reflected this observations.

Conclusion The transducer arrangement shown in Figure 3.4 has proven to be capable of capturing heartbeats for six out of seven participants in the experiments. All the BCG signals showed the characteristic BCG-J peak when the participants lay on their backs. Only two participants were tested for different positions (left side and right side), resulting in the degradation of the signal or loss of the heartbeat signal, except for one of the participants, who reported a good BCG signal when she lay on her right side. Further investigation needs to be done in order to find an arrangement robust enough to capture heartbeat signal regardless of the body types and the person's position.

Artifact introduced

To quantify the HBS system's ability to report the occurrence of heartbeats, the HBS signal was compared to the GT signal; the peak location between the transducer signal and the GT signal was used as a measure of whether or not the peak extracted using the WPPD algorithm was a heartbeat or not. To automate the detection location of the pulse signals from the ground truth, the VFM algorithm applied the WPPD algorithm to the GT signal in order to find the location of the peaks formed. The use of these approximate peak locations for the GT added an artifact to the computations of the VFM peak detector. Moreover, the Ground Truth signal is also susceptible to error caused by motion [22].

3.3 HBS System Overview

A block diagram of the new HBS system appears in Figure 3.17.

1. Inputs: BCG signals are being captured by four hydraulic transducers placed under a twin mattress with thickness of 7 inches. Each hydraulic transducer is connected to a pressure sensor [19].

2. Amplification/Filtering stage: each BCG signal is processed separately by an amplifying/filtering card, Figure 2.3. The AFC card output (F1) goes to an analog-to-digital converter (ADC). An additional output of the raw signal (for each transducer) is used to get positioning of the subject on the bed with respect to the transducer. Then, the eight output signals are digitized using an ADC connected to a PC for data storage. The sampling frequency for all channels is 100 Hz.

3. Selection of the transducer signal to be processed: the selection will be based on the voltage levels for R1, R2, R3 and R4; the two highest values will be chosen for further processing.

4. The determination of valid segments: the standard deviation of the entire signal (from the transducer selected) is computed and then used to evaluate the data every five seconds for thresholds of ± 1*std. The 5-minute segments labeled as valid segments will be saved and used for steps 6 and 7.

6. Computing heart rate using the WPPD and the Heart Detection using k means algorithm.

7. Computing respiration rate which is outside of the scope of the thesis.

8. Estimating the level of body motion and restlessness using the segments labeled as non-valid for heartbeat analysis.

Section 3.4 presents a new approach for detecting the occurrence of heartbeats, the Heartbeat Detection using k-means (HbD-KM). It also describes the estimation of the heart rate based on the beat-to-beat distance computed from the heartbeat locations detected by the WPPD algorithm and (HbD-KM).

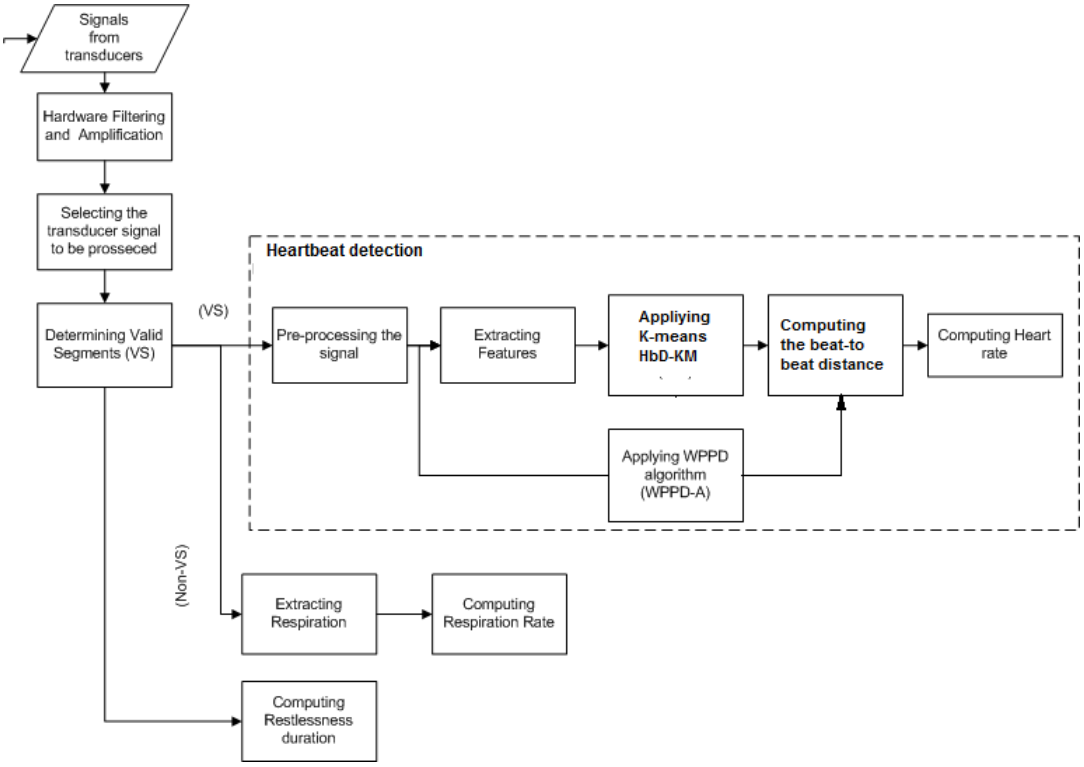

Figure 3.17: Functional block diagram of the proposed system

3.4 Heartbeat detection using K-means (HbD-KM)

A machine learning approach using clustering techniques was presented in [2]. A modified version of the k-means algorithm was applied to a BCG signal to extract the shapes of the repeating patterns. This section describes a preliminary study based on the feature extraction proposed in [2] and the k-means clustering algorithm set to two classes, for the BCG signal captured by the Hydraulic Bed Sensor system.

3.4.1 Detecting Heartbeats

The heartbeat detection process, shown in Figure 3.17 enclosed in dotted lines is described below:

1. Pre-processing the HBS signal:

The transducer signal (Fi) is bandpass filtered at [0.4 10] Hz to remove the low frequency respiratory components [1]. Additionally, an 8-point average filter was used

to smooth the signal, before feature extraction.

2. Extracting Features:

The BCG signal captured by the system, shows the occurrence of a heartbeat represented by a peak that clearly stands out (BCG-J [3]) , but unlike the data presented by [2], the BCG signal does not exhibit a self-repeating pattern for the peaks that were around the BCG-J wave.

Bruse et al. [2] parametrized the BCG signal as shown in Figure 3.18:

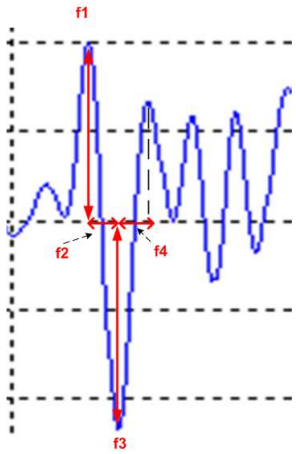

Figure 3.18: Set of Features (1) from [2]

The features shown in Figure 3.18 were computed using the subject 1 data (testing group 2) to perform a preliminary evaluation looking at the distribution of the data. Principal Component Analysis (PCA) was used to facilitate the visualization [23]. Figure 3.19 is a visualization of the data in the space of the first 3 principal components, which contains 99.9% of the variation in the data. These results and the distribution of the data (no explicit clusters) suggest that a new set of features is needed [23].

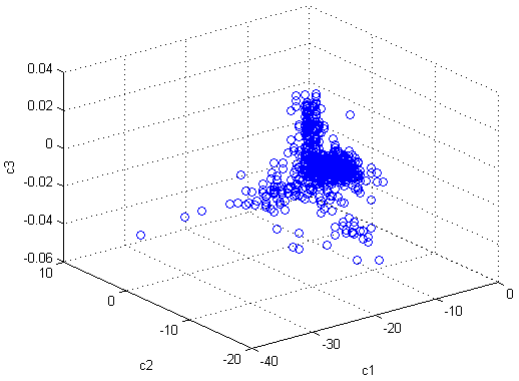

Figure 3.19: Subject 1- 4 features

Features proposed by [2] were run using the k-means algorithm along with an initialization step (two centers were chosen randomly from the data). The number of clusters was set to two, where one cluster represents the BCG-J wave of the heartbeat (HB) and the second cluster represents the other peaks (i.e., non heartbeats NHB). Then the smallest cluster will be assigned to class heartbeats (class HB) and the large cluster to class non-heartbeats (class NHB). The clustering results for this set of features reached a correct heartbeats detection of 79.6% and the number of NHB peaks that the system clustered in the HB cluster is twice the actual number (Table 3.12).

		Predicted class	
		HB	NHB
Actual class	HB (Class 1)	109	1
	NHB (Class 2)	127	390

Table 3.12: Confusion matrix-Subject 1-4 features

Feature extraction

Looking at the BCG waveform of the hydraulic bed sensor, slight modifications to the feature set proposed in [2] were made, in an attempt to capture representative features.

1) A distance between two consecutive peaks was computed (f3) and 2) features (f2) and (f4) shown in Figure 3.18 were deleted.

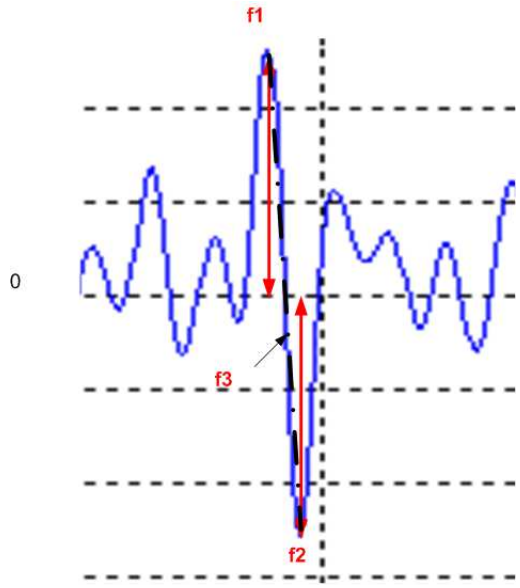

Figure 3.20: Set of Features (2)

When these data were represented in three dimensions, two clusters characterized the data. Figure 3.21 depicts the data distribution and shows the advantage of running the k-means due to the ellipsoidal shaped clusters [24].

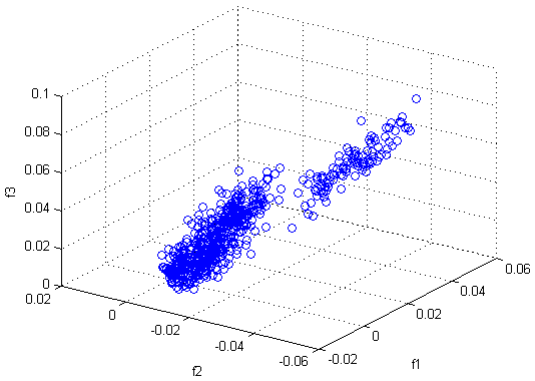

Figure 3.21: Subject 1 -3 features

3. Heartbeat detection applying k-means algorithm HbD-KM:

The k-means algorithm is tested for testing group 2 (Table 3.2), with the number of cluster set to two. The results are two vectors, in which one of them (the smallest) will contain the estimated heartbeat locations. The k-means algorithm implemented is described below.

K-means

K-means clustering aims to partition N observations into k clusters in which each observation belongs to the cluster with the nearest mean. It can be viewed as a special case of the generalized hard clustering algorithm scheme when point representatives are used and the squared Euclidean distance is adopted to measure the dissimilarity between vectors x_i and representatives θ_j [25], where θ_j is the mean of cluster j and x_i is the i-th point of the dataset X, for i=1,...,N.

The k-means algorithm is derived by minimizing a cost function of the form:

$J(\theta, r) = \sum_{i=1}^{N} \sum_{i=1}^{K} r_{ik} \left\| x_i - u_k \right\|^2$

with respect to r_{ik} and u_k, where X=$\{x_1,...,x_N,\}$ describe the dataset, $r_{ik}$is the set of binary indicator variables in [0,1], and k=1,..,m describe which of the K clusters the data point x_n is assigned to, so that if data point x_i is assigned to cluster k, then r_{ik} =1 [25].

K-means algorithm

- Choose arbitrary initial estimates $u_k(0)$ for the u_k , k=1,...,m.
- Repeat
  - For i=1 to N
    - Determine the closest representative u_k., for x_i. Compute r_{ik}
    - Set b(i)=k.
  - End (For-i)
  - For j=1 to m

  - ∗ Parameter updating: Determine $u_k.$, as the mean of the vectors $x_i$belongs to X with b(i)=k.

- End (For-j)

- Until no change in u_ks occurs between two successive iterations.

Note that θ_j: is the parametrized representative (mean) of the j-th cluster, θ_j=[,..., θ_m], b a label vector and m is the number of clusters .

4. Heartbeat detection applying WPPD algorithm (WPPD-A):

The WPPD signal was computed for ws=25 and fc2=1.5 Hz for all participants of testing group 2. Results are presented in Chapter 4.

5. Computing the beat-to-beat distance:

The estimated heartbeat locations computed for the HbD-KM approach and the WPPD algorithm are used to compute the beat-to beat interval.

6. Estimating heart rate:

A histogram built using the beat-to-beat intervals computed in step 5 is used to assess the heart rate and compared to the estimation extracted from the GT signal. The GT signal was sampled at 100 Hz and then lowpass filtered at 10 Hz to remove noise. The number of pulse signals extracted from the piezoelectric device (Section 3.1.2) and the pulse locations were computed in order to compare the heart rate measurements.

Determining heartbeat classification from clustering results

Results expected from the HbD-KM approach were stored in two vectors, where the smallest had the information about the location of the BCG-J wave. These points will be compared to the ones that were labeled manually by looking at the ballistocardiogram (BCG) signal. Labeling consisted of an identification number added to each peak of the BCG signal, along with a label of '2' if the peak is a heartbeat (HB) and '1' is it is not. Labeling was performed over a 2-minute segment of the BCG signal captured from subject 1, 2, 3, 4 and 5. Table 3.13 shows the number of instances, number of features computed and number of non-heartbeats (NHB) and heartbeats (HB) for all the participants.

	Number of Instances	Number of features	Class distribution	
			NHB	HB
Subject 1	626	3	516	110
Subject 2	493	3	475	120
Subject 3	587	3	495	92
Subject 4	677	3	570	107
Subject 5	597	3	479	118

Table 3.13: Instances and features

Finally a confusion matrix was computed to assess whether the clustering was effective grouping the BCG-J waves.

3.5 Tiger place setting

The new transducer arrangement was installed in TigerPlace in one resident's apartment. The transducer arrangement was placed under an air mattress with an adjustable firmness control (highest level of firmness). Data were recorded for the entire night; unlike the laboratory setting we did not record the Ground Truth signal. The BCG signal obtained is shown in Figure 3.23b. This heartbeat waveform, compared to the one shown in Figure 3.23a, shows a different pattern for the peaks around the BCG-J wave.

First, a 2-minute segment were selected from the collected overnight data. Second, one transducer is selected based on the waveform of the BCG signal. Last the heartbeat detection using the k-means algorithm is run.

1) Visual observation of the overnight data was made in order to identify long periods of data where the subject does not present much movement, which may indicate that he is sleeping. For this analysis the data were segmented into 1 hour-segments. The selection of the 1-hour segment was based on a visual measure of body motion and the pressure sensor outputs shown in Figure 3.22, which shows that the subject was resting on T2 and T3 for the entire hour. From this figure, T2 and T3 show higher values compared to T1 and T4, which means that more pressure is being applied on

them, since the output of the pressure sensor is directly proportional to the force exerted [19]. The 58-minute segment selected was collected starting at 12:00 pm.

2) From Figure 3.22 we know that either T2 or T3 will contain the heartbeat signal. The selection of the data transducer to be processed was based on the visual observation and comparison between their heartbeat patterns (BCG signals waveforms). The criteria for selecting T3 over T2 was the more consistent BCG signal representation by T3 [3]. The segmentation step shown in Figure 3.17 was used to separate the data into valid and noisy segments, thus the restlessness segments (non-valid segments) could be analyzed separately. The number of valid segments for the 58-minute segment was 88 using a threshold of 1 standard deviation computed for the entire signal. The selection of the segment was based on the duration and the observation of the BCG signal. The segment selected for analysis was a 15-minute long and captured by T3.

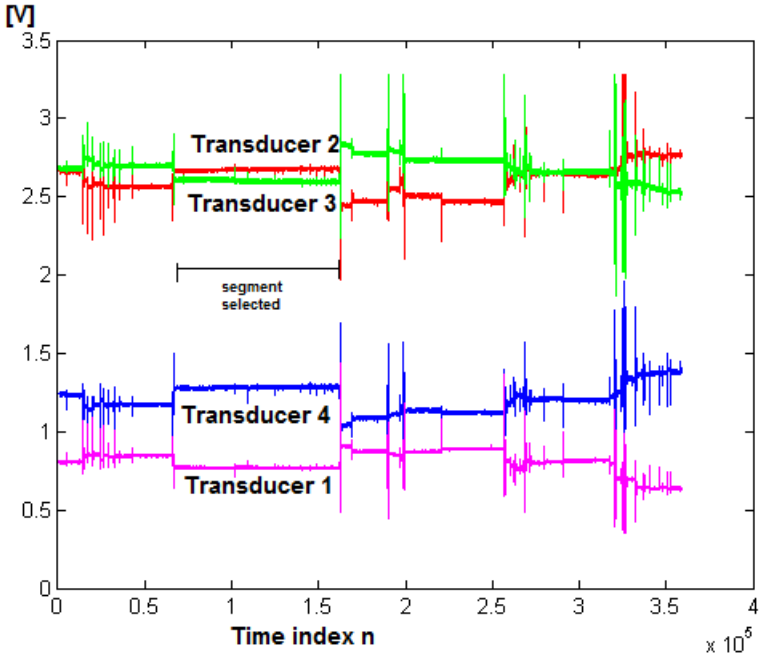

Figure 3.22: Outputs extracted from the four pressure sensors (1-hour raw data captured from TigerPlace resident collected overnight)

3) A 2-minute segment was extracted from the 15-minute segment, and each peak of the BCG signal was labeled as heartbeat (HB) and non-heartbeat (NHB) based on

(a) HBS BCG signal (coil spring mattress)

(b) HBS BCG signal (air mattress)

Figure 3.23: Hydraulic Bed Sensor (HBS) BCG signals

the occurrence of the BCG-J peak which shows the largest amplitude with respect to the other peaks [3]. The k-means algorithm was used to find the location of the BCG-J waves.

More investigation about how to determine wake and sleep segments has yet to be done as well finding a criteria for selecting a transducer when the subject is lying on more than one of them. It could be done based on the clearest representation of the BCG signal by a particular transducer.

In order to measure the correct detection of heartbeat locations, the 2-minute segment was labeled manually, table 3.14 shows the number of instances, features and heartbeats and non-heartbeats.

	Number of Instances	Number of features	Class distribution	
			NHB	HB
Subject 6	615	4	528	87

Table 3.14: Instances and features

The HbD-KM approach was tested over two-minute segment extracted from the data that were collected. Using the set of features shown in Figure 3.20. The distribution of the data as depicted by the 3D plot (Figure 3.25) did not show well-defined clusters as it did for the data that were collected in the laboratory. For this reason, a

new set of features was proposed in Figure 3.24 and was tested in a second attempt to cluster the peaks that represent the BCG-J waves .

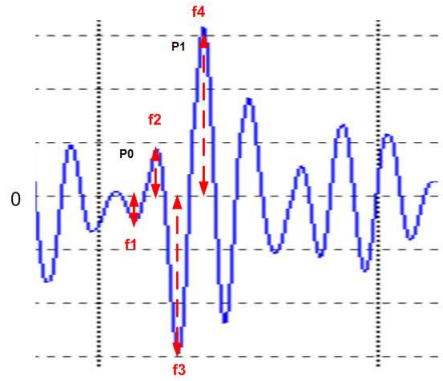

Figure 3.24: Set of features (3)

Figure 3.25 shows a plot of the set of features (3) using PCA, which shows the formation of three clusters. Although the data distribution suggests to run the k-means algorithm for k=3, the number of classes was set to 2, class heartbeats (Class HB) and class non-heartbeats (NHB) in order to identify the presence of a heartbeat and leave the rest of the peaks in the class of non-heartbeats.

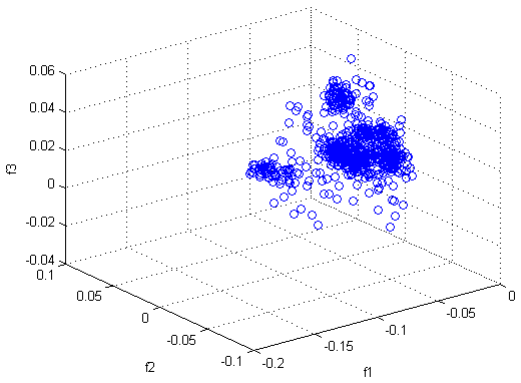

Figure 3.25: BCG Signal (Tiger Place resident) 4 features

Results from these implementations, the beat-to-beat intervals and the estimation of the heart rates for WPPD-algorithm and the HbD-KM approach are reported in Section 4.2.

Chapter 4

Results

4.1 HbD-KM results -Laboratory setting

In this section, the results of the trials carried out in a laboratory setting are presented.

Subject 1

Correct_detection =99.7%

	HB	NHB
HB (Class 1)	108	2
NHB (Class 2)	0	516

Table 4.1: Subject 1-HbD-KM-Confusion matrix

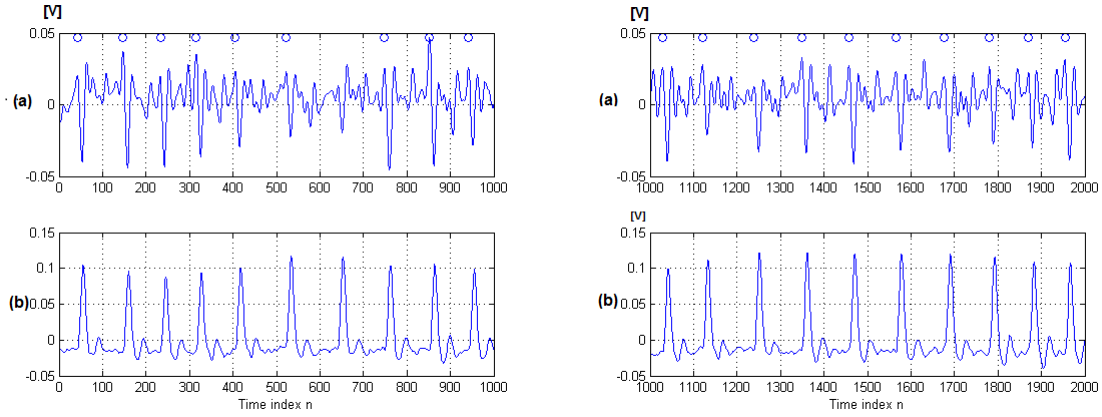

(a) (b)

Figure 4.1: Heartbeats detected by the k-means algorithm for 2 time slices (left and right) (a) processed BCG signal with a circle on top (^{O}) designating HB, (b) GT signal

Heart rate estimation

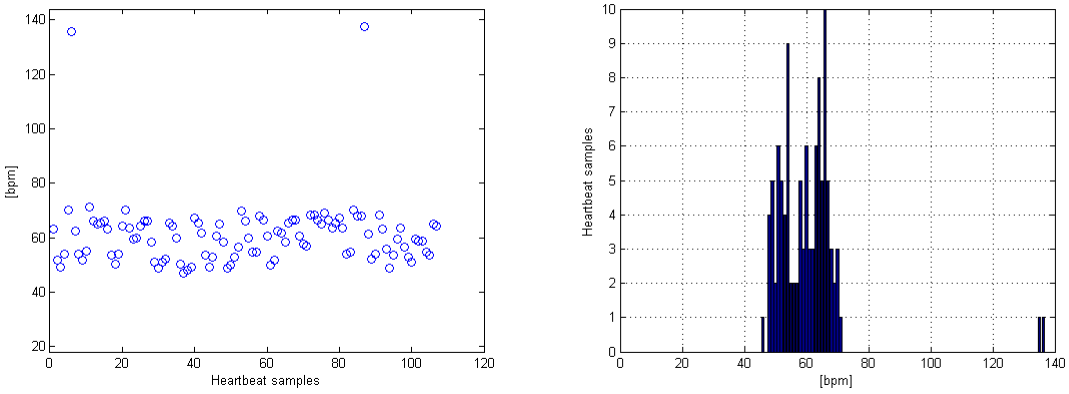

(a) Interbeat distance ID (b) Histogram ID

Figure 4.2: HbD-KmA

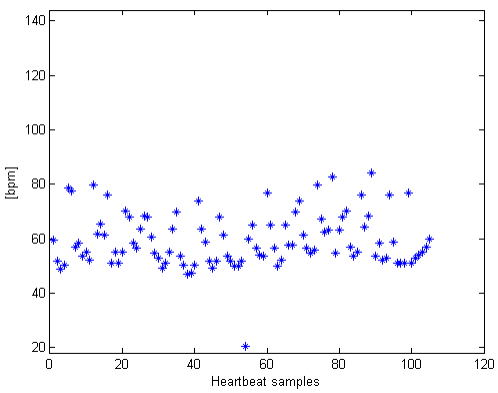

(a) Interbeat distance ID

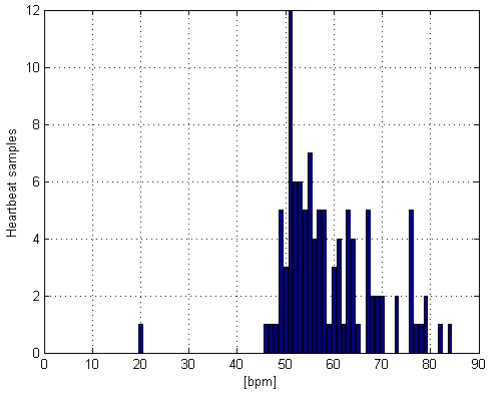

(b) Histogram ID

Figure 4.3: HBS-WPPD

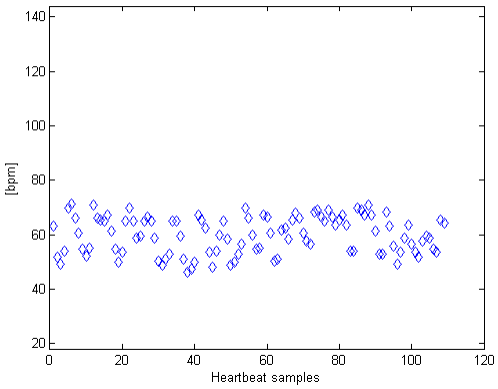

(a) Interbeat distance ID

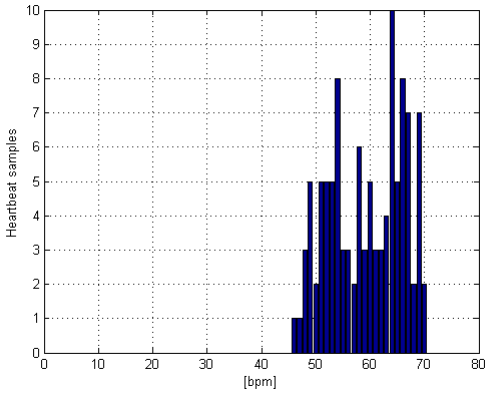

(b) Histogram ID

Figure 4.4: GT

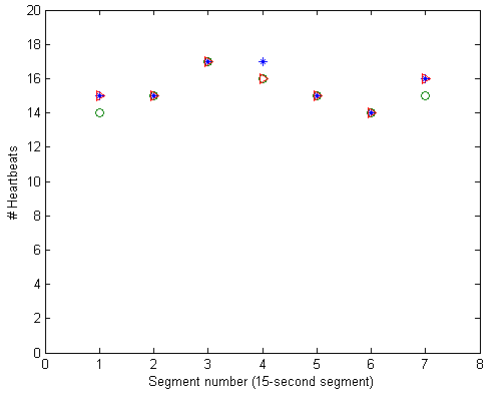

Figure 4.5: Number of Heartbeats detected by HbD-KmA(^{O}),WPPD($*$),GT($\triangleright$)

Subject 2

$$\text{Correct\_detection} = 91.4\%$$

	HB	NHB
HB (Class 1)	120	0
NHB (Class 2)	51	424

Table 4.2: Subject 2-KM-Confusion matrix

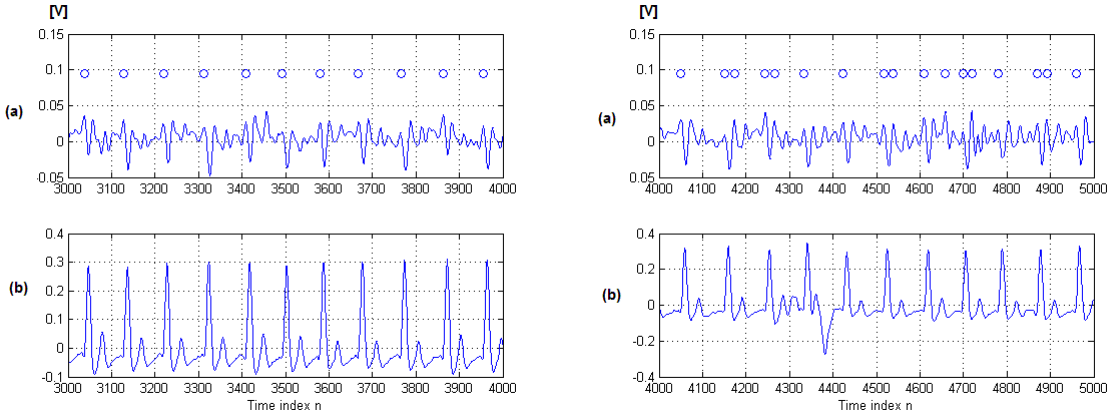

(a) (b)

Figure 4.6: Heartbeats detected by the k-means algorithm for 2 time slices (left and right) (a) processed BCG signal with a circle on top (^{O}) designating HB, (b) GT signal

Heart rate estimation

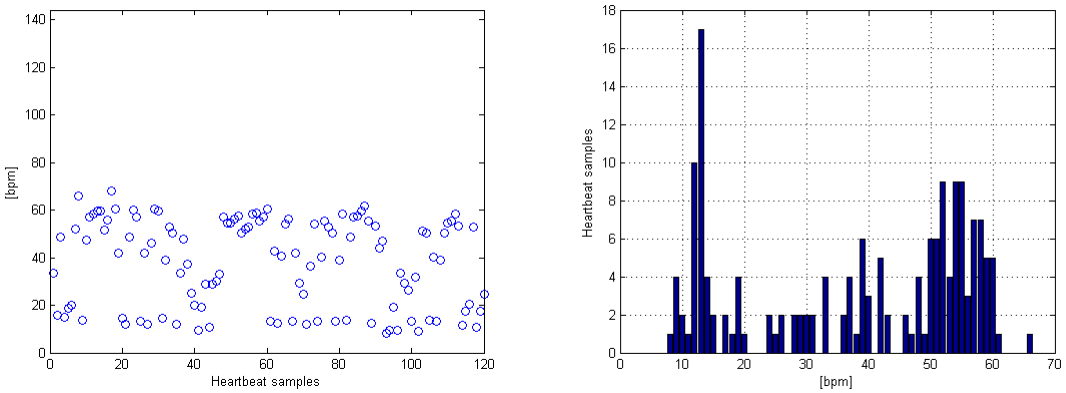

(a) Interbeat distance ID (b) Histogram ID

Figure 4.7: HbD-KmA

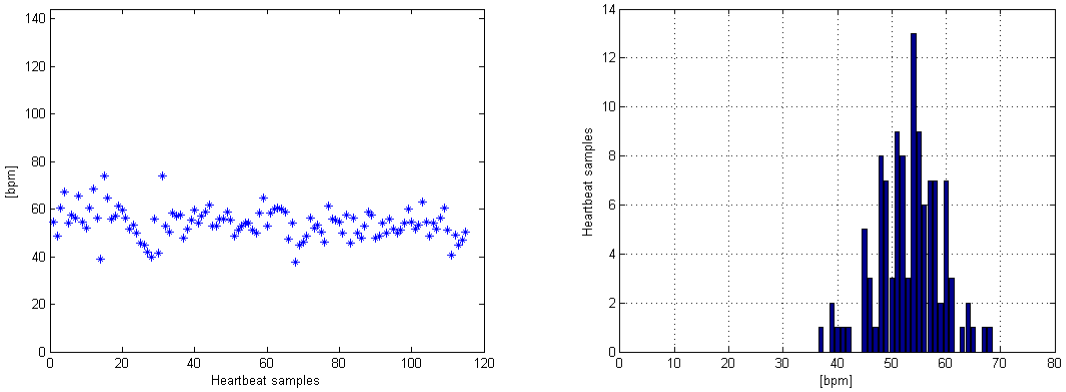

(a) Interbeat distance ID (b) Histogram ID

Figure 4.8: HBS-WPPD

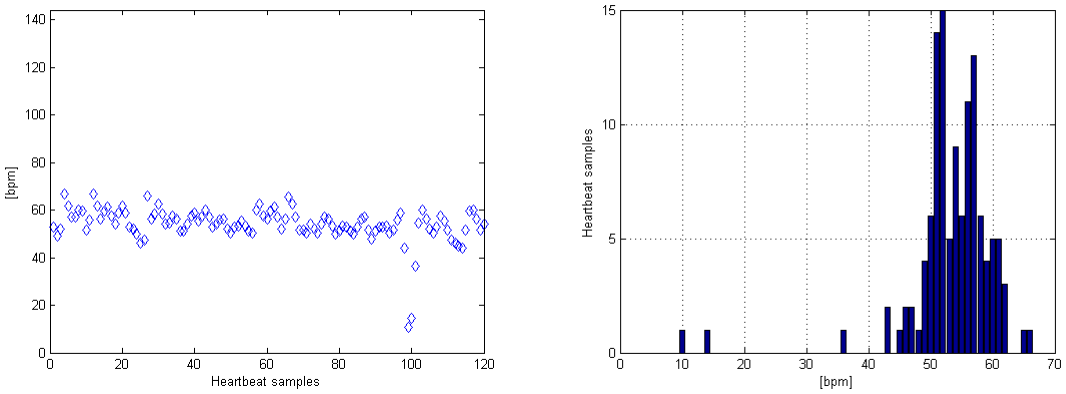

(a) Interbeat distance ID (b) Histogram ID

Figure 4.9: GT

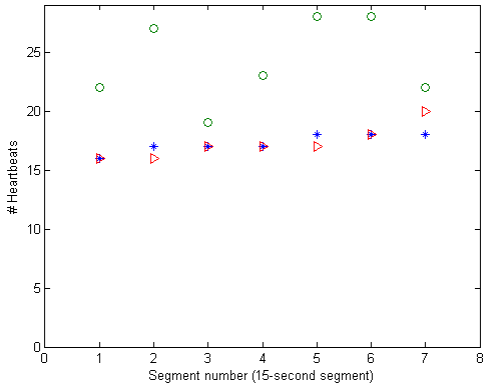

Figure 4.10: Number of Heartbeats detected by HbD-KmA(^{O}),WPPD($*$),GT($\triangleright$)

Subject 3

Correct_detection =97.3 %

	HB	NHB
HB (Class 1)	91	1
NHB (Class 2)	15	480

Table 4.3: Subject 3-KM-Confusion matrix

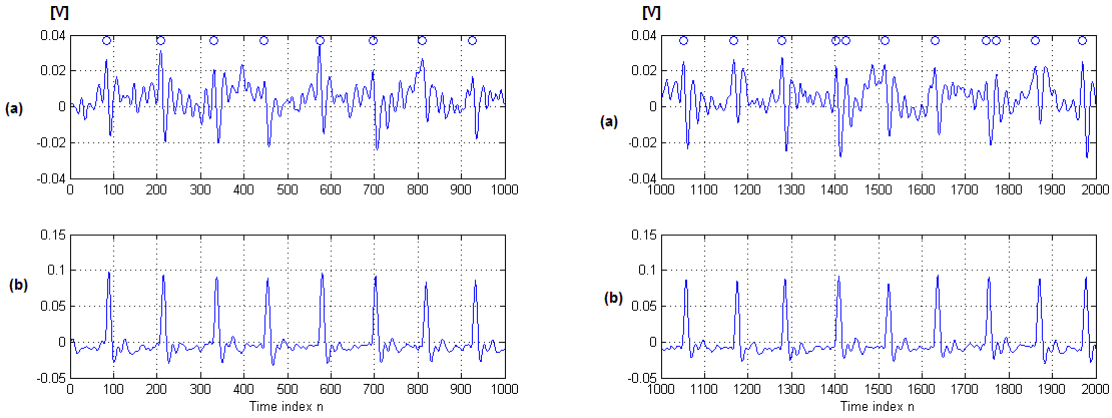

(a) (b)

Figure 4.11: Heartbeats detected by the k-means algorithm for 2 time slices (left and right) (a) processed BCG signal with a circle on top (^{O}) designating HB, (b) GT signal

Heart rate estimation

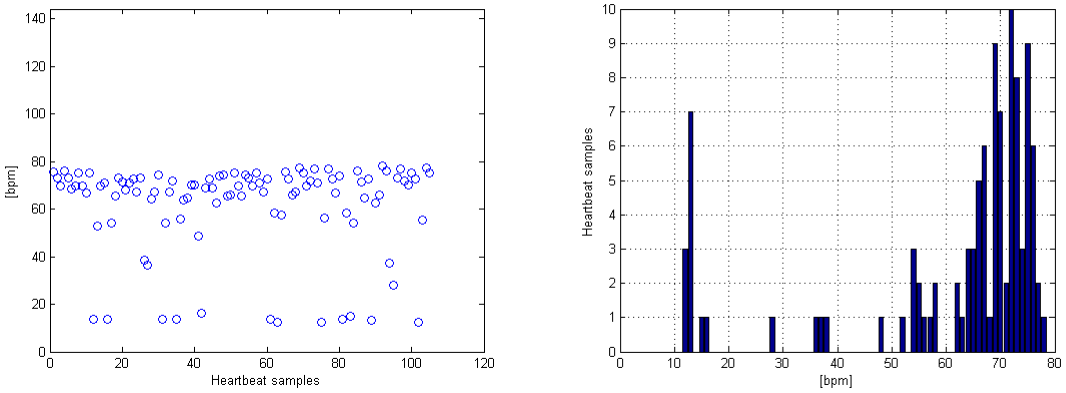

(a) Interbeat distance ID (b) Histogram ID

Figure 4.12: HbD-KmA

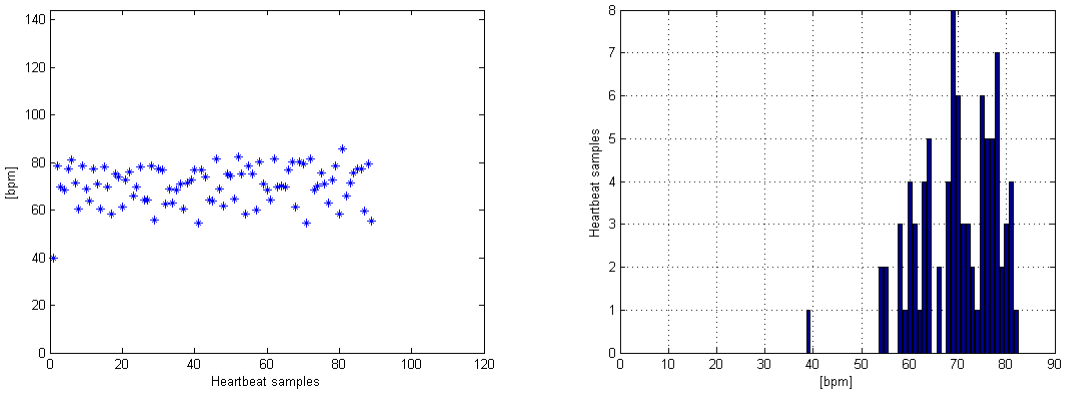

(a) Interbeat distance ID (b) Histogram ID

Figure 4.13: HBS-WPPD

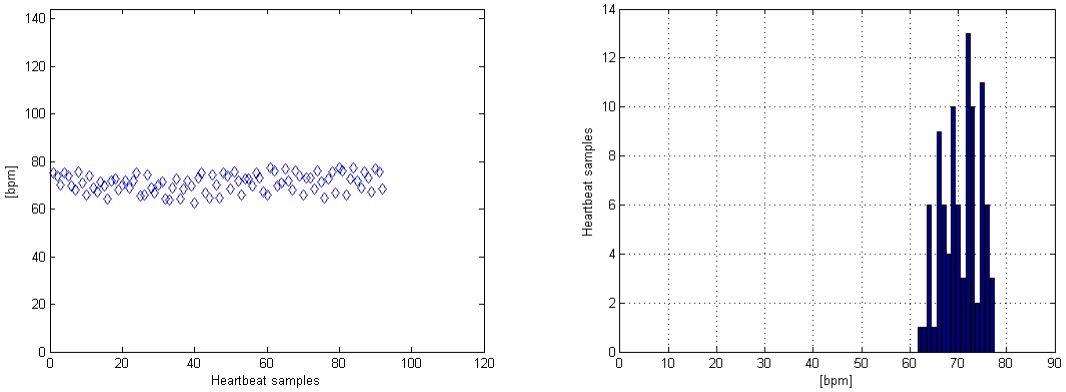

(a) Interbeat distance ID (b) Histogram ID

Figure 4.14: GT

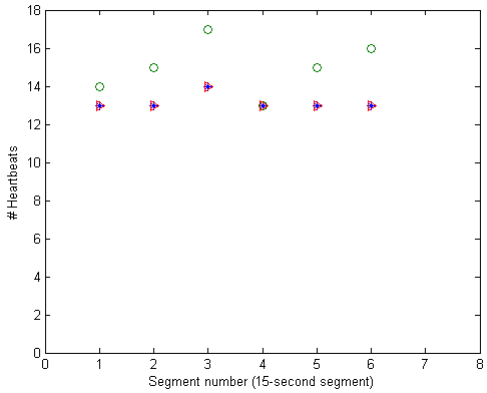

Figure 4.15: Number of Heartbeats detected by HbD-KmA(^{O}),WPPD($*$),GT($\triangleright$)

Subject 4

Correct_detection =95.6%

	HB	NHB
HB (Class 1)	115	3
NHB (Class 2)	23	456

Table 4.4: Subject 4-KM-Confusion matrix

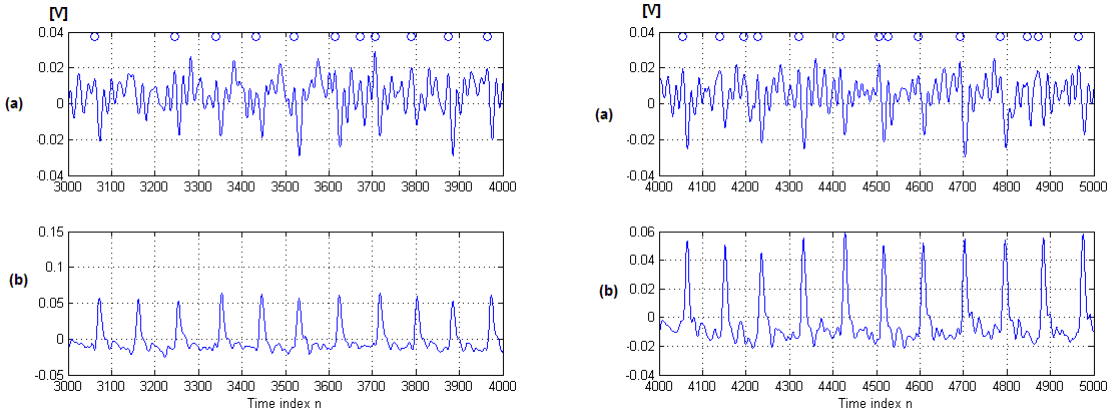

(a) (b)

Figure 4.16: Heartbeats detected by the k-means algorithm for 2 time slices (left and right) (a) processed BCG signal with a circle on top (^{O}) designating HB, (b) GT signal

Heart rate estimation

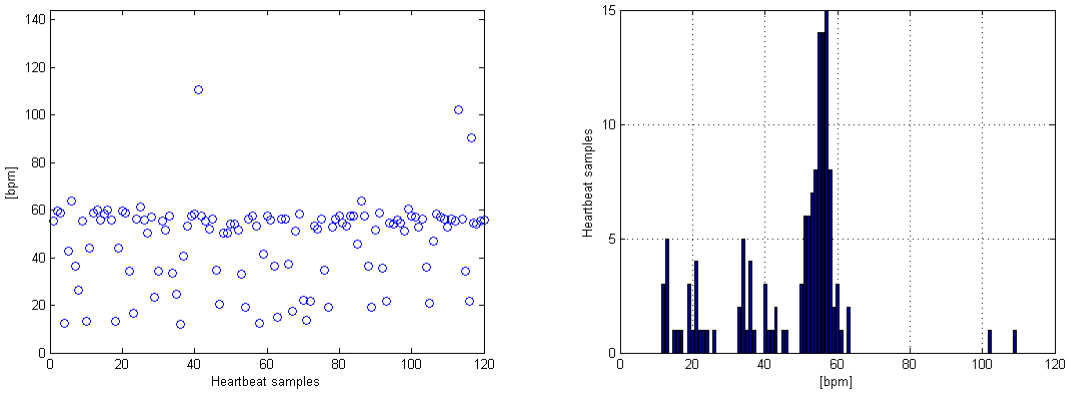

(a) Interbeat distance ID (b) Histogram ID

Figure 4.17: HbD-KmA

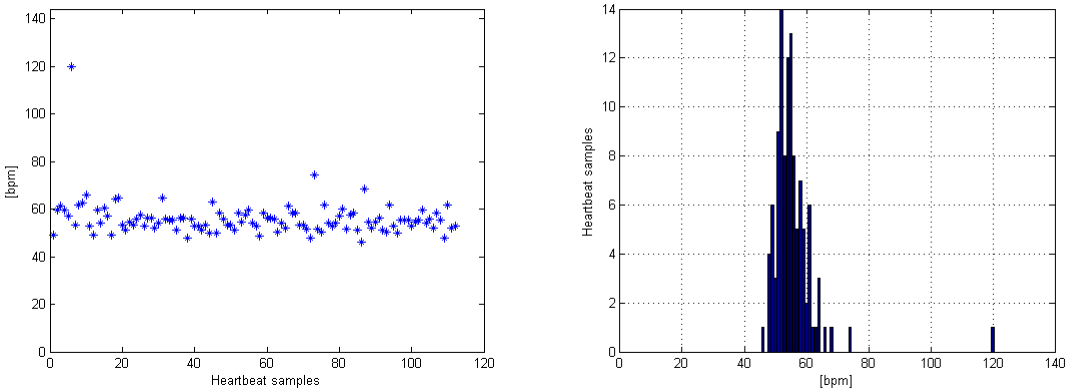

(a) Interbeat distance ID (b) Histogram ID

Figure 4.18: HBS-WPPD

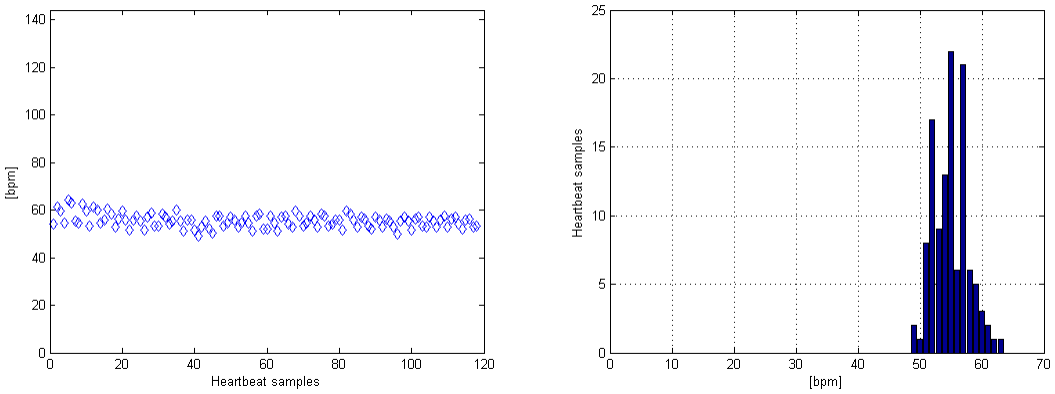

(a) Interbeat distance ID (b) Histogram ID

Figure 4.19: GT

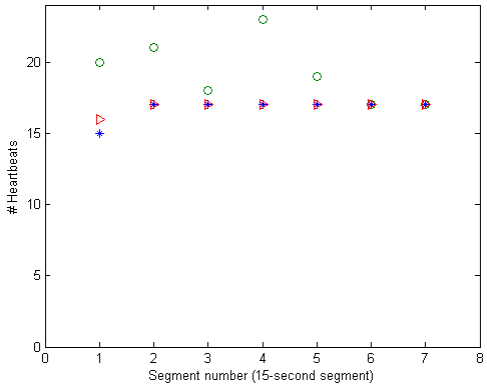

Figure 4.20: Number of Heartbeats detected by HbD-KmA(^{O}),WPPD($*$),GT($\triangleright$)

Subject 5

Correct_detection =97.2%

	HB	NHB
HB (Class 1)	104	3
NHB (Class 2)	16	554

Table 4.5: Subject 5-KM-Confusion matrix

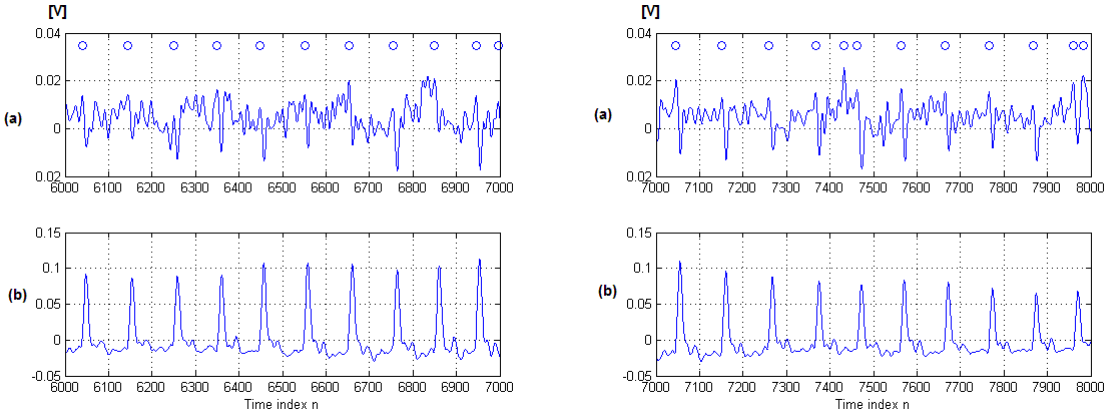

(a) (b)

Figure 4.21: Heartbeats detected by the k-means algorithm for 2 time slices (left and right) (a) processed BCG signal with a circle on top (^{O}) designating HB, (b) GT signal

Heart rate estimation

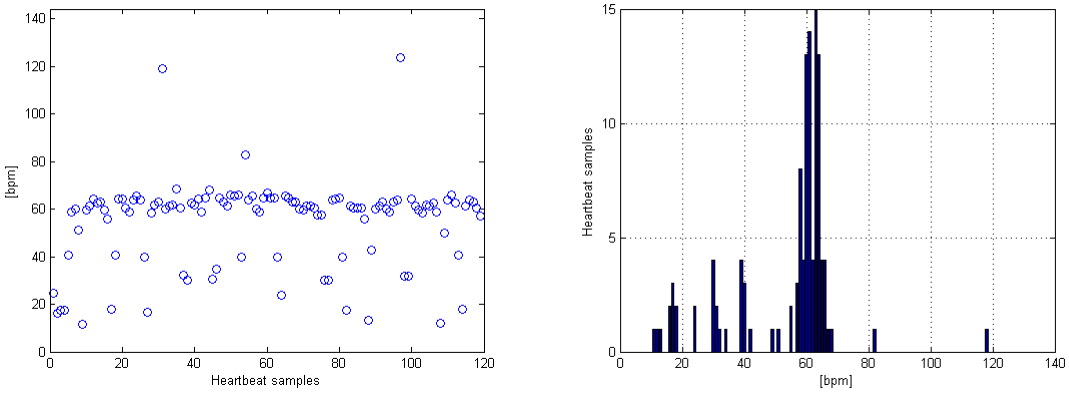

(a) Interbeat distance ID (b) Histogram ID

Figure 4.22: HbD-KmA

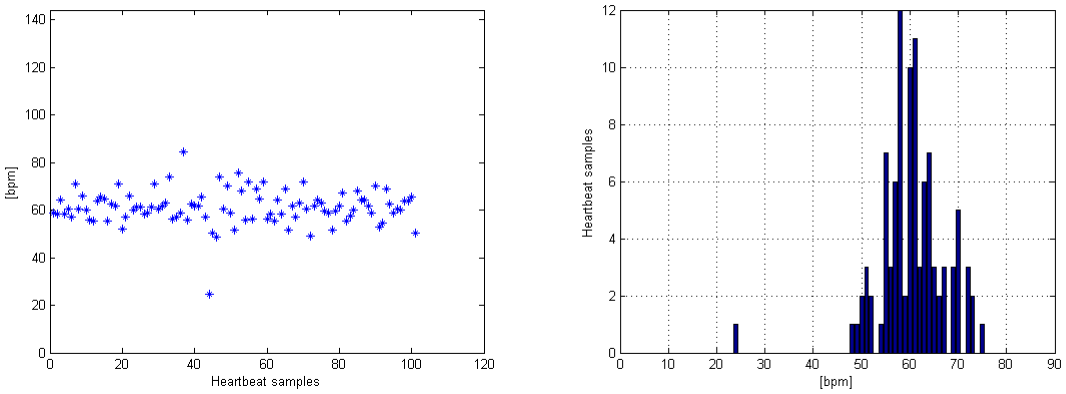

(a) Interbeat distance ID (b) Histogram ID

Figure 4.23: HBS-WPPD

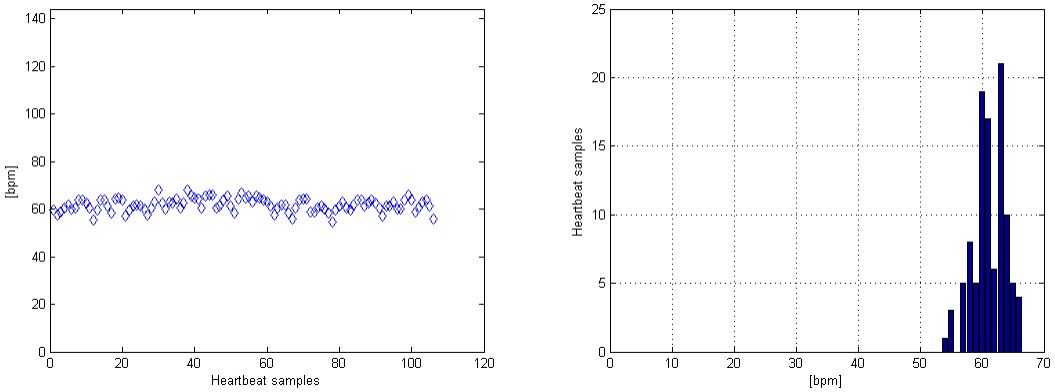

(a) Interbeat distance ID (b) Histogram ID

Figure 4.24: GT

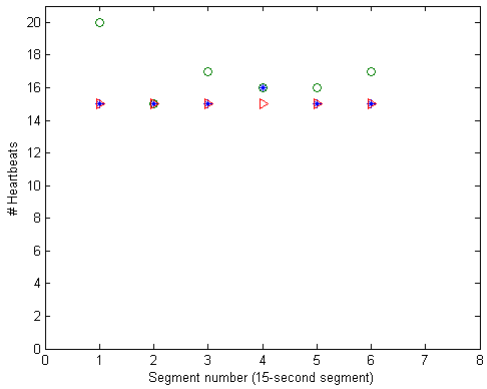

Figure 4.25: Number of Heartbeats detected by HbD-KmA(^{O}),WPPD($*$),GT($\triangleright$)

Heart rate estimation (comparison)

Measures of mean and one standard deviation were calculated for each participant, from the interbeat distances computed for the GT signal and detected by the WPPD and HbD-KM algorithms.

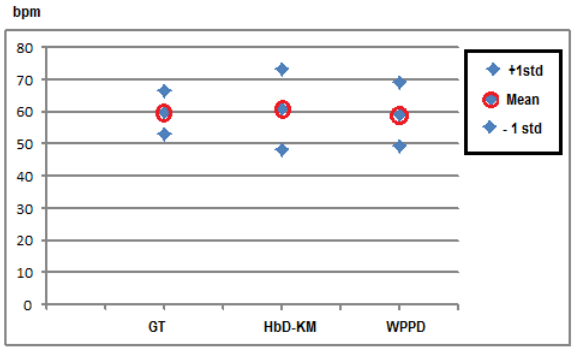

Figure 4.26: Subject 1: Heart rate estimated from the beat-to-beat interval computed using GT, HbD-KM and WPPD

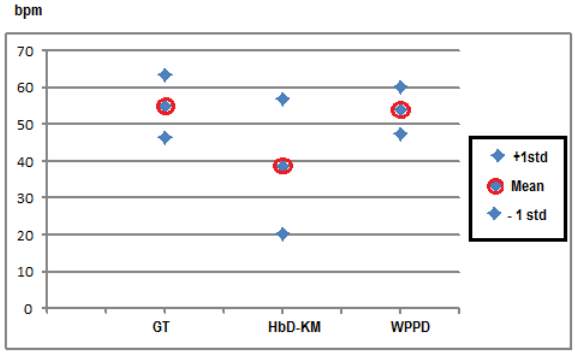

Figure 4.27: Subject 2: Heart rate estimated from the beat-to-beat interval computed using GT, HbD-KM and WPPD

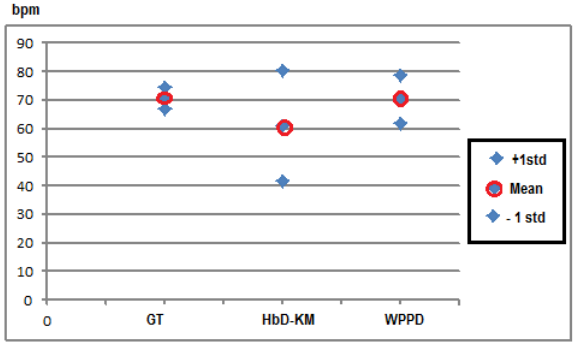

Figure 4.28: Subject 3: Heart rate estimated from the beat-to-beat interval computed using GT, HbD-KM and WPPD

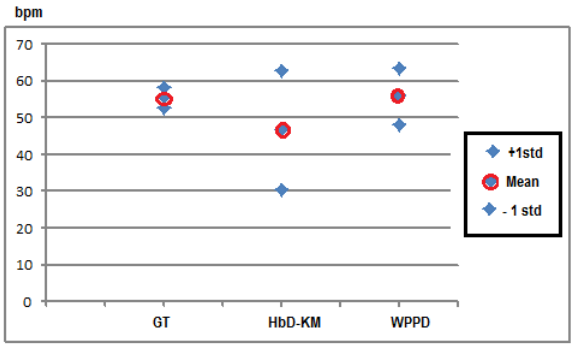

Figure 4.29: Subject 4: Heart rate estimated from the beat-to-beat interval computed using GT, HbD-KM and WPPD

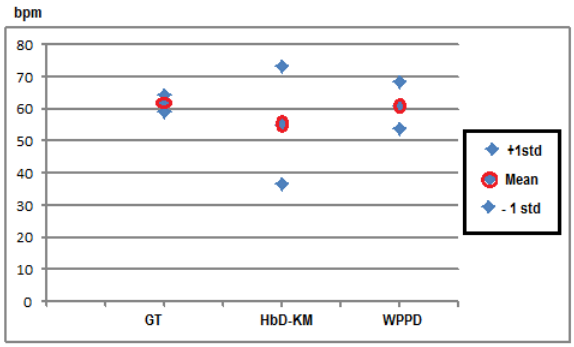

Figure 4.30: Subject 5: Heart rate estimated from the beat-to-beat interval computed using GT, HbD-KM and WPPD

4.2 HbD-KM results -TigerPlace setting

Subject 6

Correct_detection =70.3%

	HB	NHB
HB (Class 1)	85	2
NHB (Class 2)	181	348

Table 4.6: Subject 1-TG -KFCM-Confusion matrix

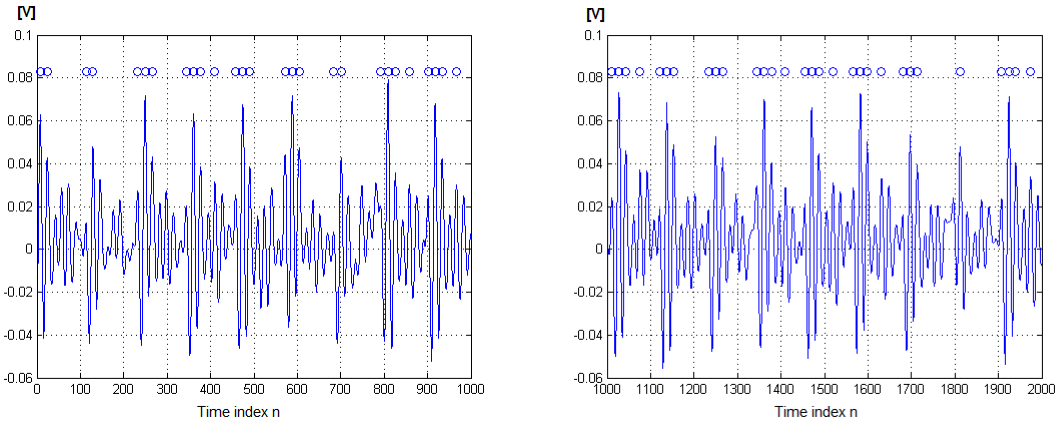

(a) (b)

Figure 4.31: Heartbeats detected by the k-means algorithm for 2 time slices processed BCG signal with a circle on top (^{O}) designating HB

Using the set of features (4 features) showed in Figure 3.24

Correct_detection =83.3%

	HB	NHB
HB (Class 1)	77	10
NHB (Class 2)	93	435

Table 4.7: Subject 1-TG -KFCM-Confusion matrix

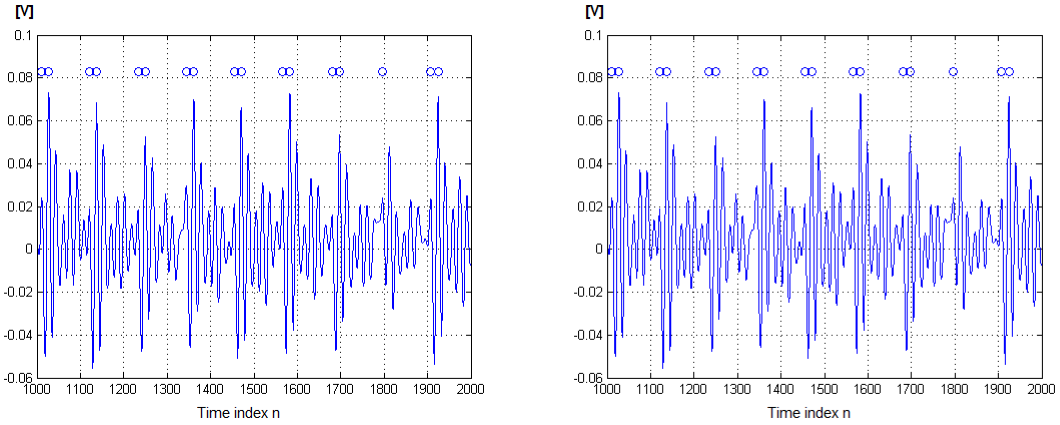

(a) (b)

Figure 4.32: Heartbeats detected by the k-means algorithm for 2 time slices processed BCG signal with a circle on top (^{O}) designating HB

Chapter 5

Discussion

Experimental results were obtained by testing the data collected from six subjects using the transducer arrangement proposed in Figure 3.4 and the Heartbeat Detection using K-means (HbD-KM approach). The arrangement was tested using a coil spring mattress and an air mattress with firmness control set to the higher level. The data collected from all the subjects were tested for the set of features described in Figure 3.20. Given the BCG waveform captured from the system with the coil spring mattress and the air mattress, a second set of features was tested for the latter. In order to verify the effectiveness of the heartbeat detection the data was labeled manually. The performance criteria used in the evaluation was the percentage of correct detection extracted from the confusion matrix. Finally, the heart rate estimated from the results reported for the HbD-KM approach and the WPPD algorithm were compared to the Ground Truth.

5.1 Transducer arrangement

The ability of the system for capturing heartbeats was tested for two types of mattresses. Five participants (testing group 2) were tested using a coil spring mattress (7 inches thick) and one participant (a TigerPlace resident) was tested on an air mattress with the firmness control set to the highest level. When a mattress firmer than coil spring bed mattress was selected, the system demonstrated the ability to capture the

heartbeat signal, but showed a different waveform pattern for the heartbeats. The BCG signals are shown in figure 3.23. Both BCG signals exhibit similar waveforms compared to BCG signals captured by other systems. Pineiro et al. [3] presented a set of typical displacement records from different ballistocardiography systems, which illustrate differences in the timing of waves and the relationship between them. Figure 5.1 shows the Starr's ballistocardiograph.

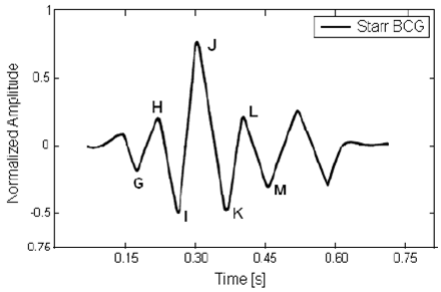

Figure 5.1: BCG signal presented in [3]

The H, I, J, K, and L waves should be dominant, forming a W shape. The H, I, J, K are the systolic waves. The W shape is certainly represented for both signals shown in Figure 3.23. The variation in number and shape for the waves around the W component may be caused by the presence of noise, motion, the system itself (the type of mattress) and the characteristics for the participant (body type and heart condition). Pineiro et al. [3] stated that all the non-systolic components are rarely perceptible and also highlights that it is very easy to produce artifacts, either by the device's architecture, or by any form of patient movement, as well as by respiration itself. Under these considerations and the observation of the BCG signals recorded from the participants with different body types, we can see that the BCG signal varies from person to person. Figures 4.1, 4.6, 4.11, 4.11, 4.16 and 4.31 illustrate this observation. But they show a different pattern if compared between the ones collected using a coil spring mattress and an air mattress. Although all the BCG signals show the occurrence of heartbeats, a personalized system could be an option to enhance the H-I-J-K-L waves. This can be achieved by varying the volume of water (experimental tests showed this).

Another consideration is the transducer arrangement, would provide the additional capability of detecting posture changes. Considering that the voltage output varies linearly with the exerted force and the four transducers are strategically placed vertically underneath the mattress stretched out across the bed width, the system is able to determine whether someone is lying on them by selecting the higher level of voltage/s measured from the transducers. This can lead to the estimation of the person's position and be used also for additional analysis of restlessness, since it can show the position changes overnight. Figure 3.22 shows a 58-minute data segment from transducers placed as shown in Figure 3.4. Voltages recorded from transducers 2 and 3 show that the participant is lying on them.

5.2 Heartbeat detection using k-means (HbD-KM)

Results for the data collected from subject 1 are shown in Table 4.1; the percentage of correct identification of heartbeats (99.7 %), shows that the feature selection was able to characterize the BCG-J wave. Looking at Figure 4.1 (a) and (b) shows the peaks clustered in class 1 (which we define as class heartbeat, because of its smaller number) with a circle on top. Only two heartbeats were clustered in the class 2 (class Non-heartbeats).

Table 4.2 shows the results for subject 2, who presented the lowest percentage of correct classification. From Figure 4.6, we can see that the k-means algorithm clustered into class heartbeats the peak prior to the occurrence of a heartbeat. This is reflected in the confusion matrix, where the algorithm clustered 51 non-heartbeat peaks in the class heartbeats. Results for subjects 3, 4 and 5, shown in Tables 4.3, 4.5 and 4.4, display that the percentages of correct identification of heartbeats was greater than 95% and the number of non-heartbeats is not as high as it was for subject 2. Although it seems acceptable, when the beat-to-beat distance is computed, the error in the detection of the exact location of the heartbeat has significant influence in the computation of the heart rate. Compared to the GT signal, only subject 1 shows a reasonable estimation when the beat-to-distance is plotted and represented in a histogram (Figure 4.2). Figures

4.7, 4.12, 4.22 and 4.17, show how the errors in the heartbeat location will introduce an artifact in the measure of the heart rate. When compared to the GT signal, the beat-to-beat distance did not show much difference in range in comparison of the data collected from subject 1. Looking at Figure 4.4 and 4.2, the difference in range may be due to the different characteristics of the pulse sensor and the pressure sensor attached to the transducer, along with the different type points measure of signal. The measure may be also influenced by the motion introduced by the piezoelectric device used as Ground Truth, as it is specified by the manufacturer on its data sheet [22].

The beat-to-beat distance computed from the GT signal compared to the results obtained from subjects 2, 3, 4 and 5 show the need for improving the feature selection, in order to get the data grouped into two clusters, where one of them will have the locations of the peaks that represent the occurrence of a heartbeat. Theodoridis highlights the importance of the selection of features for achieving a good classification [23].

If we consider the cases when the algorithm failed clustering, the peaks that represent the BCG-J wave, case 1 would be when the BCG-J is attenuated (Figure 4.6) and case 2) when the amplitude and characteristics of other peaks are increased by noise or motion, which may correspond to the case when there is body motion. Pineiro et al. [3] mentioned that it is very easy to produce artifacts, either by the device's architecture, or by any form of patient movement, as well as by respiration itself. It also says that in some cases, marked respiratory variation affects the BCG waves. Figures 5.2 and 5.3 shows the effect of respiration in the data collected from the Hydraulic Bed Sensor system.

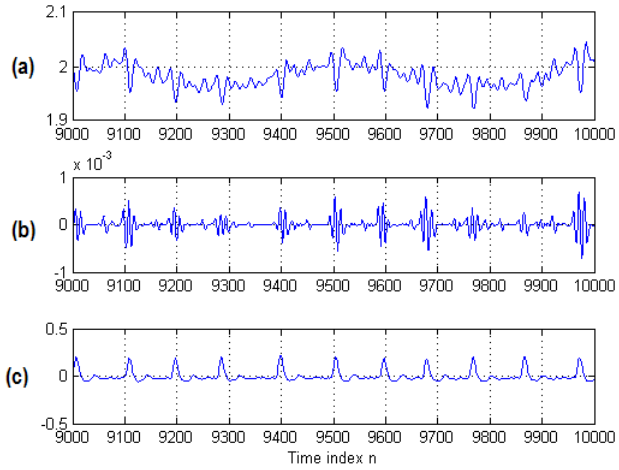

Figure 5.2: Effect of the respiration on the BCG signal lowpass filtered at 10 Hz (a) the BCG signal after bandpass filtering at 10 Hz/[0.4-10 Hz], (b) the derivative of the squared BCG signal and (c) the signal captured from the piezoelectric device used as ground truth.

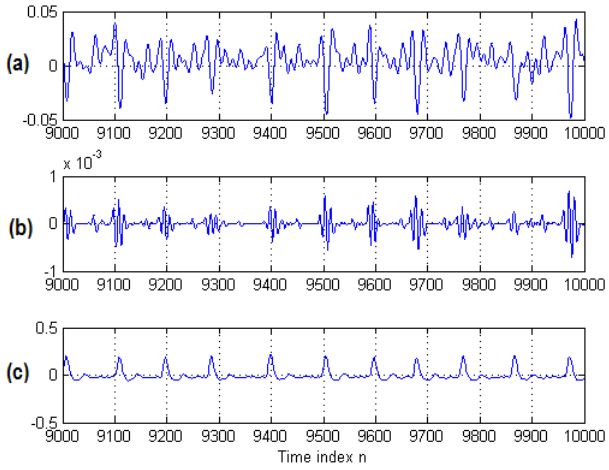

Figure 5.3: Effect of the respiration on the BCG signal bandpass filtered at 0.4 and 10 Hz
(a) the BCG signal after bandpass filtering at 10 Hz/[0.4-10 Hz], (b) the derivative of the squared BCG signal and (c) the signal captured from the piezoelectric device used as ground truth.

The variation in amplitude shown in Figure 5.2 (a) remains in Figure 5.3 (b). Two out of three features extracted from the participant's data are based on the variation

of the amplitude of the peak that represents the BCG-J wave. This may be one of the causes for the poor detection of heartbeats. Looking at the data of subject 1 compared to the rest, it is evident that the amplitude for the peak that represents the BCG-J wave is greater compared to the peaks around it.

A new set of features is also needed for the resident of TigerPlace; evaluation of the HbD-KM on the BCG data collected for an air mattress (level of firmness set to the highest level) using the features computed for the participant of the testing group 2 reported that the percentage of correct identification of heartbeats was 70.3 %. Figure 4.31 shows that more than two peaks adjacent to the BCG-J wave are clustered in the same cluster where the heartbeats are. To improve the percentage of correct detection, new features were tested (Figure 3.24). Even though the BCG signal obtained from the coil spring mattress does not look exactly like the one obtained from a coil spring mattress, both waveforms show the occurrence of the BCG-J wave. For the set of features shown in Figure 3.24, the k-means algorithm achieved 83.3% of correct detection. This time the number of non-heartbeats detected as heartbeats decreased almost 50%. Figure 4.32 shows that the k-means algorithm in this case clustered the peaks that represent heartbeats and the peaks located before them. As Web et al. [26] stated, when performing k-means, it is important to run diagnostic checks for determining the number of clusters in the data set. The author also comments that the problem of deciding how many clusters are present in the data is one common to all clustering. We looked at the distribution of the data after a dimensionality reduction (Figure 3.25), which suggested to use k=3. It is desirable to keep the number of clusters in two classes, so this estimation can be avoided. One way of doing this may be finding additional features that represents the BCG- IJKL complex and trying different clustering methods, since different clustering techniques can lead to different results [25]. If the option of exploring the 3-classes problem is considered, the first step will be to identify whether the new cluster observed in Figure 3.25 is a valid cluster [26].

5.3 Detection of the peak location -Comparison WPPD algorithm and KbD-KM

As mentioned previously Bruse et al. [2] proposed a new approach that offers heart rate estimates on a beat-to-beat basis and is designed to cope with arrhythmia. This estimation compared to other algorithms offers the possibility to compute the beat-to-beat interval, which can be used in studies of Heart Rate Variability (HRV). This approach coincides with the approach presented in [1], where the heart rate is computed based on the number of heartbeats counted in non-overlapping 15-second segments. Unlike [2] that finds the location of the heartbeat in the BCG signal, [1] finds the locations for the extracted heartbeats computed using the WPPD algorithm. Results from Figures 4.26, 4.27, 4.28, 4.29 and 4.30 show the heart rate estimation of the WPPD algorithm, the HbD-KM approach compared to the GT signal, in terms of the mean and one standard deviation.

Computing the beat-to-beat interval from the WPPD signal can lead to erroneous estimations, since the location of the peak can be affected by noise, body motion, and respiration. Experimental observation of different WPPD signals has shown that there is a possible shift of the detected heartbeats caused by the windowing of the signal. Heise et al. [1] acknowledge this when the results showed ± 1 heartbeat, when comparing 15-second segments to the GT signal. Figure 3.5 illustrates this observation. This will be an issue if it is intended to use this data for identifying abnormalities (like arrhythmia) or studies of Heart Rate Variability. To fill this gap, the Heartbeat Detection using k-means approach (HbD-KM) was developed. Since the preliminary results were successful for only one of the participants, refinements to this algorithm to ensure its robustness can improve their performance.

Heart rate computation

Figures 4.5, 4.10, 4.15, 4.25 and 4.20, show the count of heartbeats for every 15-second segment reported by the HbD-KM and WPPD-A compared to the GT signal. As before, HbD-KM did not give good estimations for subjects 2, 3, 4 and 5, while the

WPPD showed a consistent performance that in many of the cases gave the same estimate as the GT. This can be explained in part by the insensitivity of the algorithm to the respiration. Results from [1] reported that the WPPD algorithm for detecting heartbeats is relatively insensitive to changes in respiration and respiration cycle. This is not the case for the KbD-KM algorithm, which due to the features used, bases its estimations on the amplitude of the peaks and can find problems if the BCG-J peak decreases too much in amplitude.

Figures 4.26, 4.27, 4.28, 4.29 and 4.30 summarize the performances of the HbD-KM and WPPD compared to the GT, based on the computation of the mean and observation of the variability of the data (±1 std). Only subject 1 showed consistency for the three estimations when the mean (mean-GT=60 bpm, mean-HbD-KM=61 bpm and mean-WPPD=59 bpm) and the variability of the data (±1 std) were computed (var-GT=[53-67] bpm, var-HbD-KM=[48-72] bpm and var-WPPD=[49-69] bpm). Observations for subject 2, 3, 4 and 5 showed erroneous heart rate estimations for HbD-KM. The worst estimation was computed for subject 2, which reports a mean HbD-KM= 39 bpm, when the value reported by the GT was 55 bpm. WPPD showed again to be reliable on the heart rates reported, the mean compared to the GT estimated reported similar heart rates for the 2-minute data.

5.4 Artifacts

Body movements, posture changes, and leaving the bed may corrupt the measurement of the system. Watanabe and Mack [5, 11] identified the importance of minimizing the impact of movement artifacts on surrounding segments. Some considerations have to be made for our system, since the k-means algorithm will cluster peaks produced by slight movement, or portions of the segment corrupted by noise in the same class as heartbeats.

The GT signal is also susceptible to error caused by motion[ADI2011]. Figure 4.9 illustrates this, where three GT beat-to beat intervals fall between 0 to 40 bpm.

In long-term measurement, it is important to manage these artifacts in a reliable

way, [27]. The artifacts observed in ballistocardiography are chiefly related to patient motion, and complementary causes are unavoidable limitations in the device mechanical architecture, for instance sensor bandwidth limitations, or platform resonance. In addition distortion of the ballistocardiograph output may also occur due to any of a number of simple events, from breathing to posture changes, even with a seemingly calm and still patient [3].

For the selection of the transducer arrangement, we defined the output of the VFM peak detector as the reliability index. Although this output can be proven useful for identifying the presence of a well defined BCG signal, it is important to mention that it introduces artifacts related to the estimation of the location of the pulse signal used as GT signal.

Chapter 6

Conclusions and Future Work

6.1 Conclusions

The results of testing the transducer arrangement proposed for the hydraulic bed sensor system on a group of eight diverse subjects (ranging in age and body types) showed that it is capable of detecting the occurrence of heartbeats for seven out of eight participants. It was also demonstrated from the transducer placement studies, that the ability of the system for capturing heartbeats increases using this arrangement, even when positioning under an air mattress instead of a coil spring mattress.

Clustering techniques have been proposed and utilized to find the precise location of the heartbeat on BCG signal. After running preliminary tests on data collected on a coil spring mattress for the Heartbeat Detection using k-means algorithm (HbD-KM) assuming a two-class problem, it showed the potential of identifying the location of the heartbeat based on the BCG-J wave and computing the beat-to-beat interval, which can be used for studies of heart rate variability (HRV). Even so, the heartbeat detection for four out of five participants scored marginally. The results for one of the participants (subject 1) achieved 99.7 % of correct detection, 0% false positives and 1.8% false negatives while the worst was 91.4% of correct detection, 0% false positives and 42.5% false negatives for subject 2. Moreover, observation of the heartbeat signal plotted along with the locations of the peaks clustered on the smallest cluster, showed strong correlations between the heartbeat occurrence and the location detected by

the k-means algorithm. Additional testing using a different set of features used in the laboratory setting, was performed in order to improve the detection for the data collected from an air mattress (residential living), which showed that the problem can be studied as a 3-class problem.

Finally, it was demonstrated that the BCG signal captured by the new hydraulic bed sensor system, increased the robustness of our Windowed-Peak-to-Peak Deviation compared to a Ground Truth signal. This was observed for five records. The mean and the variability of the beat-to-beat distance was computed to show its performance; while HbD-KM (for four out to five records) showed the need of developing a refinement stage in order to improve the percentage of correct detection.

6.2 Future work

1. The HBS system presented shows promise as a general sleep analysis tool, since it can provide additional information regarding to:

- Presence and position of a person on the bed, using a straightforward algorithm based on the voltage values recorded by the transducers
- Estimation of respiration rate
- Detection of abnormalities in sleeping pattern such as sleep-wake periods and level of restlessness.

2. Results shown in section 3.2 for one of the participants, showed the need of determining the modifications required in order to capture his heartbeat signal. In this sense it is necessary to implement a signal to noise (S/N) ratio study in order to evaluate the reliability of the measurements for different conditions

- Sleeping postures
- Bed mattresses
- Body movements

3. Keeping in mind our goal of long-term monitoring, more investigation has to be made on developing the automated algorithms for:

- Implementing a noise reduction algorithm
- Segmenting the data into useful/noisy for heartbeat/respiration detection
- Determining wake segments and sleep segments
- Finding the criteria for selecting a transducer when the subject is lying on more than one, based on the best representation of the BCG signal
- Finding a set of features that can better represent the IJKL BCG complex.
- Applying different clustering techniques
- Exploring 3 or more classes for the number of clusters

.

Bibliography

[1] D. Heise, L. Rosales, M. Skubic, and M. J. Devaney, "Refinement and evaluation of a hydraulic bed sensor," in *Proceedings of the 33rd Annual IEEE International Conference of the IEEE Engineering in Medicine and Biology Society*, Boston, August 2010, pp. 4356–4360.

[2] C. Bruser, K. Stadlthanner, A. Brauers, and S. Leonhardt., "Applying machine learning to detect individual heart beats in ballistocardiograms," in *Proceedings of the 32rd Annual IEEE International Conference of the IEEE Engineering in Medicine and Biology Society*, Buenos Aires, Argentina, August 2010, pp. 1926–1929.

[3] E. Pinheiro, O. Postolache, and P. Girao, "Theory and developments in an unobtrusive cardiovascular system representation: Ballistocardiography," pp. 201–216, 2010.

[4] M. Rantz, M. Skubic, and S. Miller, "Using sensor technology to augment traditional healthcare," in *Proceedings of the 32rd Annual IEEE International Conference of the IEEE Engineering in Medicine and Biology Society*, November 2009, pp. 776 – 785.

[5] D. Mack, J. Patrie, P. Suratt, R. Felder, and M. Alwan, "Development and preliminary validation of heart rate and breathing rate detection using a passive, ballistocardiography-based sleep monitoring system," in *IEEE Transactions on Information Technology in Biomedicine*, vol. 13, January 2009, pp. 111 – 120.

[6] D. Heise and M. Skubic, "Monitoring pulse and respiration with a hydraulic bed sensor," in *Proceedings of the 32rd Annual IEEE International Conference of the IEEE Engineering in Medicine and Biology Society*, Buenos Aires, Argentina, August 2010, pp. 1926–1929.

[7] J. Coughlin and J. Pope, "Innovations in health, wellness, and aging-in-place," vol. 17, 2008, pp. 47 – 52.

[8] C. Fausset, A. Kelly, W. Rogers, and A. Fisk, "Challenges to aging in place: Understanding home maintenance difficulties," vol. 25, no. 2, 2011, pp. 125–141.

[9] V. Masini and P. Rossi, "Studies of quantitative ballistocardiography: The velocity of body. displacement in patients with heart desease," USA, 1953.

[10] L. Giovangrandi, O. Inan, R.Wiard, M. Etemadi, and G. Kovacs, "Ballistocardiography a method worth revisiting," in *Proceedings of the 33rd Annual International Conference of the IEEE EMBS*, Boston, Massachusetts, USA, August 2011.

[11] K. Watanabe, T. Watanabe, H. Watanabe, H. Ando, T. Ishikawa, and K. Kobayashi, "Noninvasive measurement of heartbeat, respiration, snoring and body movements of a subject in bed via a pneumatic method," in *Proceedings of the 32rd Annual IEEE International Conference of the IEEE Engineering in Medicine and Biology Society*, vol. 52, no. 12, December 2005, pp. 2100–2107.

[12] X. Zhu, W. Chen, T. Nemoto, Y. Kanemitsu, K. Kitamura, K.Yamakoshi, and D. Wei, "Real-time monitoring of respiration rhythm and pulse rate during sleep," *IEEE Transactions on Biomedical Engineering*, vol. 53, no. 12, pp. 2553–2563, December 2006.

[13] Z. Beattie, C. Hagen, and T. Hayes, "Classification of lying position using load cells under the bed," in *Proceedings of the 33rd Annual International Conference of the IEEE EMBS*, Boston, Massachusetts, USA, August 2011.

[14] Y. Xinsheng, D. Dent, and C. Osborn, "Classification of ballistocardiography using wavelet transform and neural networks," vol. 3, 1996, pp. 937 – 938.

[15] A. Gaddam, S. Mukhopadhyay, and G. Gupta, "Intelligent bed sensor system: Design, expermentation and results," in *Sensors Applications Symposium (SAS)*, February 2010, pp. 220–225, 23–25.

[16] S. Nukaya, T. Shino, Y. Kurihara, K. Watanabe, and H. Tanaka, "Noninvasive bed sensing of human biosignals via piezoceramic devices sandwiched between the floor and bed," vol. PP, November 2010, p. 1.

[17] TigerPlace, "Tigerplace independent living by americare," 2011. [Online]. Available: www.americareusa.net

[18] M. J. Rantz, M. Skubic, S. J. Miller, and J. Krampe, "Using technology to enhance aging in placer," in *Proceedings of the International Conference on Smart Home and Health Telematics*, Ames, IA, June 2008, pp. 169–176.

[19] F. semiconductor, "Mxp 5010," 2011. [Online]. Available: http://cache.freescale.com

[20] N. Semiconductor, "Lm741," 2011. [Online]. Available: http://www.national.com/mpf/LM/LM741.html

[21] MAXIM, "Max7401," 2011. [Online]. Available: http://www.maxim-ic.com/datasheet/index.mvp/id/1920

[22] ADINSTRUMENTSi, "Mlt1010/d pulse transducer," 2011. [Online]. Available: http://www.adinstruments.com/products/hardware/research/product/MLT1010–D

[23] S. Theodoridis and K. K. F. Edition, *Pattern RecogKnition.* Canada: Elsevier, 2009, ,.

[24] C. Ding and X. He, "Principal component analysis and effective k-means clustering," Berkeley, 2004.

[25] C. Bishop, *Pattern Recognition and Machine Learning , First Edition.* USA: Springer, 2006.

[26] A. Web, *Statistical Pattern Recognition*. John Wiley and Sons, Ltd, l 2002.

[27] Q. Wang, P. Yang, and Y. Zhang, "Artifact reduction based on empirical mode decomposition (emd) in photoplethysmography for pulse rate detection," August 2010, pp. 959 – 962.

[28] Z. Aihua and Y. Fengxia, "Study on recognition of sub-health from pulse signal," in *Proceedings of the XX Annual International Conference on Neural Networks and Brain*, vol. 3, no. 12, October 2005, pp. 1516–1518.

[29] G. Demiris and H. Thompson, "Smart homes and ambient assisted living applications: From data to knowledge-empowering or overwhelming older adults? contribution of the imia smart homes and ambiant assisted living working group.s," vol. 6, no. 1, 2011, pp. 51–57.

[30] A. Lotherington and F. Olsen.

[31] D. Obeid, S. Sadek, G. Zaharia, and G. Zein, "Touch-less heartbeat detection and measurement-based cardiopulmonary modeling,," in *Proceedings of the 32rd Annual IEEE International Conference of the IEEE Engineering in Medicine and Biology Society*, August 2010, pp. 658–661.

[32] H. Chan, G. Chen, and M. L. S. Fang, "Touch-less heartbeat detection and measurement-based cardiopulmonary modeling," in *Proceedings of the 32rd Annual IEEE International Conference of the IEEE Engineering in Medicine and Biology Society*, January 2006, pp. 6668–6670.

[33] J. Kortelainen, M. Mendez, A. Bianchi, M. Matteucci, and S. Cerutti, "Sleep staging based on signals acquired through bed sensor," in *Proceedings of the 32rd Annual IEEE International Conference of the IEEE Engineering in Medicine and Biology Society*, May 2010, pp. 776 – 785.

[34] R. W. Pew and S. B. V. Hemel, "Technology for adaptive aging," 2004.

[35] J. Rafiee, M. Rafiee, and N. Prause, "Biosignals: Psychophysio-signal processing concept," April 2010, pp. 1 – 2.

Appendix A

Evaluation Trial presented in [1]

A.1 Combination of ws and fc2 - Subject 5

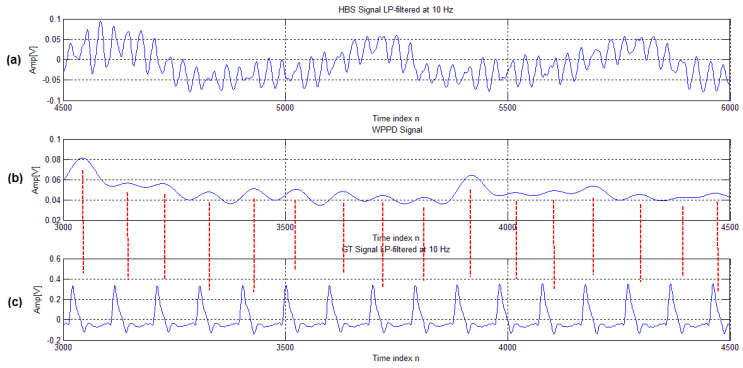

Figure A.1: Fifteen-second data segment being processed to extract heartbeats using the WPPD algorithm
(a) shows the signal after 10 Hz lowpass filtering, (b) shows the WPPD signal computed using a ws = 15 and fc2 = 1 Hz; and (c) shows the corresponding signal from the piezoresistive pulse sensor, used as ground truth for showing heartbeats.

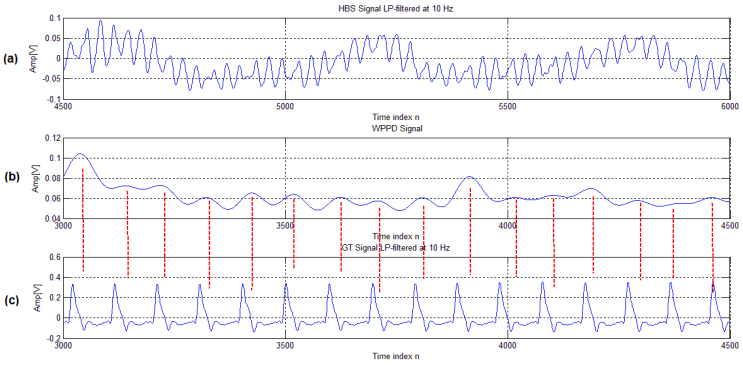

Figure A.2: Fifteen-second data segment being processed to extract heartbeats using the WPPD algorithm
(a) shows the signal after 10 Hz lowpass filtering, (b) shows the WPPD signal computed using a ws = 25 and fc2 = 1 Hz; and (c) shows the corresponding signal from the piezoresistive pulse sensor, used as ground truth for showing heartbeats.

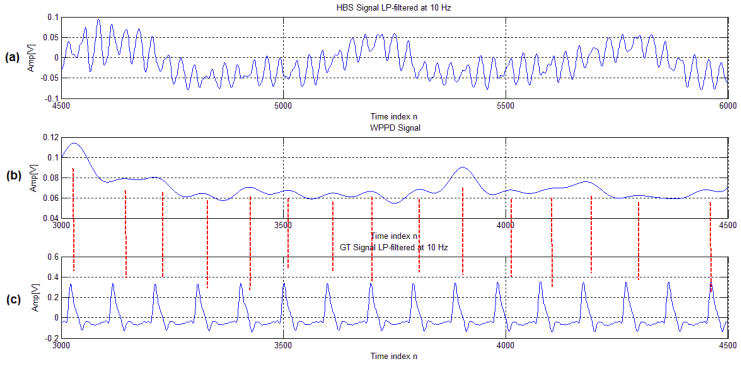

Figure A.3: Fifteen-second data segment being processed to extract heartbeats using the WPPD algorithm
(a) shows the signal after 10 Hz lowpass filtering, (b) shows the WPPD signal computed using a ws = 40 and fc2 = 1 Hz; and (c) shows the corresponding signal from the piezoresistive pulse sensor, used as ground truth for showing heartbeats.

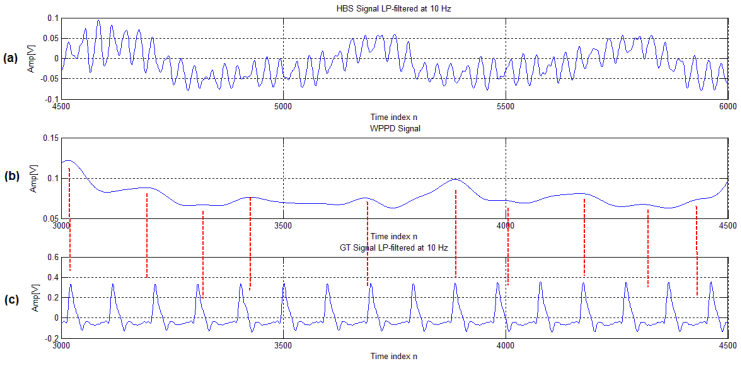

Figure A.4: Fifteen-second data segment being processed to extract heartbeats using the WPPD algorithm
(a) shows the signal after 10 Hz lowpass filtering, (b) shows the WPPD signal computed using a ws = 60 and fc2 = 1 Hz; and (c) shows the corresponding signal from the piezoresistive pulse sensor, used as ground truth for showing heartbeats.

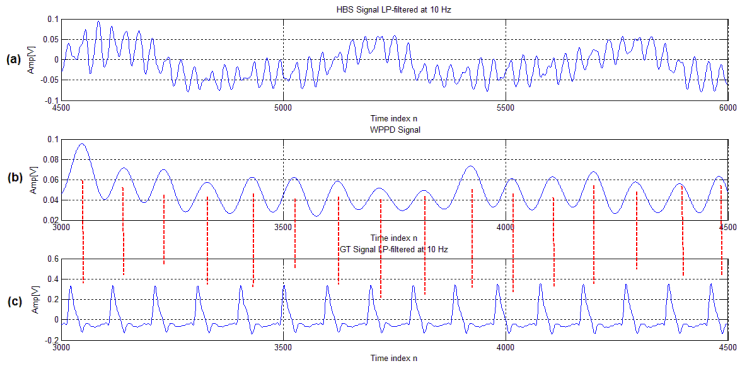

Figure A.5: Fifteen-second data segment being processed to extract heartbeats using the WPPD algorithm
(a) shows the signal after 10 Hz lowpass filtering, (b) shows the WPPD signal computed using a ws = 15 and fc2 = 1.5 Hz; and (c) shows the corresponding signal from the piezoresistive pulse sensor, used as ground truth for showing heartbeats.

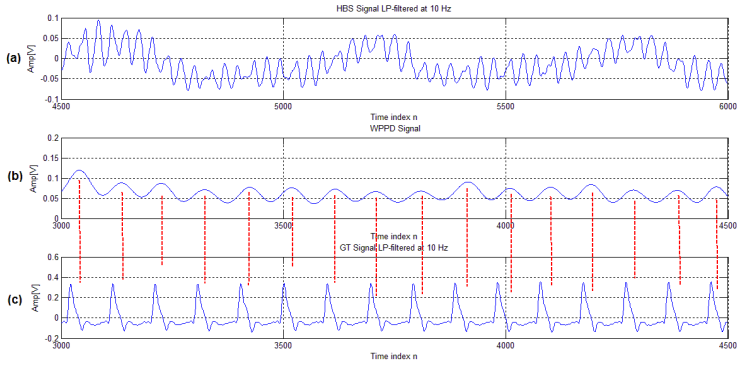

Figure A.6: Fifteen-second data segment being processed to extract heartbeats using the WPPD algorithm
(a) shows the signal after 10 Hz lowpass filtering, (b) shows the WPPD signal computed using a ws = 25 and fc2 = 1.5 Hz; and (c) shows the corresponding signal from the piezoresistive pulse sensor, used as ground truth for showing heartbeats.

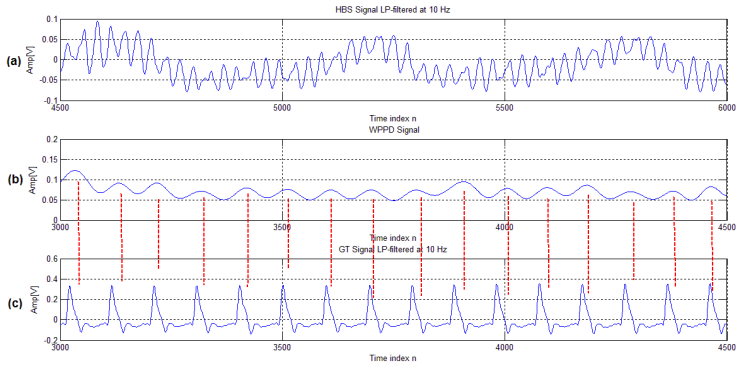

Figure A.7: Fifteen-second data segment being processed to extract heartbeats using the WPPD algorithm
(a) shows the signal after 10 Hz lowpass filtering, (b) shows the WPPD signal computed using a ws = 40 and fc2 = 1.5 Hz; and (c) shows the corresponding signal from the piezoresistive pulse sensor, used as ground truth for showing heartbeats.

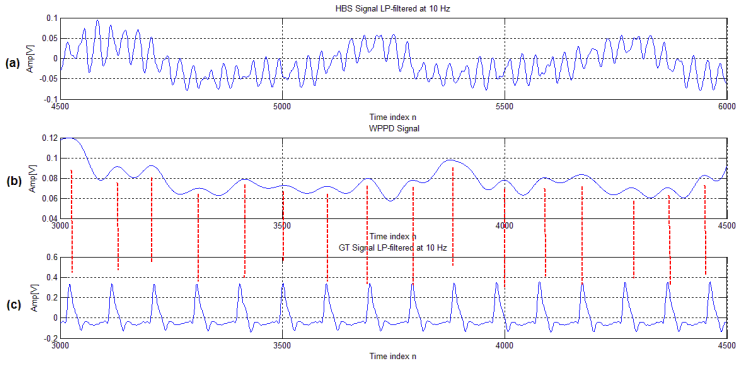

Figure A.8: Fifteen-second data segment being processed to extract heartbeats using the WPPD algorithm
(a) shows the signal after 10 Hz lowpass filtering, (b) shows the WPPD signal computed using a ws = 60 and fc2 = 1.5 Hz; and (c) shows the corresponding signal from the piezoresistive pulse sensor, used as ground truth for showing heartbeats.

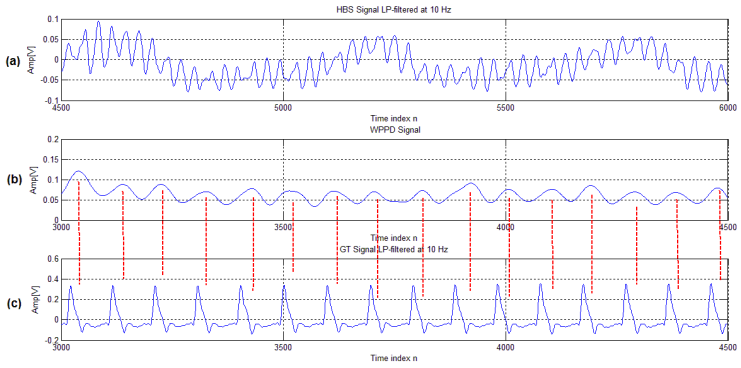

Figure A.9: Fifteen-second data segment being processed to extract heartbeats using the WPPD algorithm
(a) shows the signal after 10 Hz lowpass filtering, (b) shows the WPPD signal computed using a ws = 15 and fc2 = 2 Hz; and (c) shows the corresponding signal from the piezoresistive pulse sensor, used as ground truth for showing heartbeats.

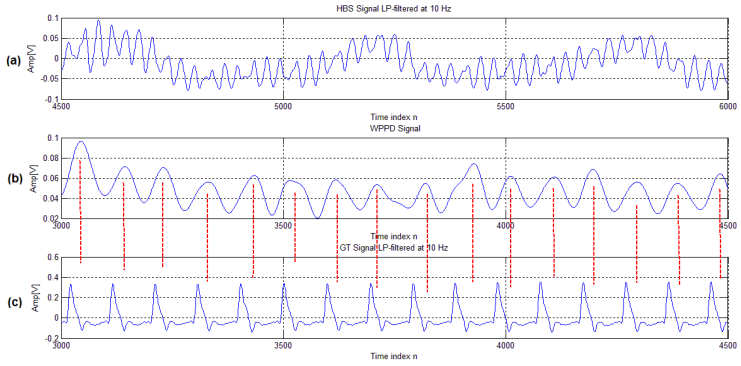

Figure A.10: Fifteen-second data segment being processed to extract heartbeats using the WPPD algorithm
(a) shows the signal after 10 Hz lowpass filtering, (b) shows the WPPD signal computed using a ws = 25 and fc2 = 2 Hz; and (c) shows the corresponding signal from the piezoresistive pulse sensor, used as ground truth for showing heartbeats.

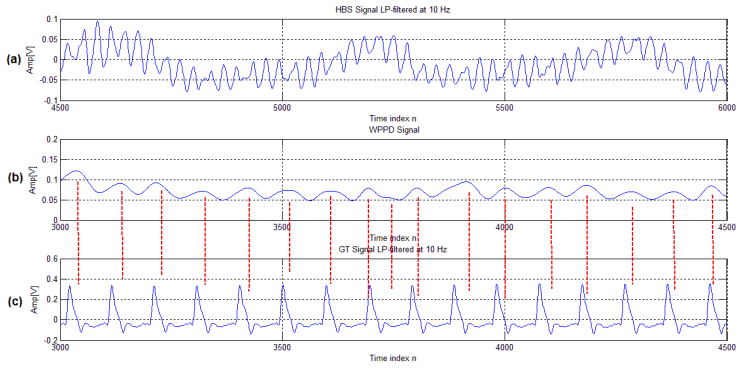

Figure A.11: Fifteen-second data segment being processed to extract heartbeats using the WPPD algorithm
\(a) shows the signal after 10 Hz lowpass filtering, (b) shows the WPPD signal computed using a ws = 40 and fc2 = 2 Hz; and (c) shows the corresponding signal from the piezoresistive pulse sensor, used as ground truth for showing heartbeats.

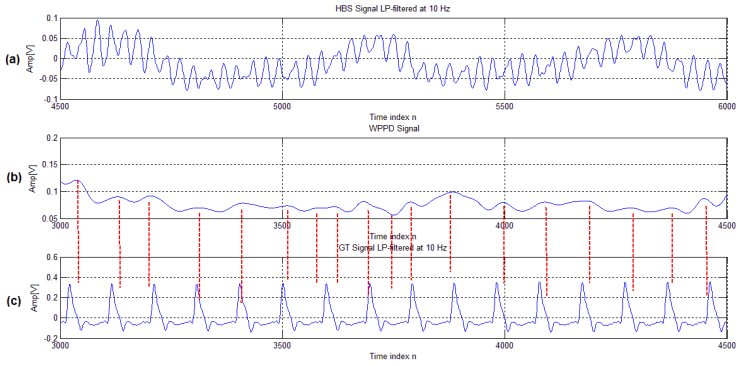

Figure A.12: Fifteen-second data segment being processed to extract heartbeats using the WPPD algorithm
(a) shows the signal after 10 Hz lowpass filtering, (b) shows the WPPD signal computed using a ws = 60 and fc2 = 2 Hz; and (c) shows the corresponding signal from the piezoresistive pulse sensor, used as ground truth for showing heartbeats.

A.2 HBS signal after lowpass filtering at 10 Hz-Subject 2

Figure A.13: Fifteen-second segment, Subject 2-B2-segment according to Figure 2.5 (a) shows the signal after 10 Hz lowpass filtering, (b) shows the corresponding signal from the piezoresistive pulse sensor, used as ground truth for showing heartbeats.

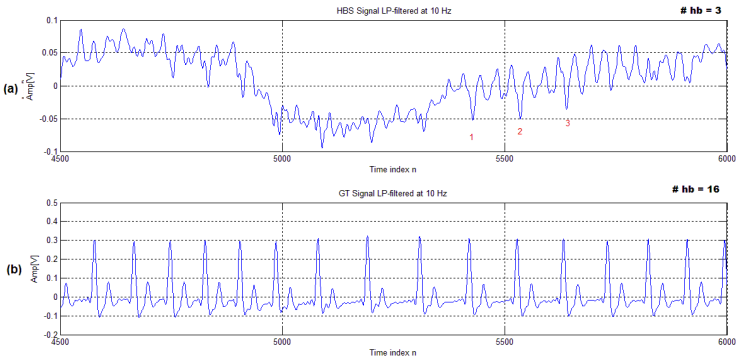

Figure A.14: Fifteen-second segment, Subject 2-B2-segment according to Figure 2.5 (a) shows the signal after 10 Hz lowpass filtering, (b) shows the corresponding signal from the piezoresistive pulse sensor, used as ground truth for showing heartbeats.

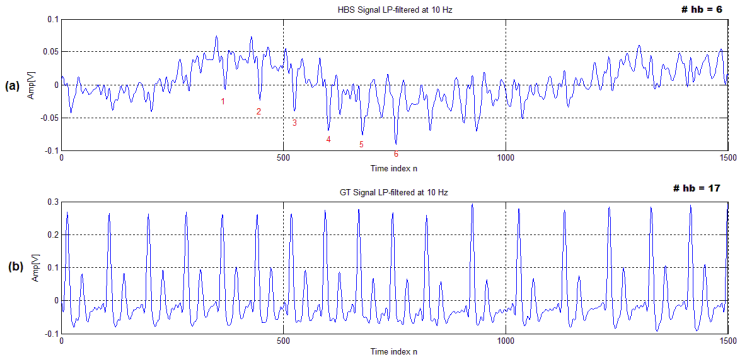

Figure A.15: Fifteen-second segment, Subject 2-B3-segment according to Figure 2.5 (a) shows the signal after 10 Hz lowpass filtering, (b) shows the corresponding signal from the piezoresistive pulse sensor, used as ground truth for showing heartbeats.

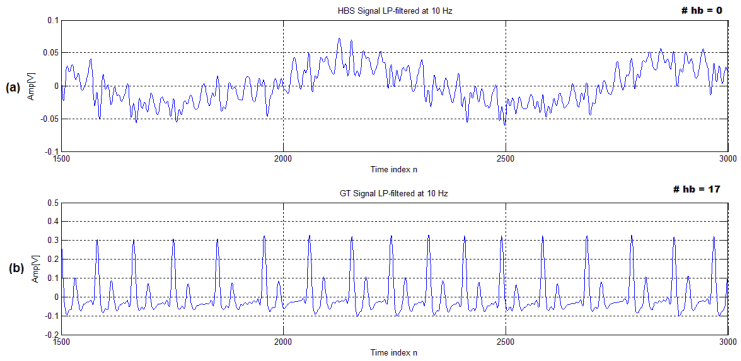

Figure A.16: Fifteen-second segment, Subject 2-B3-segment according to Figure 2.5 (a) shows the signal after 10 Hz lowpass filtering, (b) shows the corresponding signal from the piezoresistive pulse sensor, used as ground truth for showing heartbeats.

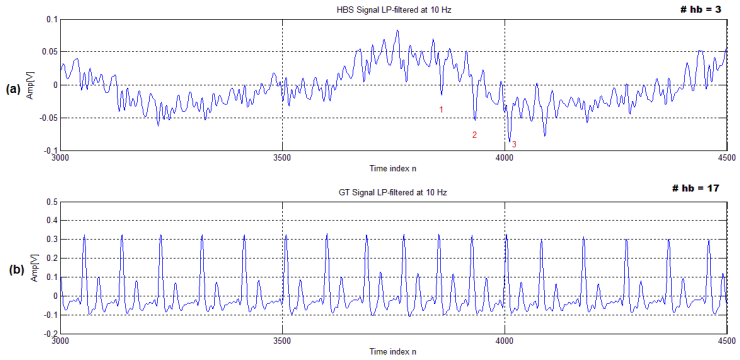

Figure A.17: Fifteen-second segment, Subject 2-B3-segment according to Figure 2.5 (a) shows the signal after 10 Hz lowpass filtering, (b) shows the corresponding signal from the piezoresistive pulse sensor, used as ground truth for showing heartbeats.

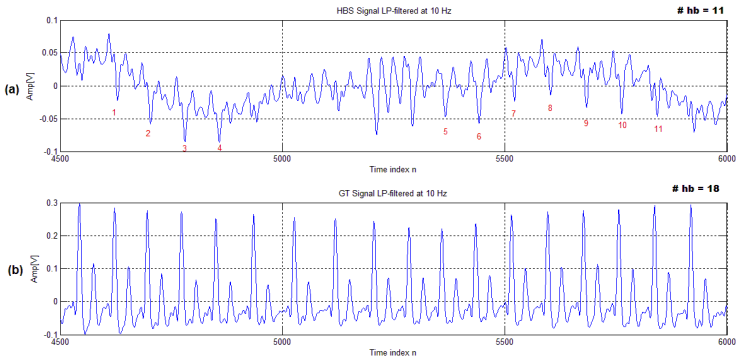

Figure A.18: Fifteen-second segment, Subject 2-B3-segment according to Figure 2.5 (a) shows the signal after 10 Hz lowpass filtering, (b) shows the corresponding signal from the piezoresistive pulse sensor, used as ground truth for showing heartbeats.

A.3 HBS signal after lowpass filtering at 10 Hz-Subject 4

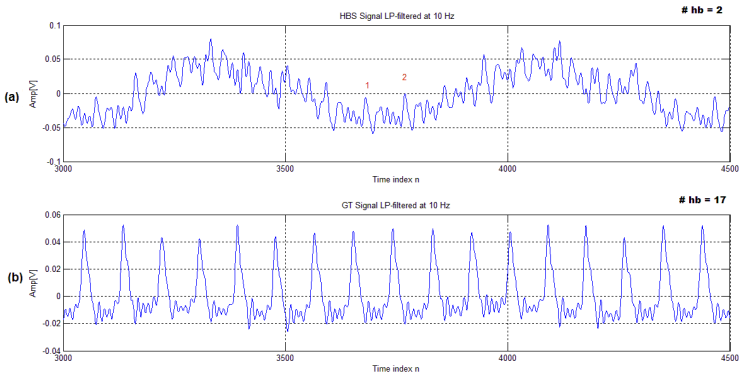

Figure A.19: Fifteen-second segment, Subject 4-B1-segment according to Figure 2.5 (a) shows the signal after 10 Hz lowpass filtering, (b) shows the corresponding signal from the piezoresistive pulse sensor, used as ground truth for showing heartbeats.

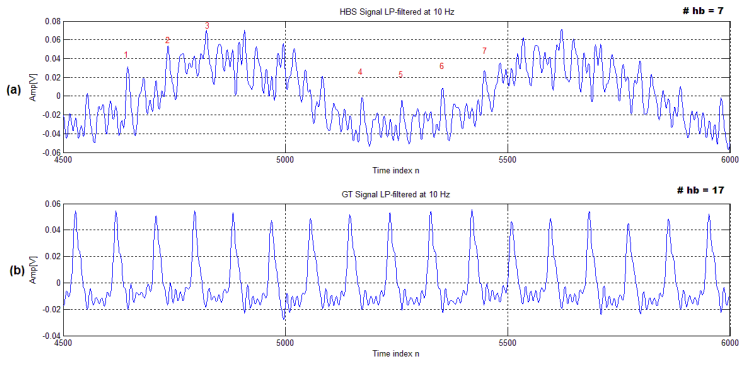

Figure A.20: Fifteen-second segment, Subject 4-B1-segment according to Figure 2.5 (a) shows the signal after 10 Hz lowpass filtering, (b) shows the corresponding signal from the piezoresistive pulse sensor, used as ground truth for showing heartbeats.

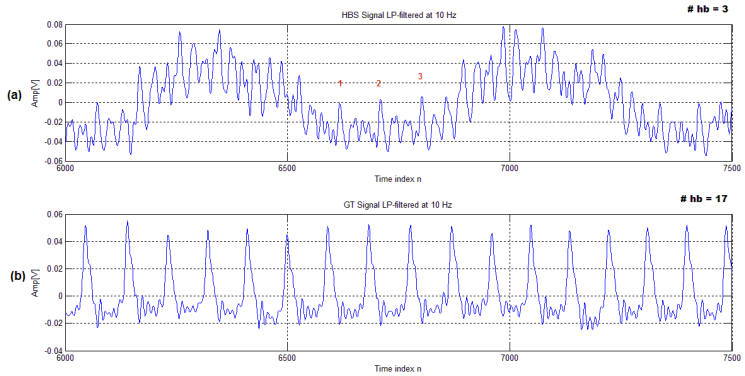

Figure A.21: Fifteen-second segment, Subject 4-B1-segment according to Figure 2.5 (a) shows the signal after 10 Hz lowpass filtering, (b) shows the corresponding signal from the piezoresistive pulse sensor, used as ground truth for showing heartbeats.

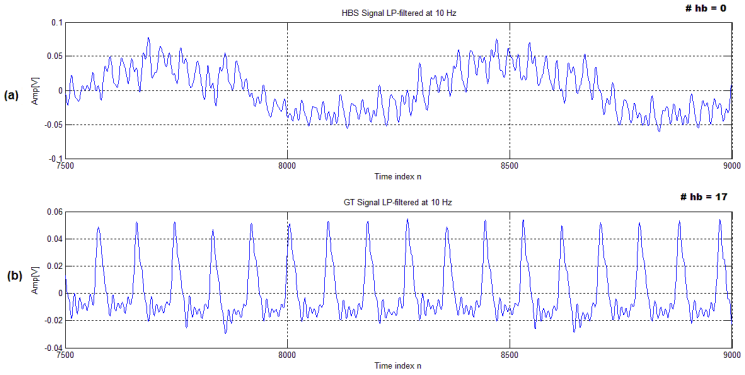

Figure A.22: Fifteen-second segment, Subject 4-B1-segment according to Figure 2.5 (a) shows the signal after 10 Hz lowpass filtering, (b) shows the corresponding signal from the piezoresistive pulse sensor, used as ground truth for showing heartbeats.

Appendix B

Transducer placement selection

B.1 Experiment 1

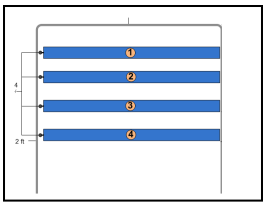

Figure B.1: 36 in. long trandsucers filled with 20 oz. of water

Subject 1

		fc2=1 Hz		fc2=1.5 Hz		fc2=2 Hz	
		V [%]	F [%]	V [%]	F [%]	V [%]	F [%]
T1	ws=15	0.0	0.0	56.9	35.8	69.9	52.8
	ws=25	0.0	0.0	36.6	46.3	48.8	57.7
	ws=40	0.0	0.0	0.0	0.0	28.5	38.2
	ws=60	0.0	0.0	0.0	0.0	24.4	27.6
T2	ws=15	0.0	0.0	4.1	62.6	0.0	0.0
	ws=25	0.0	0.0	0.0	0.0	0.0	0.0
	ws=40	0.0	0.0	0.0	0.0	0.0	0.0
	ws=60	0.0	0.0	8.1	56.9	0.0	0.0
T3	ws=15	24.4	22.0	59.3	37.4	0.0	0.0
	ws=25	0.0	0.0	48.0	47.2	0.0	0.0
	ws=40	0.0	0.0	26.8	67.5	0.0	0.0
	ws=60	0.0	0.0	0.0	0.0	36.6	63.4
T4	ws=15	0.0	0.0	38.2	57.7	49.6	56.9
	ws=25	0.0	0.0	15.4	61.8	30.1	74.0
	ws=40	0.0	0.0	0.0	0.0	0.0	0.0
	ws=60	0.0	0.0	0.0	0.0	0.0	0.0

Table B.1: Experiment 1-Subject 1-Test 1
V% and F% are the percentages of valid and false peaks respectively for twelve combinations of ws&fc2 computed for transducers T1, T2 , T3 and T4. Window sizes: ws=[15, 25, 40, 60] and cutoff frequencies: fc2=[1, 1.5, 2] Hz.

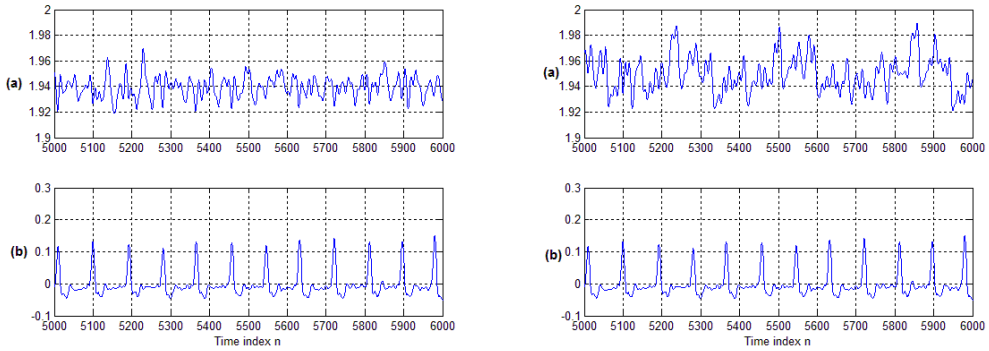

(a) T1 (b) T2

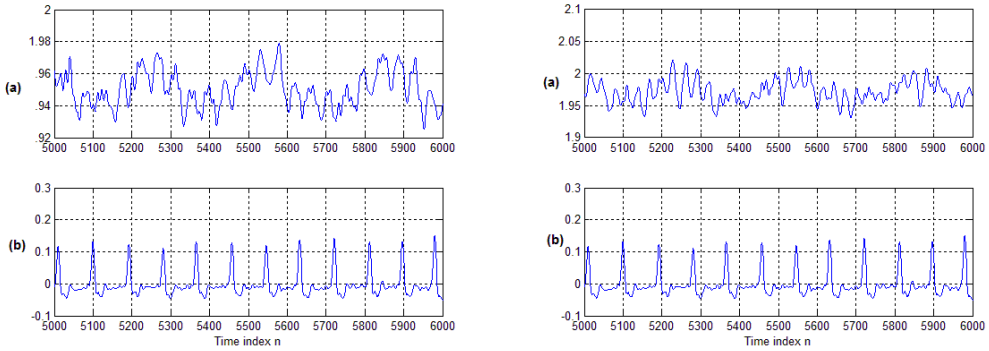

(c) T3 (d) T4

Figure B.2: Experiment 1-Subject 1-Test 1
(a) shows the HBS signal after lowpass filtering at 10 Hz. (b) GT signal captured by a piezoelectric device worn on the subject's finger. T1, T2, T3 and T4 are the transducers tested.

Subject 2

		fc2=1 Hz		fc2=1.5 Hz		fc2=2 Hz	
		V [%]	F [%]	V [%]	F [%]	V [%]	F [%]
T1	ws=15	0.0	0.0	34.8	43.5	0.0	0.0
	ws=25	23.9	20.7	0.0	0.0	31.5	55.4
	ws=40	19.6	17.4	30.4	34.8	41.3	47.8
	ws=60	0.0	0.0	39.1	19.6	54.3	35.9
T2	ws=15	0.0	0.0	41.8	37.3	0.0	0.0
	ws=25	0.0	0.0	33.6	43.6	0.0	0.0
	ws=40	0.0	0.0	36.4	28.2	55.5	51.8
	ws=60	0.0	0.0	31.8	25.5	54.5	45.5
T3	ws=15	0.0	0.0	63.6	9.1	54.5	22.7
	ws=25	0.0	0.0	31.8	9.1	59.1	18.2
	ws=40	0.0	0.0	36.4	0.0	0.0	0.0
	ws=60	0.0	0.0	36.4	0.0	36.4	0.0
T4	ws=15	22.7	19.5	83.6	9.4	84.4	25.0
	ws=25	21.9	19.5	93.0	3.1	91.4	14.8
	ws=40	21.9	18.0	87.5	4.7	87.5	13.3
	ws=60	17.2	19.5	69.5	13.3	75.8	20.3

Table B.2: Experiment 1-Subject 2-Test 1
V% and F% are the percentages of valid and false peaks respectively for twelve combinations of ws&fc2 computed for transducers T1, T2 , T3 and T4. Window sizes: ws=[15, 25, 40, 60] and cutoff frequencies: fc2=[1, 1.5, 2] Hz.

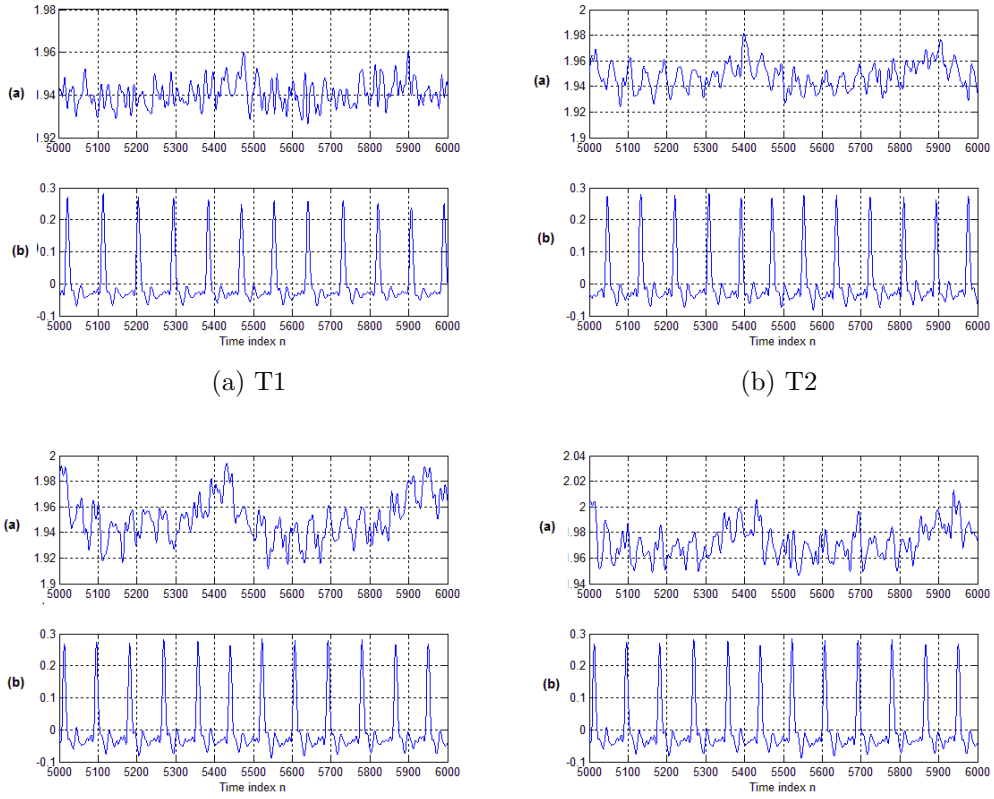

(a) T1 (b) T2

(c) T3 (d) T4

Figure B.3: Experiment 1-Subject 2-Test 1
(a) shows the HBS signal after lowpass filtering at 10 Hz. (b) GT signal captured by a piezoelectric device worn on the subject's finger. T1, T2, T3 and T4 are the transducers tested.

B.2 Experiment 2

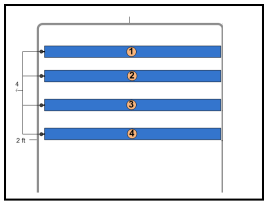

Figure B.4: 36 in. long trandsucers filled with 30 oz.of water

Subject 1

		fc2=1 Hz		fc2=1.5 Hz		fc2=2 Hz	
		V [%]	F [%]	V [%]	F [%]	V [%]	F [%]
T1	ws=15	0.0	0.0	0.0	0.0	2.9	31.1
	ws=25	0.0	0.0	0.0	0.0	0.0	0.0
	ws=40	0.0	0.0	19.4	19.4	40.8	58.3
	ws=60	0.0	0.0	44.7	21.4	62.1	35.0
T2	ws=15	0.0	0.0	0.0	0.0	0.0	0.0
	ws=25	0.0	0.0	0.0	0.0	0.0	0.0
	ws=40	0.0	0.0	0.0	0.0	0.0	0.0
	ws=60	0.0	0.0	0.0	0.0	0.0	0.0
T3	ws=15	0.0	0.0	80.6	20.4	85.4	34.0
	ws=25	0.0	0.0	56.3	38.8	59.2	53.4
	ws=40	0.0	0.0	35.9	57.3	46.6	65.0
	ws=60	0.0	0.0	34.0	47.6	37.9	55.3
T4	ws=15	0.0	0.0	78.6	24.3	75.7	45.6
	ws=25	0.0	0.0	76.7	26.2	84.5	35.0
	ws=40	0.0	0.0	63.1	31.1	71.8	35.0
	ws=60	0.0	0.0	56.3	14.6	73.8	27.2

Table B.3: Experiment 2-Subject 1-Test 1
V% and F% are the percentages of valid and false peaks respectively for twelve combinations of ws&fc2 computed for transducers T1, T2 , T3 and T4. Window sizes: ws=[15, 25, 40, 60] and cutoff frequencies: fc2=[1, 1.5, 2] Hz.

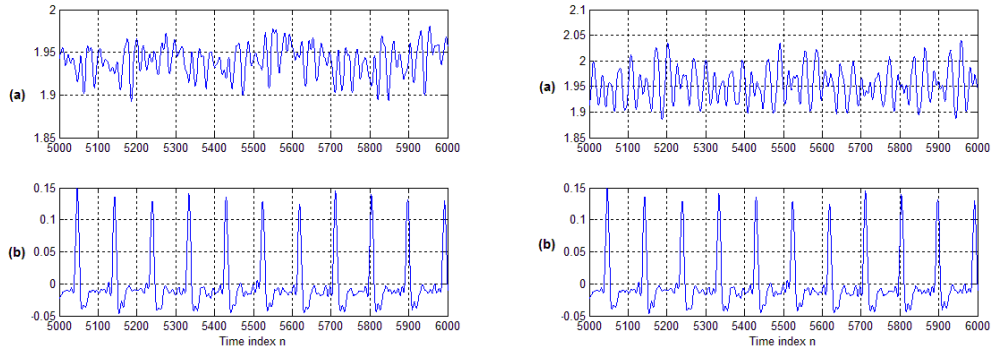

(a) T1 (b) T2

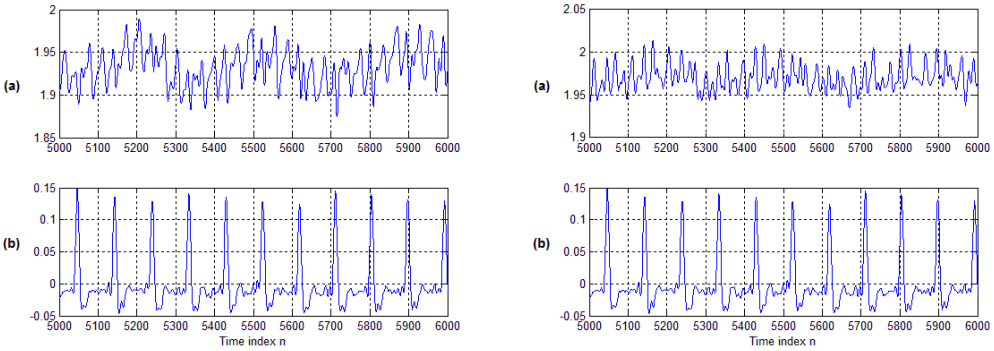

(c) T3 (d) T4

Figure B.5: Experiment 2-Subject 1-Test 1
(a) shows the HBS signal after lowpass filtering at 10 Hz. (b) GT signal captured by a piezoelectric device worn on the subject's finger. T1, T2, T3 and T4 are the transducers tested.

Subject 2

		fc2=1 Hz		fc2=1.5 Hz		fc2=2 Hz	
		V [%]	F [%]	V [%]	F [%]	V [%]	F [%]
T1	ws=15	0.0	0.0	90.5	5.6	88.9	7.9
	ws=25	0.0	0.0	81.7	11.1	82.5	17.5
	ws=40	0.0	0.0	69.8	16.7	74.6	23.0
	ws=60	0.0	0.0	0.0	0.0	50.0	39.7
T2	ws=15	0.0	0.0	18.3	75.4	27.0	77.0
	ws=25	0.0	0.0	26.2	64.3	31.0	69.0
	ws=40	0.0	0.0	46.0	44.4	50.0	46.8
	ws=60	0.0	0.0	0.0	0.0	81.0	11.9
T3	ws=15	0.0	0.0	52.4	45.2	69.8	50.8
	ws=25	0.0	0.0	56.3	32.5	71.4	42.9
	ws=40	0.0	0.0	52.4	25.4	67.5	40.5
	ws=60	0.0	0.0	48.4	27.8	62.7	36.5
T4	ws=15	0.0	0.0	64.3	28.6	70.6	40.5
	ws=25	0.0	0.0	87.3	9.5	81.0	24.6
	ws=40	0.0	0.0	85.7	6.3	85.7	13.5
	ws=60	0.0	0.0	0.0	0.0	73.8	27.8

Table B.4: Experiment 2-Subject 2-Test 1
V% and F% are the percentages of valid and false peaks respectively for twelve combinations of ws&fc2 computed for transducers T1, T2 , T3 and T4. Window sizes: ws=[15,25,40,60] and cutoff frequencies: fc2=[1, 1.5, 2] Hz.

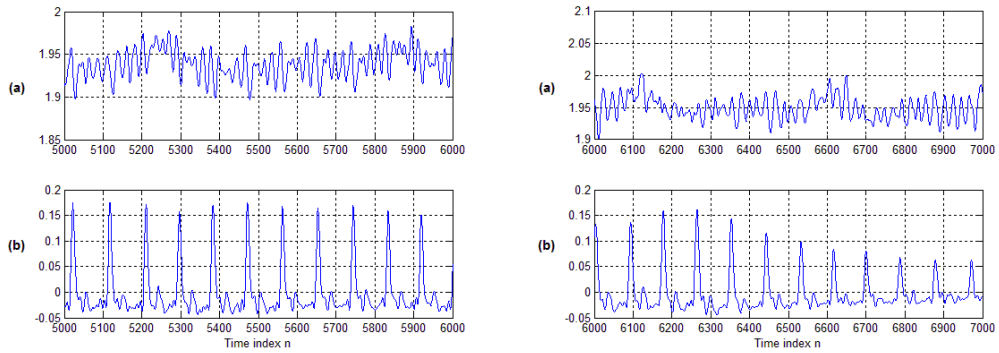

(a) T1 (b) T2

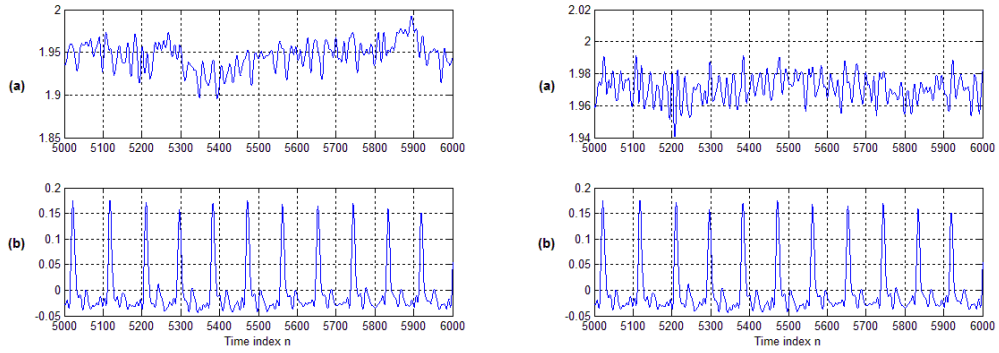

(c) T3 (d) T4

Figure B.6: Experiment 2-Subject 2-Test 1
(a) shows the HBS signal after lowpass filtering at 10 Hz. (b) GT signal captured by a piezoelectric device worn on the subject's finger. T1, T2, T3 and T4 are the transducers tested.

B.3 Experiment 3

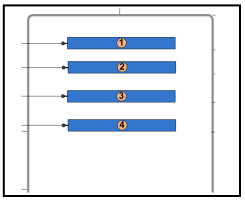

Figure B.7: 22 in. long trandsucers filled with 16 oz. of water

Subject 1

		fc2=1 Hz		fc2=1.5 Hz		fc2=2 Hz	
		V [%]	F [%]	V [%]	F [%]	V [%]	F [%]
T1	ws=15	0.0	0.0	42.4	48.3	53.0	55.6
	ws=25	0.0	0.0	66.2	25.2	66.2	39.1
	ws=40	0.0	0.0	79.5	5.3	80.8	22.5
	ws=60	0.0	0.0	0.0	0.0	70.2	29.1
T2	ws=15	0.0	0.0	96.0	0.7	94.0	2.0
	ws=25	0.0	0.0	94.7	0.0	94.7	0.0
	ws=40	0.0	0.0	94.7	0.0	94.7	0.0
	ws=60	0.0	0.0	0.0	0.0	88.7	7.3
T3	ws=15	0.0	0.0	10.6	85.4	13.9	82.1
	ws=25	0.0	0.0	38.4	57.0	40.4	56.3
	ws=40	0.0	0.0	82.8	8.6	80.8	15.9
	ws=60	0.0	0.0	0.0	0.0	80.1	20.5
T4	ws=15	0.0	0.0	42.4	48.3	53.0	55.6
	ws=25	0.0	0.0	66.2	25.2	66.2	39.1
	ws=40	0.0	0.0	79.5	5.3	80.8	22.5
	ws=60	0.0	0.0	0.0	0.0	70.2	29.1

Table B.5: Experiment 3-Subject 1-Test 1
V% and F% are the percentages of valid and false peaks respectively for twelve combinations of ws&fc2 computed for transducers T1, T2 , T3 and T4. Window sizes: ws=[15, 25, 40, 60] and cutoff frequencies: fc2=[1, 1.5, 2] Hz.

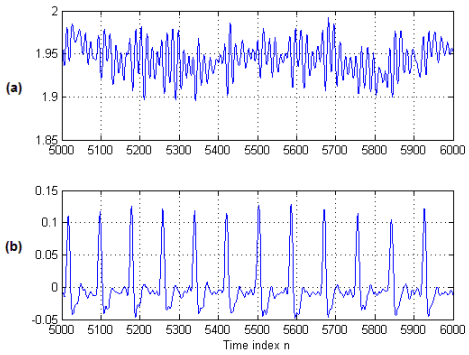

(a) T1

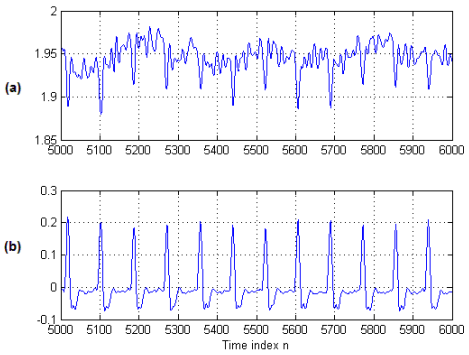

(b) T2

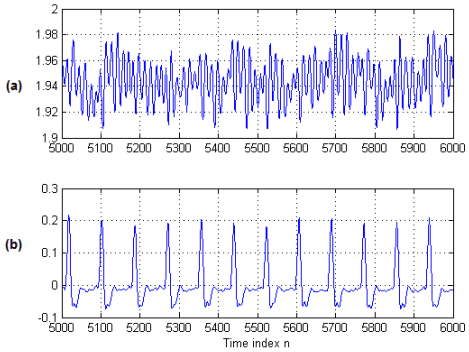

(c) T3

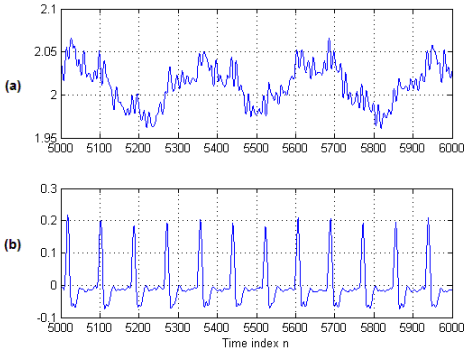

(d) T4

Figure B.8: Experiment 3-Subject 1-Test 1
(a) shows the HBS signal after lowpass filtering at 10 Hz. (b) GT signal captured by a piezoelectric device worn on the subject's finger. T1, T2, T3 and T4 are the transducers tested.

Subject 2

		fc2=1 Hz		fc2=1.5 Hz		fc2=2 Hz	
		V [%]	F [%]	V [%]	F [%]	V [%]	F [%]
T1	ws=15	0.0	0.0	45.2	45.2	0.0	0.0
	ws=25	0.0	0.0	60.6	26.9	65.4	45.2
	ws=40	0.0	0.0	67.3	16.3	76.0	29.8
	ws=60	0.0	0.0	66.3	14.4	71.2	27.9
T2	ws=15	29.8	23.1	41.3	51.0	0.0	0.0
	ws=25	0.0	0.0	55.8	36.5	0.0	0.0
	ws=40	0.0	0.0	78.8	12.5	81.7	26.0
	ws=60	0.0	0.0	67.3	13.5	69.2	25.0
T3	ws=15	0.0	0.0	33.7	55.8	39.4	54.8
	ws=25	0.0	0.0	63.5	26.9	66.3	30.8
	ws=40	0.0	0.0	80.8	6.7	81.7	16.3
	ws=60	0.0	0.0	80.8	3.8	82.7	12.5
T4	ws=15	0.0	0.0	45.2	45.2	0.0	0.0
	ws=25	0.0	0.0	60.6	26.9	65.4	45.2
	ws=40	0.0	0.0	67.3	16.3	76.0	29.8
	ws=60	0.0	0.0	66.3	14.4	71.2	27.9

Table B.6: Experiment 3-Subject 2-Test 1
V% and F% are the percentages of valid and false peaks respectively for twelve combinations of ws&fc2 computed for transducers T1, T2 , T3 and T4. Window sizes: ws=[15, 25, 40, 60] and cutoff frequencies: fc2=[1, 1.5, 2] Hz.

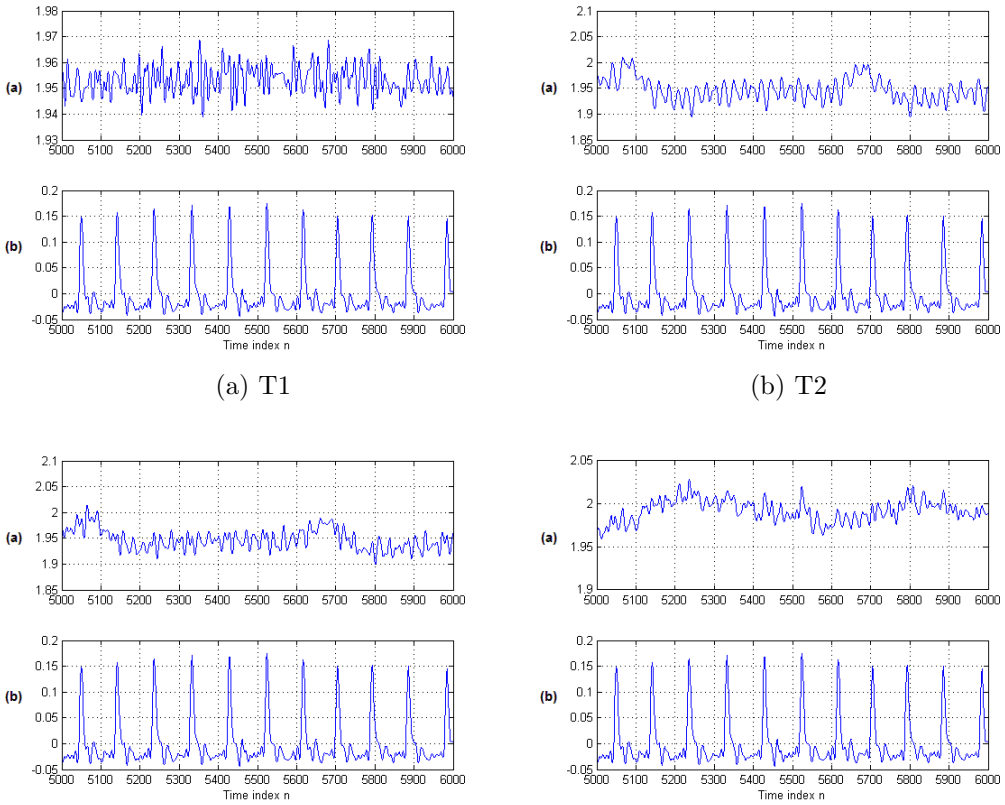

(a) T1 (b) T2

(c) T3 (d) T4

Figure B.9: Experiment 3-Subject 2-Test 1
(a) shows the HBS signal after lowpass filtering at 10 Hz. (b) GT signal captured by a piezoelectric device worn on the subject's finger. T1, T2, T3 and T4 are the transducers tested.

B.4 Experiment 4

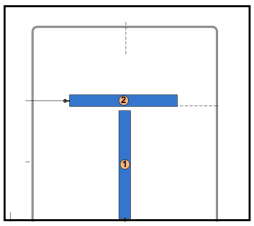

Figure B.10: 22 in. long trandsucers filled with 16 oz.of water

Subject 1

		fc2=1 Hz		fc2=1.5 Hz		fc2=2 Hz	
		V [%]	F [%]	V [%]	F [%]	V [%]	F [%]
T1	ws=15	0.0	0.0	67.1	27.1	69.3	46.4
	ws=25	0.0	0.0	62.9	29.3	62.1	47.9
	ws=40	0.0	0.0	62.9	23.6	67.1	33.6
	ws=60	0.0	0.0	40.0	19.3	57.1	41.4
T2	ws=15	0.0	0.0	93.6	2.9	83.6	12.1
	ws=25	0.0	0.0	94.3	2.1	92.1	2.9
	ws=40	0.0	0.0	95.0	1.4	92.1	0.0
	ws=60	0.0	0.0	87.1	5.0	85.0	7.9

Table B.7: Experiment 4-Subject 1-Test 1

V% and F% are the percentages of valid and false peaks respectively for twelve combinations of ws&fc2 computed for transducers T1 and T2. Window sizes: ws=[15, 25, 40, 60] and cutoff frequencies: fc2=[1, 1.5, 2] Hz.

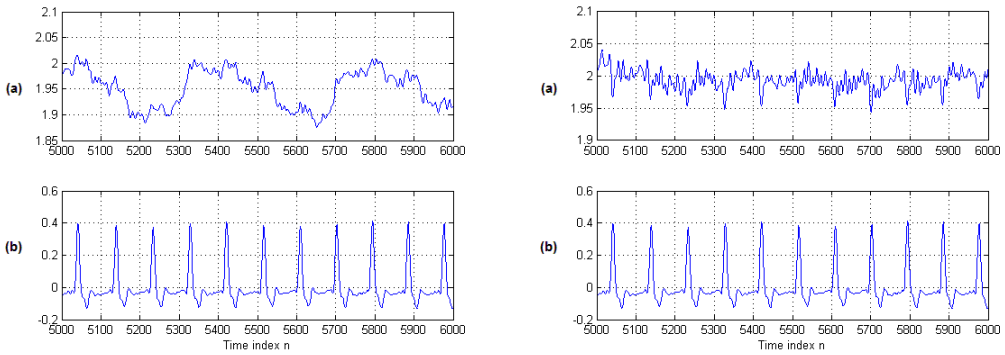

(a) T1 (b) T2

Figure B.11: Experiment 4-Subject 1-Test 1-2

(a) shows the HBS signal after lowpass filtering at 10 Hz. (b) GT signal captured by a piezoelectric device worn on the subject's finger. T1 and T2 are the transducers tested.

Subject 2

		fc2=1 Hz		fc2=1.5 Hz		fc2=2 Hz	
		V [%]	F [%]	V [%]	F [%]	V [%]	F [%]
T1	ws=15	0.0	0.0	77.4	25.2	0.0	0.0
	ws=25	0.0	0.0	80.0	18.3	0.0	0.0
	ws=40	0.0	0.0	71.3	7.8	87.0	31.3
	ws=60	0.0	0.0	45.2	19.1	53.9	33.0
T2	ws=15	0.0	0.0	73.0	23.5	77.4	48.7
	ws=25	34.8	14.8	86.1	14.8	83.5	40.0
	ws=40	37.4	9.6	85.2	9.6	86.1	23.5
	ws=60	30.4	13.9	85.2	11.3	83.5	23.5

Table B.8: Experiment 4-Subject 2-Test 1
V% and F% are the percentages of valid and false peaks respectively for twelve combinations of ws&fc2 computed for transducers T1 and T2. Window sizes: ws=[15, 25, 40, 60] and cutoff frequencies: fc2=[1, 1.5, 2] Hz.

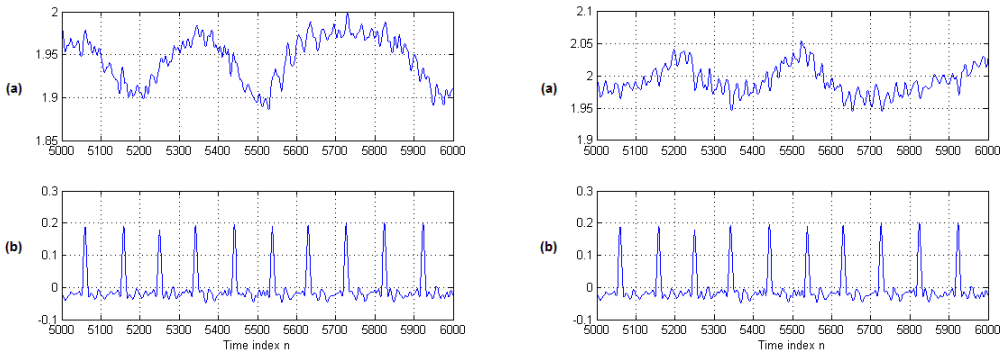

(a) T1 (b) T2

Figure B.12: Experiment 4-Subject 2-Test 1
(a) shows the HBS signal after lowpass filtering at 10 Hz. (b) GT signal captured by a piezoelectric device worn on the subject's finger. T1 and T2 are the transducers tested.

B.5 Experiment 5

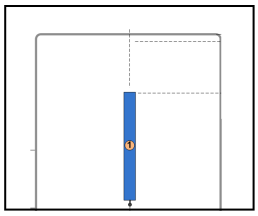

Figure B.13: 22 in. long trandsucer filled with 16 oz. of water

Subject 1

		fc2=1 Hz		fc2=1.5 Hz		fc2=2 Hz	
		V [%]	F [%]	V [%]	F [%]	V [%]	F [%]
T1	ws=15	20.1	16.9	42.9	23.4	61.0	40.9
	ws=25	20.1	17.5	34.4	22.7	59.1	46.1
	ws=40	17.5	18.8	26.0	29.2	44.8	55.2
	ws=60	17.5	18.2	0.0	0.0	0.0	0.0

Table B.9: Experiment 5-Suject 1-Test 1
V% and F% are the percentages of valid and false peaks respectively for twelve combinations of ws&fc2 computed for transducer T1. Window sizes: ws=[15, 25, 40, 60] and cutoff frequencies: fc2=[1, 1.5, 2] Hz.

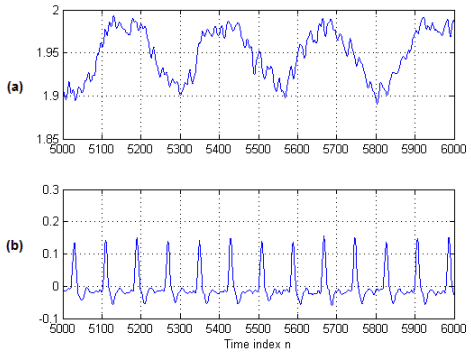

(a) T1

Figure B.14: Experiment 5-Subject 1-Test 1
(a) shows the HBS signal after lowpass filtering at 10 Hz. (b) GT signal captured by a piezoelectric device worn on the subject's finger. T1is the transducer tested.

Subject 2

		fc2=1 Hz		fc2=1.5 Hz		fc2=2 Hz	
		V [%]	F [%]	V [%]	F [%]	V [%]	F [%]
T1	ws=15	25.6	17.9	61.5	37.6	72.6	57.3
	ws=25	23.9	18.8	62.4	35.9	76.1	51.3
	ws=40	0.0	0.0	57.3	35.0	72.6	48.7
	ws=60	0.0	0.0	35.0	34.2	47.9	47.9

Table B.10: Experiment 5-Subject 2-Test 1
V% and F% are the percentages of valid and false peaks respectively for twelve combinations of ws&fc2 computed for transducer T1. Window sizes: ws=[15, 25, 40, 60] and cutoff frequencies: fc2=[1, 1.5, 2] Hz.

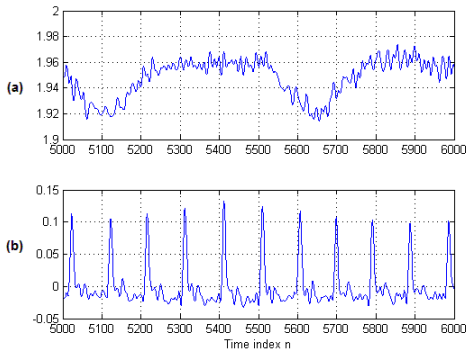

(a) T1

Figure B.15: Experiment 5-Subject 2-Test 1-2
(a) shows the HBS signal after lowpass filtering at 10 Hz. (b) GT signal captured by a piezoelectric device worn on the subject's finger. T1 is the transducer tested.

B.6 Experiment 6

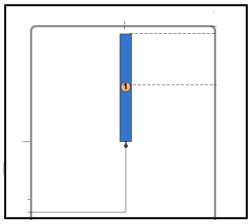

Figure B.16: 22 in. long trandsucer filled with 16 oz. of water

Subject 1

		fc2=1 Hz		fc2=1.5 Hz		fc2=2 Hz	
		V [%]	F [%]	V [%]	F [%]	V [%]	F [%]
T1	ws=15	0.0	0.0	90.2	5.3	91.0	24.8
	ws=25	0.0	0.0	93.2	1.5	93.2	12.8
	ws=40	0.0	0.0	91.7	2.3	91.0	8.3
	ws=60	0.0	0.0	75.2	12.0	74.4	26.3

Table B.11: Experiment 6-Subject 1-Test 1
V% and F% are the percentages of valid and false peaks respectively for twelve combinations of ws&fc2 computed for transducer T1. Window sizes: ws=[15, 25, 40, 60] and cutoff frequencies: fc2=[1, 1.5, 2] Hz.

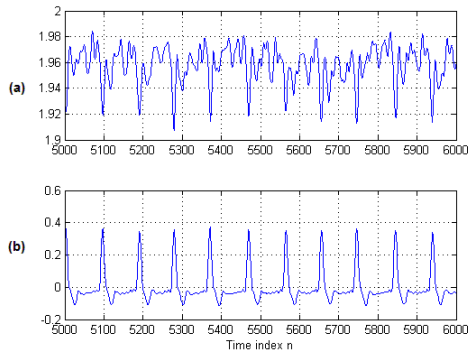

(a) T1

Figure B.17: Experiment 6-Subject 1-Test 1
(a) shows the HBS signal after lowpass filtering at 10 Hz. (b) GT signal captured by a piezoelectric device worn on the subject's finger. T1 is the transducer tested.

Subject 2

		fc2=1 Hz		fc2=1.5 Hz		fc2=2 Hz	
		V [%]	F [%]	V [%]	F [%]	V [%]	F [%]
T1	ws=15	0.0	0.0	91.0	4.5	91.7	13.5
	ws=25	0.0	0.0	93.2	3.8	92.5	6.8
	ws=40	56.4	12.0	93.2	3.8	94.0	3.8
	ws=60	39.1	13.5	89.5	6.8	92.5	7.5

Table B.12: Experiment 6-Subject 2-Test 1

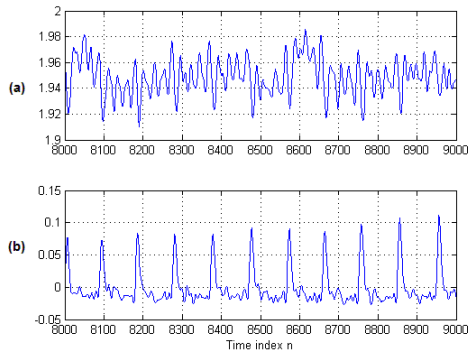

(a) T1

Figure B.18: Experiment 6-Subject 2-Test 1-2
(a) shows the HBS signal after lowpass filtering at 10 Hz. (b) GT signal captured by a piezoelectric device worn on the subject's finger. T1 is the transducer tested.

B.7 Experiment 7

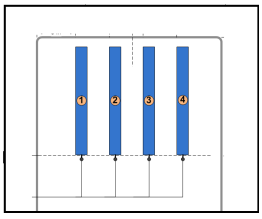

Figure B.19: 22 in. long trandsucers filled with 16 oz. of water

Subject 1

		fc2=1 Hz		fc2=1.5 Hz		fc2=2 Hz	
		V [%]	F [%]	V [%]	F [%]	V [%]	F [%]
T1	ws=15	21.4	17.1	46.2	52.1	53.0	70.1
	ws=25	0.0	0.0	28.2	56.4	47.9	71.8
	ws=40	0.0	0.0	19.7	40.2	0.0	0.0
	ws=60	0.0	0.0	29.1	44.4	45.3	54.7
T2	ws=15	31.6	30.8	28.2	57.3	43.6	56.4
	ws=25	35.9	23.1	65.0	29.1	65.0	36.8
	ws=40	0.0	0.0	82.9	11.1	75.2	22.2
	ws=60	0.0	0.0	70.1	8.5	87.2	28.2
T3	ws=15	43.6	17.9	81.2	14.5	79.5	27.4
	ws=25	53.8	11.1	92.3	3.4	90.6	12.0
	ws=40	50.4	7.7	94.0	1.7	94.0	6.8
	ws=60	36.8	12.0	82.9	14.5	88.0	14.5
T4	ws=15	30.8	21.4	39.3	56.4	0.0	0.0
	ws=25	32.5	20.5	63.2	33.3	63.2	43.6
	ws=40	29.9	20.5	75.2	21.4	76.1	25.6
	ws=60	29.1	16.2	68.4	17.9	76.1	24.8

Table B.13: Experiment 8-Subject 4-Test 1
V% and F% are the percentages of valid and false peaks respectively for twelve combinations of ws&fc2 computed for transducers T1, T2, T3 and T4. Window sizes: ws=[15, 25, 40, 60] and cutoff frequencies: fc2=[1, 1.5, 2] Hz.

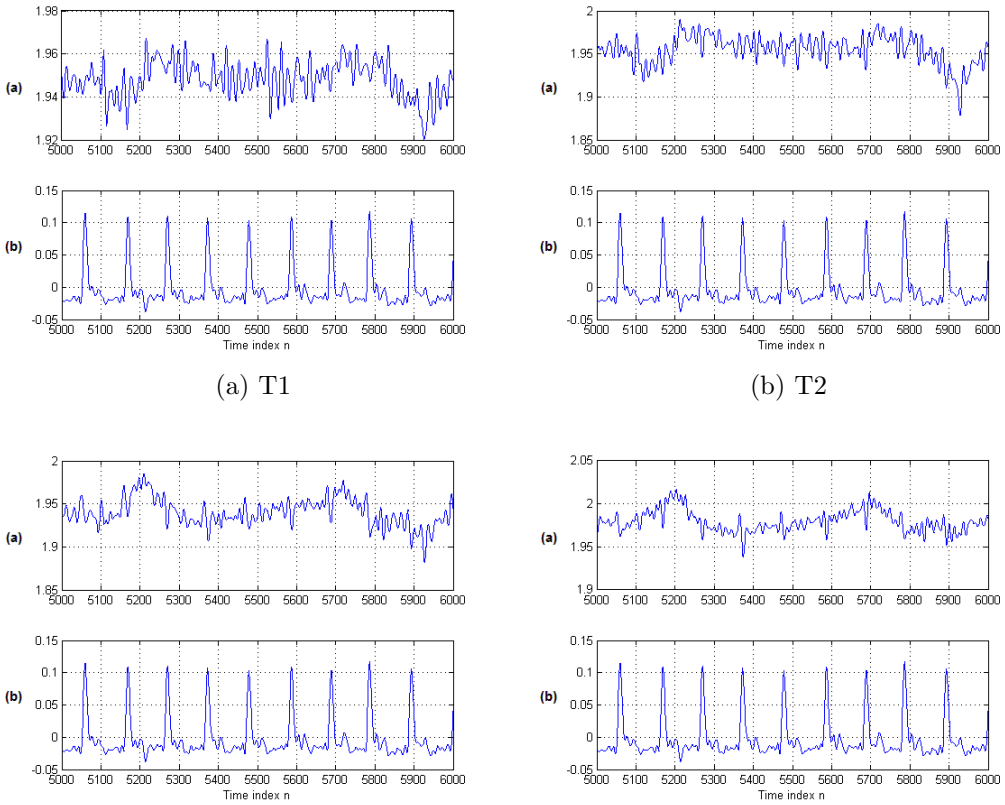

(a) T1 (b) T2

(c) T3 (d) T4

Figure B.20: Experiment 7-Subject 1 Test 1
(a) shows the HBS signal after lowpass filtering at 10 Hz. (b) GT signal captured by a piezoelectric device worn on the subject's finger. T1, T2, T3 and T4 are the transducers tested.

Subject 2

		fc2=1 Hz		fc2=1.5 Hz		fc2=2 Hz	
		V [%]	F [%]	V [%]	F [%]	V [%]	F [%]
T1	ws=15	9.5	60.0	26.7	73.3	0.0	0.0
	ws=25	8.6	58.1	26.7	71.4	0.0	0.0
	ws=40	0.0	0.0	21.9	79.0	0.0	0.0
	ws=60	0.0	0.0	19.0	66.7	0.0	0.0
T2	ws=15	36.4	33.3	33.3	42.4	0.0	0.0
	ws=25	30.3	27.3	42.4	30.3	0.0	0.0
	ws=40	33.3	21.2	45.5	27.3	0.0	0.0
	ws=60	0.0	0.0	51.5	30.3	57.6	30.3
T3	ws=15	79.0	12.4	80.0	20.0	92.4	80.0
	ws=25	90.5	2.9	85.7	13.3	95.2	70.5
	ws=40	90.5	2.9	92.4	6.7	91.4	31.4
	ws=60	72.4	2.9	91.4	6.7	92.4	34.3
T4	ws=15	85.7	1.9	85.7	10.5	0.0	0.0
	ws=25	91.4	0.0	90.5	4.8	92.4	76.2
	ws=40	89.5	1.0	92.4	2.9	94.3	32.4
	ws=60	84.8	3.8	92.4	2.9	86.7	40.0

Table B.14: Experiment 8-Subject 5-Test 1
V% and F% are the percentages of valid and false peaks respectively for twelve combinations of ws&fc2 computed for transducers T1, T2, T3 and T4. Window sizes: ws=[15, 25, 40, 60] and cutoff frequencies: fc2=[1, 1.5, 2] Hz.

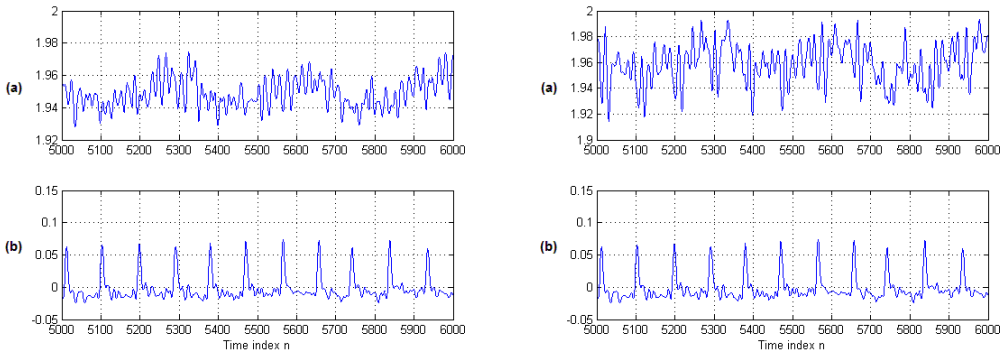

(a) T1 (b) T2

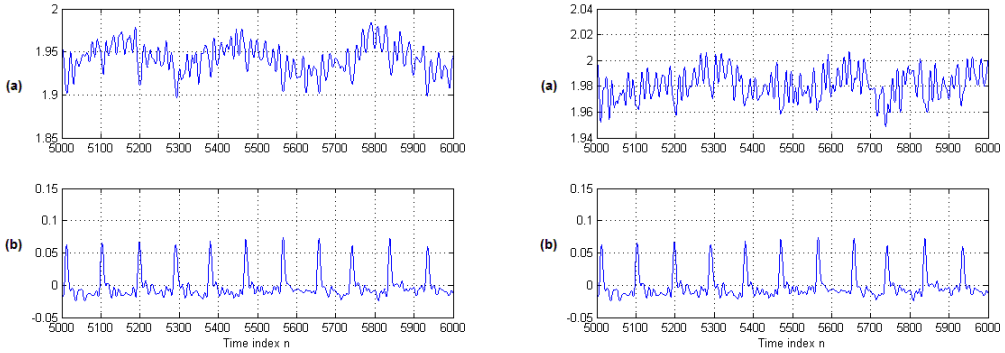

(c) T3 (d) T4

Figure B.21: Experiment 7-Subject 2 Test 1
(a) shows the HBS signal after lowpass filtering at 10 Hz. (b) GT signal captured by a piezoelectric device worn on the subject's finger. T1, T2, T3 and T4 are the transducers tested.

B.8 Experiment 8

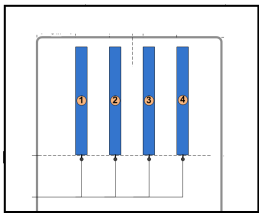

Figure B.22: 22 in. long trandsucers filled with 16 oz. of water

Subject 1

		fc2=1 Hz		fc2=1.5 Hz		fc2=2 Hz	
		V [%]	F [%]	V [%]	F [%]	V [%]	F [%]
T1	ws=15	0.0	0.0	13.6	50.0	0.0	0.0
	ws=25	0.0	0.0	8.5	38.1	0.0	0.0
	ws=40	0.0	0.0	16.1	55.9	0.0	0.0
	ws=60	0.0	0.0	0.0	0.0	43.2	55.9
T2	ws=15	57.3	10.0	80.0	21.8	90.9	57.3
	ws=25	67.3	5.5	87.3	13.6	90.0	51.8
	ws=40	61.8	8.2	90.9	7.3	92.7	23.6
	ws=60	45.5	15.5	83.6	12.7	79.1	34.5
T3	ws=15	74.5	4.5	95.5	3.6	95.5	58.2
	ws=25	75.5	3.6	95.5	0.9	95.5	46.4
	ws=40	72.7	4.5	95.5	0.9	95.5	15.5
	ws=60	61.8	12.7	94.5	0.9	92.7	14.5
T4	ws=15	78.2	2.7	91.8	3.6	95.5	57.3
	ws=25	81.8	4.5	93.6	2.7	95.5	50.0
	ws=40	80.9	3.6	95.5	0.0	95.5	22.7
	ws=60	70.0	6.4	95.5	0.0	94.5	8.2

Table B.15: Experiment 8-Subject 1-Test 1
V% and F% are the percentages of valid and false peaks respectively for twelve combinations of ws&fc2 computed for transducers T1, T2, T3 and T4. Window sizes: ws=[15, 25, 40, 60] and cutoff frequencies: fc2=[1, 1.5, 2] Hz.

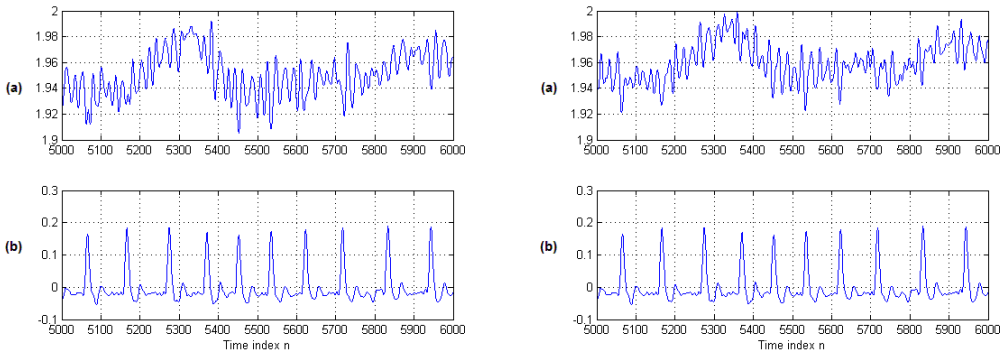

(a) T1 (b) T2

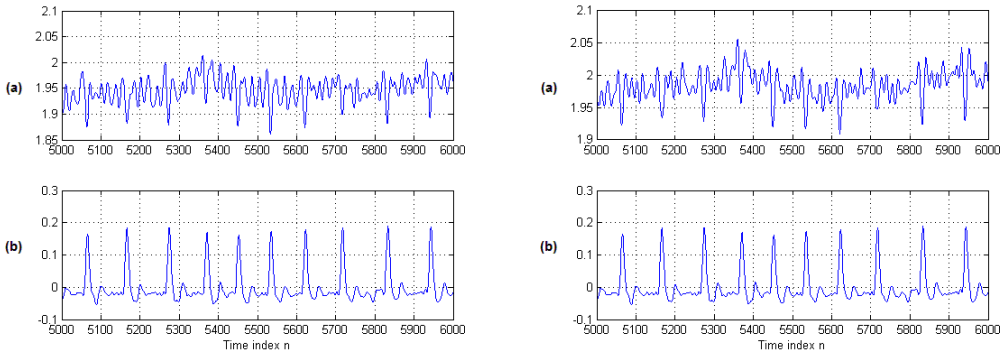

(c) T3 (d) T4

Figure B.23: Experiment 8-Subject 1-Test 1
(a) shows the HBS signal after lowpass filtering at 10 Hz. (b) GT signal captured by a piezoelectric device worn on the subject's finger. T1, T2, T3 and T4 are the transducers tested.

Subject 2

		fc2=1 Hz		fc2=1.5 Hz		fc2=2 Hz	
		V [%]	F [%]	V [%]	F [%]	V [%]	F [%]
T1	ws=15	0.0	0.0	53.4	40.9	64.8	48.9
	ws=25	0.0	0.0	60.2	31.8	69.3	34.1
	ws=40	0.0	0.0	72.7	15.9	73.9	29.5
	ws=60	29.5	18.2	0.0	0.0	63.6	34.1
T2	ws=15	35.2	10.2	78.4	18.2	77.3	36.4
	ws=25	35.2	12.5	80.7	14.8	83.0	27.3
	ws=40	34.1	12.5	84.1	10.2	78.4	23.9
	ws=60	23.9	12.5	61.4	20.5	67.0	28.4
T3	ws=15	35.0	18.3	85.8	9.2	90.0	27.5
	ws=25	47.5	10.8	87.5	4.2	90.0	19.2
	ws=40	40.8	11.7	90.8	2.5	92.5	7.5
	ws=60	28.3	17.5	82.5	7.5	86.7	15.0
T4	ws=15	41.7	18.3	85.8	11.7	87.5	16.7
	ws=25	45.0	12.5	91.7	5.8	92.5	9.2
	ws=40	45.8	10.0	94.2	3.3	93.3	5.0
	ws=60	40.0	12.5	90.0	5.0	90.0	9.2

Table B.16: Experiment 8-Subject 2-Test 1
V% and F% are the percentages of valid and false peaks respectively for twelve combinations of ws&fc2 computed for transducers T1, T2, T3 and T4. Window sizes: ws=[15, 25, 40, 60] and cutoff frequencies: fc2=[1, 1.5, 2] Hz.

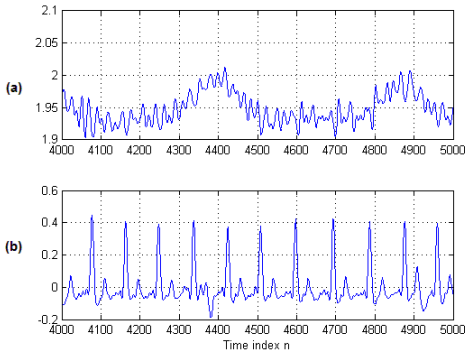

(a) T1

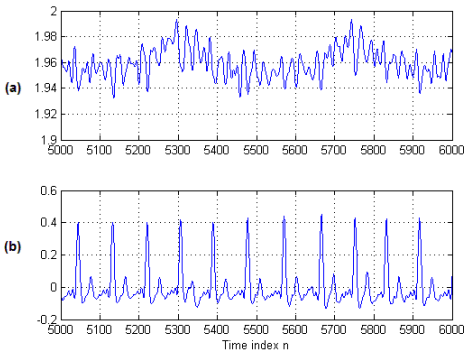

(b) T2

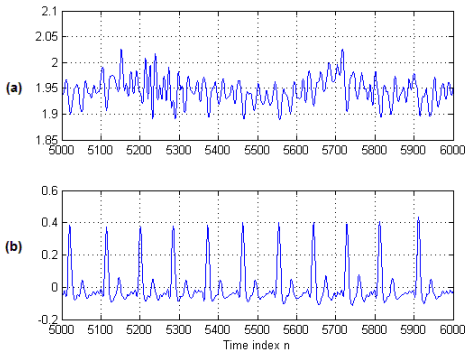

(c) T3

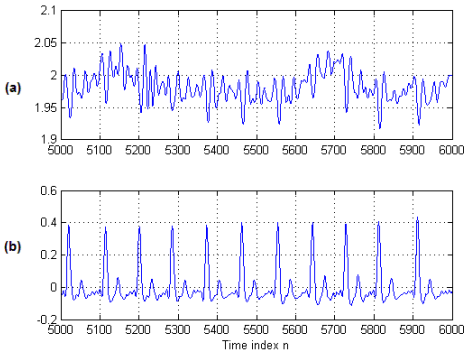

(d) T4

Figure B.24: Experiment 8-Subject 2 Test 1
(a) shows the HBS signal after lowpass filtering at 10 Hz. (b) GT signal captured by a piezoelectric device worn on the subject's finger. T1, T2, T3 and T4 are the transducers tested.

Subject 3

		fc2=1 Hz		fc2=1.5 Hz		fc2=2 Hz	
		V [%]	F [%]	V [%]	F [%]	V [%]	F [%]
T1	ws=15	12.9	54.8	23.7	46.2	0.0	0.0
	ws=25	38.7	41.9	48.4	44.1	91.4	72.0
	ws=40	92.5	2.2	79.6	16.1	88.2	26.9
	ws=60	94.6	0.0	89.2	7.5	88.2	21.5
T2	ws=15	75.3	19.4	76.3	32.3	0.0	0.0
	ws=25	89.2	5.4	87.1	19.4	0.0	0.0
	ws=40	88.2	2.2	89.2	15.1	0.0	0.0
	ws=60	76.3	4.3	81.7	16.1	0.0	0.0
T3	ws=15	94.6	0.0	93.5	3.2	0.0	0.0
	ws=25	94.6	0.0	94.6	0.0	0.0	0.0
	ws=40	94.6	0.0	94.6	0.0	0.0	0.0
	ws=60	93.5	0.0	93.5	2.2	92.5	12.9
T4	ws=15	94.6	0.0	89.2	15.1	0.0	0.0
	ws=25	94.6	0.0	93.5	6.5	0.0	0.0
	ws=40	94.6	0.0	93.5	2.2	91.4	36.6
	ws=60	94.6	0.0	93.5	0.0	93.5	9.7

Table B.17: Experiment 8-Subject 3-Test 1
V% and F% are the percentages of valid and false peaks respectively for twelve combinations of ws&fc2 computed for transducers T1, T2, T3 and T4. Window sizes: ws=[15, 25, 40, 60] and cutoff frequencies: fc2=[1, 1.5, 2] Hz.

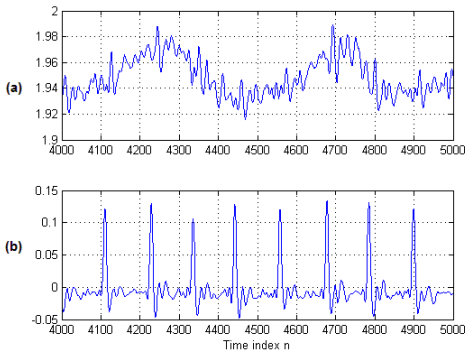

(a) T1

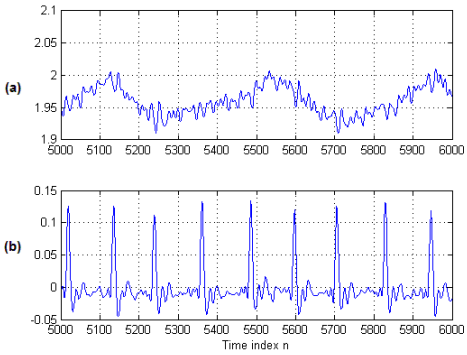

(b) T2

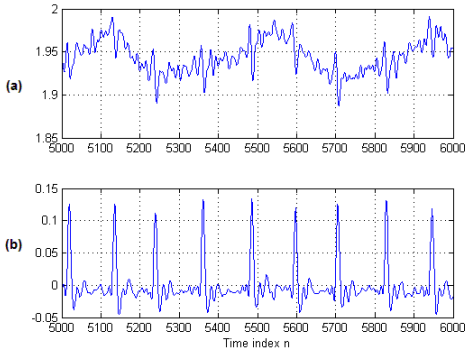

(c) T3

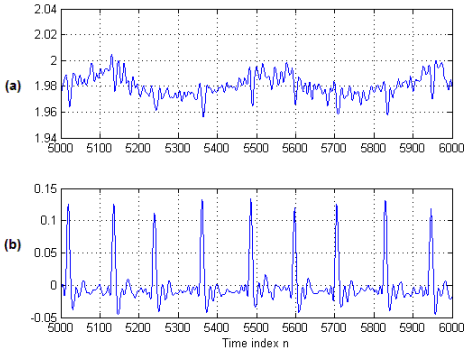

(d) T4

Figure B.25: Experiment 8-Subject 3 Test 1
(a) shows the HBS signal after lowpass filtering at 10 Hz. (b) GT signal captured by a piezoelectric device worn on the subject's finger. T1, T2, T3 and T4 are the transducers tested.

Subject 4

		fc2=1 Hz		fc2=1.5 Hz		fc2=2 Hz	
		V [%]	F [%]	V [%]	F [%]	V [%]	F [%]
T1	ws=15	0.0	0.0	13.6	50.0	0.0	0.0
	ws=25	0.0	0.0	8.5	38.1	0.0	0.0
	ws=40	0.0	0.0	16.1	55.9	0.0	0.0
	ws=60	0.0	0.0	0.0	0.0	43.2	55.9
T2	ws=15	0.0	0.0	34.7	61.0	46.6	60.2
	ws=25	31.4	29.7	66.1	29.7	65.3	39.0
	ws=40	0.0	0.0	89.0	6.8	82.2	18.6
	ws=60	0.0	0.0	78.8	3.4	90.7	18.6
T3	ws=15	32.2	13.6	94.1	1.7	83.9	22.0
	ws=25	37.3	10.2	94.1	0.8	91.5	13.6
	ws=40	35.6	9.3	94.1	1.7	94.1	12.7
	ws=60	30.5	9.3	89.8	5.9	0.0	0.0
T4	ws=15	28.0	16.1	62.7	21.2	0.0	0.0
	ws=25	30.5	12.7	78.0	14.4	79.7	26.3
	ws=40	37.3	7.6	83.9	6.8	88.1	18.6
	ws=60	0.0	0.0	63.6	12.7	76.3	28.8

Table B.18: Experiment 7-Subject 1-Test 1
V% and F% are the percentages of valid and false peaks respectively for twelve combinations of ws&fc2 computed for transducers T1, T2, T3 and T4. Window sizes: ws=[15, 25, 40, 60] and cutoff frequencies: fc2=[1, 1.5, 2] Hz.

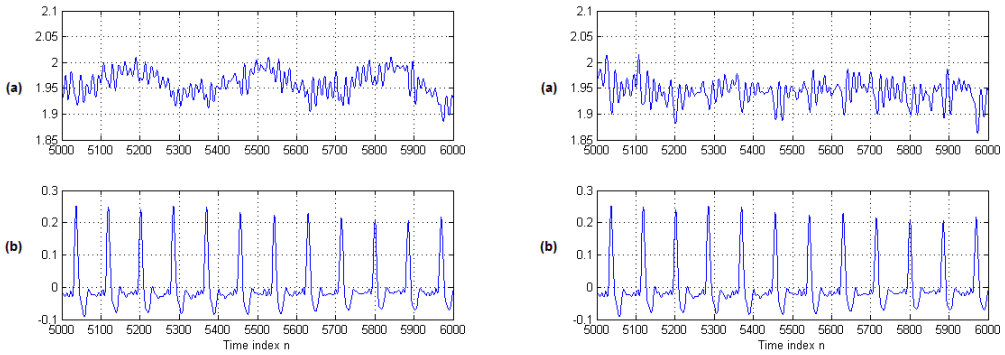

(a) T1 (b) T2

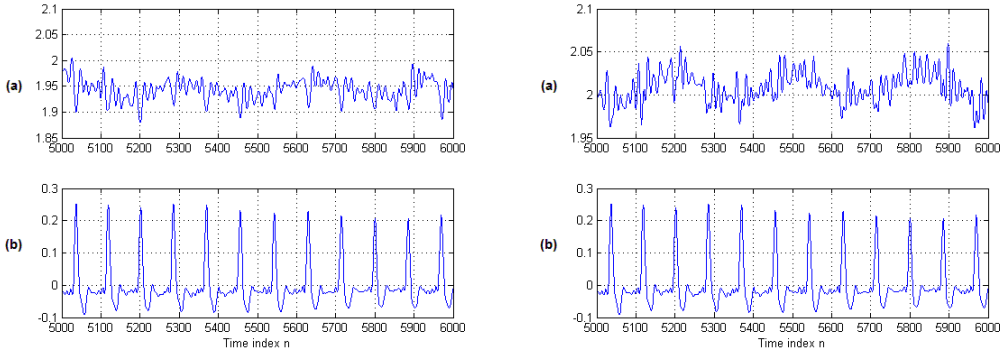

(c) T3 (d) T4

Figure B.26: Experiment 7-Subject 1-Test 1
(a) shows the HBS signal after lowpass filtering at 10 Hz. (b) GT signal captured by a piezoelectric device worn on the subject's finger. T1, T2, T3 and T4 are the transducers tested.

Subject 5

		fc2=1 Hz		fc2=1.5 Hz		fc2=2 Hz	
		V [%]	F [%]	V [%]	F [%]	V [%]	F [%]
T1	ws=15	0.0	0.0	23.4	75.7	0.0	0.0
	ws=25	0.0	0.0	24.3	74.8	0.0	0.0
	ws=40	0.0	0.0	18.7	61.7	36.4	74.8
	ws=60	0.0	0.0	22.4	62.6	0.0	0.0
T2	ws=15	58.9	18.7	72.0	29.9	0.0	0.0
	ws=25	64.5	11.2	72.9	20.6	89.7	63.6
	ws=40	0.0	0.0	76.6	16.8	82.2	46.7
	ws=60	0.0	0.0	68.2	18.7	84.1	45.8
T3	ws=15	90.7	0.0	83.2	9.3	0.0	0.0
	ws=25	90.7	0.0	89.7	2.8	94.4	43.0
	ws=40	91.6	1.9	90.7	0.0	90.7	15.9
	ws=60	0.0	0.0	88.8	2.8	89.7	23.4
T4	ws=15	86.9	1.9	89.7	7.5	0.0	0.0
	ws=25	92.5	0.9	93.5	2.8	0.0	0.0
	ws=40	92.5	0.9	93.5	0.0	93.5	28.0
	ws=60	83.2	3.7	92.5	0.9	86.9	25.2

Table B.19: Experiment 7-Subject 2-Test 1
V% and F% are the percentages of valid and false peaks respectively for twelve combinations of ws&fc2 computed for transducers T1, T2, T3 and T4. Window sizes: ws=[15, 25, 40, 60] and cutoff frequencies: fc2=[1, 1.5, 2] Hz.

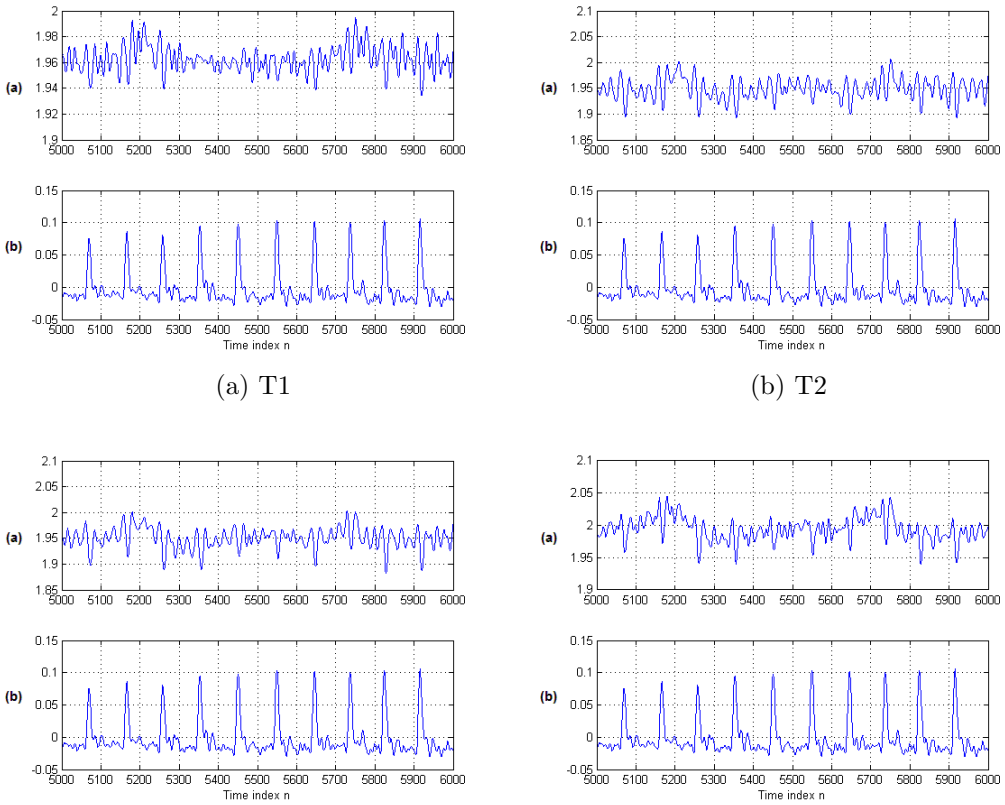

(a) T1 (b) T2

(c) T3 (d) T4

Figure B.27: Experiment 7-Subject 1-Test 2
(a) shows the HBS signal after lowpass filtering at 10 Hz. (b) GT signal captured by a piezoelectric device worn on the subject's finger. T1, T2, T3 and T4 are the transducers tested.

B.9 Experiment 9

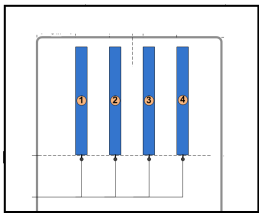

Figure B.28: 22 in. long trandsucers filled with 16 oz. of water

Subject 1

		fc2=1 Hz		fc2=1.5 Hz		fc2=2 Hz	
		V [%]	F [%]	V [%]	F [%]	V [%]	F [%]
T1	ws=15	0.0	0.0	86.5	3.8	87.2	15.0
	ws=25	20.3	21.8	80.5	5.3	82.7	18.8
	ws=40	0.0	0.0	62.4	12.0	72.9	30.1
	ws=60	0.0	0.0	0.0	0.0	48.9	45.1
T2	ws=15	0.0	0.0	93.5	3.6	91.7	7.7
	ws=25	0.0	0.0	97.0	0.0	96.4	1.2
	ws=40	0.0	0.0	94.1	1.8	95.3	3.6
	ws=60	0.0	0.0	63.3	15.4	73.4	27.8
T3	ws=15	18.9	17.8	39.6	42.6	63.9	59.2
	ws=25	16.0	18.3	47.3	36.1	59.2	58.6
	ws=40	0.0	0.0	40.2	30.8	55.6	43.2
	ws=60	16.6	11.8	32.5	18.3	46.7	36.1
T4	ws=15	0.0	0.0	47.9	47.3	47.3	50.3
	ws=25	0.0	0.0	89.3	5.9	85.2	12.4
	ws=40	0.0	0.0	88.2	3.0	87.0	10.1
	ws=60	0.0	0.0	50.9	14.2	58.0	27.2

Table B.20: Experiment 9-Subject 1, [1]-B1

V% and F% are the percentages of valid and false peaks respectively for twelve combinations of ws&fc2 computed for transducers T1, T2, T3 and T4. Window sizes: ws=[15, 25, 40, 60] and cutoff frequencies: fc2=[1, 1.5, 2] Hz.

B1 indicates the position of the person according to the protocol shown in Figure 2.5.

Subject 2

		fc2=1 Hz		fc2=1.5 Hz		fc2=2 Hz	
		V [%]	F [%]	V [%]	F [%]	V [%]	F [%]
T1	ws=15	0.0	0.0	0.0	0.0	8.2	73.1
	ws=25	0.0	0.0	48.0	42.7	55.6	43.3
	ws=40	0.0	0.0	79.5	8.2	77.2	17.0
	ws=60	0.0	0.0	59.1	13.5	76.0	24.6
T2	ws=15	0.0	0.0	76.6	19.9	76.0	21.1
	ws=25	0.0	0.0	95.9	1.2	94.7	2.3
	ws=40	0.0	0.0	95.9	0.0	95.9	1.2
	ws=60	26.9	11.7	84.2	1.8	87.7	5.8
T3	ws=15	0.0	0.0	96.5	0.0	94.2	1.8
	ws=25	0.0	0.0	96.5	0.0	95.9	0.0
	ws=40	0.0	0.0	95.9	0.0	95.3	0.6
	ws=60	19.3	15.2	88.3	3.5	90.6	4.7
T4	ws=15	0.0	0.0	96.5	0.6	93.6	5.3
	ws=25	0.0	0.0	97.1	0.0	97.1	1.8
	ws=40	0.0	0.0	96.5	0.0	95.3	4.1
	ws=60	0.0	0.0	59.1	17.5	71.9	21.6

Table B.21: Experiment 9-Subject 2, [1]-B1

V% and F% are the percentages of valid and false peaks respectively for twelve combinations of ws&fc2 computed for transducers T1, T2, T3 and T4. Window sizes: ws=[15, 25, 40, 60] and cutoff frequencies: fc2=[1, 1.5, 2] Hz.

B1 indicates the position of the person according to the protocol shown in Figure 2.5.

		fc2=1 Hz		fc2=1.5 Hz		fc2=2 Hz	
		V [%]	F [%]	V [%]	F [%]	V [%]	F [%]
T1	ws=15	0.0	0.0	52.0	27.3	66.7	49.3
	ws=25	0.0	0.0	58.0	23.3	70.7	34.0
	ws=40	0.0	0.0	0.0	0.0	67.3	33.3
	ws=60	0.0	0.0	0.0	0.0	54.7	42.0
T2	ws=15	0.0	0.0	44.0	36.0	56.0	46.0
	ws=25	0.0	0.0	57.3	19.3	67.3	32.7
	ws=40	0.0	0.0	60.0	16.0	73.3	27.3
	ws=60	0.0	0.0	0.0	0.0	30.7	7.3
T3	ws=15	0.0	0.0	36.7	60.0	46.7	60.7
	ws=25	0.0	0.0	74.0	18.7	75.3	26.7
	ws=40	0.0	0.0	79.3	10.7	82.7	14.7
	ws=60	0.0	0.0	70.0	6.7	80.7	14.7
T4	ws=15	0.0	0.0	58.7	35.3	0.0	0.0
	ws=25	0.0	0.0	56.7	14.7	72.7	30.0
	ws=40	0.0	0.0	0.0	0.0	87.3	16.7
	ws=60	0.0	0.0	0.0	0.0	80.7	14.0

Table B.22: Experiment 9-Subject 2, [1]R

V% and F% are the percentages of valid and false peaks respectively for twelve combinations of ws&fc2 computed for transducers T1, T2, T3 and T4. Window sizes: ws=[15, 25, 40, 60] and cutoff frequencies: fc2=[1, 1.5, 2] Hz.

R indicates the position of the person according to the protocol shown in Figure 2.5.

		fc2=1 Hz		fc2=1.5 Hz		fc2=2 Hz	
		V [%]	F [%]	V [%]	F [%]	V [%]	F [%]
T1	ws=15	0.0	0.0	0.0	0.0	0.0	0.0
	ws=25	0.0	0.0	33.2	56.7	35.3	54.5
	ws=40	0.0	0.0	94.7	1.6	92.0	5.3
	ws=60	0.0	0.0	73.3	5.3	89.8	14.4
T2	ws=15	0.0	0.0	38.5	57.8	42.2	48.1
	ws=25	0.0	0.0	95.7	1.6	90.4	5.9
	ws=40	0.0	0.0	97.3	0.0	97.3	0.0
	ws=60	0.0	0.0	90.9	1.6	93.6	3.7
T3	ws=15	0.0	0.0	94.1	3.2	89.3	8.0
	ws=25	0.0	0.0	96.8	0.5	95.7	1.6
	ws=40	0.0	0.0	97.3	0.0	96.3	2.1
	ws=60	0.0	0.0	91.4	1.1	95.2	3.7
T4	ws=15	0.0	0.0	87.2	10.2	77.5	19.8
	ws=25	0.0	0.0	94.1	3.2	89.8	9.1
	ws=40	0.0	0.0	89.8	4.3	90.9	9.1
	ws=60	0.0	0.0	59.4	12.8	82.4	18.2

Table B.23: Experiment 9-Subject 2, [1]-B2
V% and F% are the percentages of valid and false peaks respectively for twelve combinations of ws&fc2 computed for transducers T1, T2, T3 and T4. Window sizes: ws=[15, 25, 40, 60] and cutoff frequencies: fc2=[1, 1.5, 2] Hz.
B2 indicates the position of the person according to the protocol shown in Figure 2.5.

		fc2=1 Hz		fc2=1.5 Hz		fc2=2 Hz	
		V [%]	F [%]	V [%]	F [%]	V [%]	F [%]
T1	ws=15	0.0	0.0	0.0	0.0	4.7	69.8
	ws=25	0.0	0.0	5.4	69.1	8.1	64.4
	ws=40	0.0	0.0	69.8	26.8	68.5	28.9
	ws=60	0.0	0.0	73.8	7.4	86.6	12.1
T2	ws=15	0.0	0.0	0.0	0.0	2.0	72.5
	ws=25	0.0	0.0	10.1	64.4	20.8	75.8
	ws=40	0.0	0.0	81.2	14.1	78.5	17.4
	ws=60	0.0	0.0	0.0	0.0	83.2	6.7
T3	ws=15	0.0	0.0	0.0	0.0	0.0	0.0
	ws=25	0.0	0.0	8.7	87.9	10.7	84.6
	ws=40	0.0	0.0	83.2	14.1	83.9	12.8
	ws=60	0.0	0.0	0.0	0.0	87.2	6.7
T4	ws=15	0.0	0.0	7.4	79.2	20.1	86.6
	ws=25	0.0	0.0	14.1	75.8	23.5	80.5
	ws=40	0.0	0.0	43.0	46.3	48.3	55.0
	ws=60	0.0	0.0	0.0	0.0	70.5	19.5

Table B.24: Experiment 9-Subject 2, [1]L

V% and F% are the percentages of valid and false peaks respectively for twelve combinations of ws&fc2 computed for transducers T1, T2, T3 and T4. Window sizes: ws=[15, 25, 40, 60] and cutoff frequencies: fc2=[1, 1.5, 2] Hz.

L indicates the position of the person according to the protocol shown in Figure 2.5.

		fc2=1 Hz		fc2=1.5 Hz		fc2=2 Hz	
		V [%]	F [%]	V [%]	F [%]	V [%]	F [%]
T1	ws=15	21.9	20.3	55.5	39.1	51.6	39.8
	ws=25	25.0	14.8	95.3	0.8	85.2	10.2
	ws=40	0.0	0.0	96.1	0.0	94.5	1.6
	ws=60	0.0	0.0	80.5	6.3	85.9	10.9
T2	ws=15	22.7	16.4	84.4	11.7	77.3	17.2
	ws=25	23.4	21.1	95.3	0.8	92.2	3.9
	ws=40	31.3	14.8	96.1	0.0	94.5	0.8
	ws=60	25.0	14.8	93.8	0.8	91.4	7.8
T3	ws=15	21.9	20.3	91.4	4.7	87.5	10.2
	ws=25	22.7	19.5	96.1	0.0	94.5	2.3
	ws=40	28.1	15.6	96.1	0.0	95.3	0.8
	ws=60	23.4	13.3	96.1	0.0	95.3	1.6
T4	ws=15	0.0	0.0	53.9	42.2	45.3	44.5
	ws=25	0.0	0.0	79.7	14.8	77.3	27.3
	ws=40	0.0	0.0	87.5	9.4	84.4	19.5
	ws=60	0.0	0.0	57.0	13.3	75.8	21.9

Table B.25: Experiment 9-Subject 2, [1]-B3
V% and F% are the percentages of valid and false peaks respectively for twelve combinations of ws&fc2 computed for transducers T1, T2, T3 and T4. Window sizes: ws=[15, 25, 40, 60] and cutoff frequencies: fc2=[1, 1.5, 2] Hz.
B3 indicates the position of the person according to the protocol shown in Figure 2.5.

Subject 3

		fc2=1 Hz		fc2=1.5 Hz		fc2=2 Hz	
		V [%]	F [%]	V [%]	F [%]	V [%]	F [%]
T1	ws=15	0.0	0.0	26.1	55.0	32.4	53.2
	ws=25	0.0	0.0	92.8	2.7	85.6	9.9
	ws=40	0.0	0.0	95.5	0.0	95.5	0.0
	ws=60	0.0	0.0	82.0	9.9	83.8	13.5
T2	ws=15	0.0	0.0	95.5	0.0	95.5	0.0
	ws=25	0.0	0.0	95.5	0.0	95.5	0.0
	ws=40	0.0	0.0	95.5	0.0	95.5	0.0
	ws=60	0.0	0.0	92.8	1.8	93.7	1.8
T3	ws=15	0.0	0.0	95.5	0.0	95.5	0.0
	ws=25	0.0	0.0	95.5	0.0	95.5	0.0
	ws=40	0.0	0.0	95.5	0.0	95.5	0.0
	ws=60	0.0	0.0	94.6	0.0	95.5	0.0
T4	ws=15	0.0	0.0	95.5	0.0	95.5	0.9
	ws=25	0.0	0.0	95.5	0.0	94.6	0.9
	ws=40	0.0	0.0	95.5	0.0	95.5	0.0
	ws=60	0.0	0.0	94.6	0.0	95.5	0.9

Table B.26: Experiment 9-Subject 3, [1]-B1

V% and F% are the percentages of valid and false peaks respectively for twelve combinations of ws&fc2 computed for transducers T1, T2, T3 and T4. Window sizes: ws=[15, 25, 40, 60] and cutoff frequencies: fc2=[1, 1.5, 2] Hz.

B1 indicates the position of the person according to the protocol shown in Figure 2.5.

		fc2=1 Hz		fc2=1.5 Hz		fc2=2 Hz	
		V [%]	F [%]	V [%]	F [%]	V [%]	F [%]
T1	ws=15	0.0	0.0	34.8	52.3	33.3	44.7
	ws=25	0.0	0.0	87.9	8.3	83.3	12.9
	ws=40	0.0	0.0	95.5	0.0	95.5	0.0
	ws=60	0.0	0.0	95.5	0.0	96.2	0.0
T2	ws=15	0.0	0.0	94.7	1.5	93.9	2.3
	ws=25	0.0	0.0	96.2	0.0	95.5	0.8
	ws=40	0.0	0.0	94.7	0.0	95.5	0.8
	ws=60	0.0	0.0	0.0	0.0	90.9	2.3
T3	ws=15	0.0	0.0	81.1	14.4	75.8	18.9
	ws=25	0.0	0.0	93.2	2.3	88.6	6.1
	ws=40	0.0	0.0	94.7	0.8	93.9	3.0
	ws=60	0.0	0.0	0.0	0.0	86.4	9.1
T4	ws=15	15.2	22.7	29.5	59.1	45.5	57.6
	ws=25	0.0	0.0	56.8	35.6	61.4	41.7
	ws=40	0.0	0.0	68.9	21.2	75.8	22.0
	ws=60	0.0	0.0	40.9	25.0	51.5	29.5

Table B.27: Experiment 9-Subject 3, [1]-R
V% and F% are the percentages of valid and false peaks respectively for twelve combinations of ws&fc2 computed for transducers T1, T2, T3 and T4. Window sizes: ws=[15, 25, 40, 60] and cutoff frequencies: fc2=[1, 1.5, 2] Hz.
R indicates the position of the person according to the protocol shown in Figure 2.5.

		fc2=1 Hz		fc2=1.5 Hz		fc2=2 Hz	
		V [%]	F [%]	V [%]	F [%]	V [%]	F [%]
T1	ws=15	19.6	19.6	7.1	10.7	7.1	10.7
	ws=25	22.3	13.4	36.6	56.3	42.9	50.9
	ws=40	0.0	0.0	87.5	6.3	86.6	10.7
	ws=60	0.0	0.0	0.0	0.0	71.4	17.9
T2	ws=15	0.0	0.0	95.5	0.0	95.5	1.8
	ws=25	0.0	0.0	95.5	0.0	95.5	1.8
	ws=40	0.0	0.0	95.5	0.0	95.5	0.9
	ws=60	0.0	0.0	92.0	1.8	93.8	2.7
T3	ws=15	0.0	0.0	95.5	0.0	95.5	0.9
	ws=25	0.0	0.0	95.5	0.0	95.5	0.9
	ws=40	0.0	0.0	95.5	0.0	95.5	0.0
	ws=60	0.0	0.0	95.5	0.0	95.5	0.0
T4	ws=15	0.0	0.0	93.8	0.9	91.1	3.6
	ws=25	0.0	0.0	95.5	0.0	94.6	0.9
	ws=40	0.0	0.0	95.5	0.0	95.5	0.0
	ws=60	0.0	0.0	95.5	0.0	92.0	3.6

Table B.28: Experiment 9-Subject 3, [1]-B2
V% and F% are the percentages of valid and false peaks respectively for twelve combinations of ws&fc2 computed for transducers T1, T2, T3 and T4. Window sizes: ws=[15, 25, 40, 60] and cutoff frequencies: fc2=[1, 1.5, 2] Hz.
B2 indicates the position of the person according to the protocol shown in Figure 2.5.

		fc2=1 Hz		fc2=1.5 Hz		fc2=2 Hz	
		V [%]	F [%]	V [%]	F [%]	V [%]	F [%]
T1	ws=15	0.0	0.0	4.3	66.7	0.0	0.0
	ws=25	0.0	0.0	0.0	0.0	0.0	0.0
	ws=40	0.0	0.0	0.0	0.0	0.0	0.0
	ws=60	21.3	17.7	27.7	42.6	27.7	30.5
T2	ws=15	0.0	0.0	4.3	64.5	0.0	0.0
	ws=25	0.0	0.0	11.3	57.4	0.0	0.0
	ws=40	0.0	0.0	33.3	49.6	41.1	60.3
	ws=60	0.0	0.0	0.0	0.0	51.1	40.4
T3	ws=15	0.0	0.0	7.8	23.4	24.8	81.6
	ws=25	0.0	0.0	0.0	0.0	17.7	63.1
	ws=40	0.0	0.0	0.0	0.0	52.5	44.7
	ws=60	0.0	0.0	0.0	0.0	81.6	16.3
T4	ws=15	0.0	0.0	0.0	0.0	0.0	0.0
	ws=25	0.0	0.0	0.0	0.0	45.4	52.5
	ws=40	0.0	0.0	0.0	0.0	61.0	41.8
	ws=60	0.0	0.0	0.0	0.0	0.0	0.0

Table B.29: Experiment 9-Subject 3, [1]-L
V% and F% are the percentages of valid and false peaks respectively for twelve combinations of ws&fc2 computed for transducers T1, T2, T3 and T4. Window sizes: ws=[15, 25, 40, 60] and cutoff frequencies: fc2=[1, 1.5, 2] Hz.
L indicates the position of the person according to the protocol shown in Figure 2.5.

		fc2=1 Hz		fc2=1.5 Hz		fc2=2 Hz	
		V [%]	F [%]	V [%]	F [%]	V [%]	F [%]
T1	ws=15	0.0	0.0	12.1	7.7	0.0	0.0
	ws=25	0.0	0.0	57.1	19.8	56.0	23.1
	ws=40	0.0	0.0	84.6	4.4	85.7	9.9
	ws=60	0.0	0.0	74.7	16.5	72.5	19.8
T2	ws=15	0.0	0.0	94.5	0.0	94.5	0.0
	ws=25	0.0	0.0	94.5	0.0	94.5	0.0
	ws=40	0.0	0.0	94.5	0.0	94.5	0.0
	ws=60	0.0	0.0	89.0	5.5	87.9	4.4
T3	ws=15	0.0	0.0	93.7	0.0	94.6	0.9
	ws=25	0.0	0.0	93.7	0.0	93.7	2.7
	ws=40	0.0	0.0	93.7	0.0	91.9	0.0
	ws=60	0.0	0.0	0.0	0.0	0.0	0.0
T4	ws=15	0.0	0.0	94.6	0.9	91.0	4.5
	ws=25	0.0	0.0	95.5	0.0	93.7	0.9
	ws=40	0.0	0.0	95.5	0.0	93.7	0.0
	ws=60	0.0	0.0	0.0	0.0	0.0	0.0

Table B.30: Experiment 9-Subject 3, [1]-B3
V% and F% are the percentages of valid and false peaks respectively for twelve combinations of ws&fc2 computed for transducers T1, T2, T3 and T4. Window sizes: ws=[15, 25, 40, 60] and cutoff frequencies: fc2=[1, 1.5, 2] Hz.
B3 indicates the position of the person according to the protocol shown in Figure 2.5.